Assessment of Metabolic Therapy for Acute Heart Failure

By

Charlene Patricia Kimar

Thesis presented in fulfilment of the requirements for the degree

of Doctor of Philosophy (Physiological Sciences) in the Faculty of Science at Stellenbosch University

Supervisor: Professor M Faadiel Essop

March 2017

DECLARATION

By submitting this thesis/dissertation, I declare that the entirety of the work contained therein is my own, original work, that I am the sole author thereof (save to the extent explicitly otherwise stated), that reproduction and publication thereof by Stellenbosch University will not infringe any third party rights and that I have not previously in its entirety or in part submitted it for obtaining any qualification.

Charlene P Kimar

_____

March 2017

ABSTRACT

Introduction

Acute heart failure (AHF) is the most common primary diagnosis for hospitalized heart disease cases in Africa. Increased fatty acid oxidation (FAO) with heart failure (HF) triggers detrimental effects on the myocardium, we hypothesized that diabetic rat hearts subjected to AHF display lower cardiac function *vs.* controls and that Trimetazidine (TMZ) (a partial FAO inhibitor) counters this effect.

Aims

1) To establish an *ex vivo* AHF model for diabetic hearts; 2) Assess whether TMZ treatment offers cardioprotection to diabetic rat hearts subjected to an AHF protocol; and 3) Delineate underlying mechanisms by evaluating markers for oxidative stress, mitochondrial uncoupling, apoptosis and metabolic dysregulation.

Methods

Vehicle control male Wistar rats were injected with citrate buffer. To induce diabetes rats were administered streptozotocin (60 mg/kg) for one week *vs.* non-diabetic controls. Hearts were perfused on the Langendorff retrograde perfusion system for three phases: Stabilization - (11 mM glucose- non-diabetic, and 30 mM glucose- diabetic hearts) at 100 cm H_2O (30 min); AHF – (1.5 mM palmitic acid, 2.5 mM glucose) at 20 cm H_2O (35 min); and Recovery– (1.5 mM palmitic acid, 11 mM glucose or 30 mM glucose) at 100 cm H_2O (30 min). 1 µM TMZ was administered at the start of recovery. In addition, we evaluated necrosis and infarct size by tetrazolium (TTC) staining at the end of the AHF phase. Western blotting was performed for

markers of apoptosis (pBAD/BAD), oxidative stress (superoxide dismutase 2 [SOD2], conjugated dienes [CDs], thiobarbituric acid reactive substances (TBARS), reduced/oxidized glutathione [GSH/GSSG] analysis, oxygen radical absorbance capacity [ORAC]), mitochondrial uncoupling (uncoupling protein 2 [UCP2]) and metabolic dysregulation (advanced glycation end product [AGE] and polyol pathway analyses). We investigated direct effects of TMZ (1 µM) in H9c2 cardiomyoblasts exposed to 500 µM palmitate for 21 hours and assessed the effects of TMZ treatment on fatty acid-induced oxidative stress and apoptosis.

Results

Reduced function was seen for all groups in recovery *vs.* controls, while AHF-diabetic showed worse outcomes *vs.* AHF alone. TMZ treatment resulted in a robust increase in left ventricular developed pressure (LVDP) for diabetic hearts *vs.* controls. Infarct size assessment showed no differences. TMZ treated diabetic hearts also displayed lower AGE and higher polyol pathway activation *vs.* respective controls. However, several markers of the AGE pathway did not show any significant differences for any groups. Non-diabetic and diabetic hearts displayed increased oxidative stress (TBARS) compared to their counterparts. TMZ treatment resulted in anti-apoptotic effects in hearts subjected to AHF. TMZ exhibited antioxidant effects by lowering fatty acid-induced mitochondrial oxidative stress in cells.

Conclusion

This study successfully established a novel *ex vivo* model of AHF for the diabetic rat heart, and TMZ treatment resulted in cardioprotection for diabetic hearts. Our data suggest that TMZ may mediate some of its cardioprotective effects by acting as an anti-oxidant to lower myocardial oxidative stress triggered during AHF. The findings also indicate that TMZ treatment may lower

the formation of damaging AGEs in the diabetic heart. TMZ therefore, emerges as a putative therapeutic target to be considered as sole and/or combined treatment (with more conventional drugs) for AHF patients.

OPSOMMING

Inleiding

Akute hartversaking (AHV) is die mees algemene primêre diagnose vir gehospitaliseerde hartsiekte gevalle in Afrika. Verhoogde vetsuuroksidasie (VSO) met hartversaking (HV) veroorsaak skadelike effekte op die miokardium. Ons hipotiseer dat diabetiese rotharte blootgestel aan AHV verlaagde hartfunksie vertoon vs. kontroles en dat Trimetazidien (TMZ) (‘n gedeeltelike VSO inhibitor), hierdie effek teenwerk.

Doelwitte

1) Om ‘n *ex vivo* AHV model vir diabetiese harte te vestig; 2) Assesseer of TMZ behandeling kardiobeskerming verleen aan diabetiese rotharte blootgestel aan ‘n AHV protokol; en 3) Karakterisering van onderliggende meganismes deur merkers vir oksidatiewe stres, mitochondriese ontkoppeling, apoptose en metaboliese wanregulering te ondersoek.

Metodes

Draer kontrole Wistar rot mannetjies was met sitraat buffer ingespuit. Om diabetes te induseer was rotte met streptozotosien (60 mg/kg) vir een week toegedien vs. nie-diabetiese kontroles. Harte is geperfuseer op die Langendorff retrograad perfusie sisteem vir drie fases: Stabilisasie – (11 mM glukose-nie-diabeties, en 30 mM glukose-diabetiese harte) teen 100 cm H_2O (30 min); AHV – (1.5 mM palmitiensuur, 2.5 mM glukose) teen 20 cm H_2O (35 min); en Herstel – (1.5 mM palmitiensuur, 11 mM glukose of 30 mM glukose) teen 100 cm H_2O (30 min). 1 µM TMZ is aan die begin van herstel toegedien. Ons het addisioneel nekrose en infarktgrootte aan die einde van die AHV fase geevalueer met tetrazolium (TTC) kleuring. Western klad-analise is

uitgevoer vir merkers van apoptose (pBAD/BAD), oksidatiewe stres (superoksieddismutase 2 [SOD2], gekonjugeerde diëne [CDs], tiobarbituursuur reaktiewe stowwe (TBARS), gereduseerde/geoksideerde glutatioon [GSH/GSSG] analise, suurstof radikaal absorbansie kapasiteit [ORAC]), mitochondriese ontkoppeling (ontkoppelingproteïen 2 [UCP2]) en metaboliese wanregulering (gevorderde glukasie eindproduk [AGE] en poliolpad analise). Ons het die direkte effek van TMZ (1 µM) in H9c2 kardiomioblaste, blootgestel aan 500 µM palmitaat vir 21 ure, ondersoek en die effek van TMZ behandeling op vetsuur-geïnduseerde oksidatiewe stres en apoptose, geassesseer.

Resultate

Verminderde funksie is waargeneem vir alle groepe in herstel vs. kontrole, terwyl AHV-diabete slegter uitkomste getoon het vs. slegs AHV. TMZ behandeling het gelei tot ‘n sterk toename in linker ventrikulêre ontwikkelde druk (LVDP) vir diabetiese harte vs. kontroles. Infarktgrootte assessering het geen verskille getoon nie. TMZ behandelde diabetiese harte het ook laer AGE en hoër poliolpad aktivering vs. onderskeidelike kontroles, getoon. ‘n Aantal merkers van die AGE pad het egter nie betekenisvolle verskille vir enige groepe gedemonstreer nie. Nie-diabetiese en diabetiese harte het verhoogde oksidatiewe stres (TBARS) in vergelyking met hul ekwivalente getoon. TMZ behandeling het anti-apoptotiese effekte teweeggebring in harte blootgestel aan AHV. TMZ het anti-oksidant effekte getoon deur die verlaging van vetsuur-geïnduseerde mitochondriese oksidatiewe stres in selle.

Gevolgtrekking

Hierdie studie het suksesvol ‘n nuwe *ex vivo* model vir AHV vir die diabetiese rothart gevestig, en TMZ behandeling het gelei tot kardiobeskerming vir diabetiese harte. Ons data stel voor dat

TMZ die kardiobeskermende effekte daarvan medieer deur op te tree as anti-oksidant om miokardiale oksidatiewe stres veroorsaak tydens AHV, te verlaag. Die bevindinge dui ook aan dat TMZ behandeling die vorming van skadelike AGE in die diabetiese hart mag verlaag. TMZ verskyn dus as ‘n putatiewe terapeutiese teiken om in ag te neem as enkel en/of gekombineerde behandeling (met meer konvensionele geneesmiddels) vir AHV pasiënte.

ACKNOWLEDGEMENTS

First and foremost, I thank God almighty for all the countless blessings and the strength and perseverance to see this study through.

I would like to express my sincere gratitude to the following people for their significant contribution towards this study:

To my mentor and PhD supervisor, **Professor M. Faadiel Essop**, thank you for granting me the opportunity to be apart of the CMRG research group and for all the valuable advice, guidance, support and intellectual input throughout my PhD.

I would like to thank and acknowledge **Dr Lydia Lacerda** for her guidance (both on the technical and intellectual front) with establishing our perfusion model, and for never hesitating to offer her assistance.

I would like to acknowledge **Dr Dirk Bester** and **Dr Fanie Rautenbach** from the Oxidative Stress Research Centre at the Cape Peninsula University of Technology and the contributions of **Dr Danzil Joseph** and **Natasha Driescher** towards this body of work.

Dr Rudo Mapanga - For her patience with regard to perfusion training, technical guidance and proof-reading of this thesis.

Dr Gaurang Deshpande – For proof-reading of this thesis and always being so willing and cheerful in assisting when needed.

To **Dr Theo Nel,** thank you for all your assistance, mentorship and guidance.

Ms. Veronique Human – Thank you for the Afrikaans translation of my abstract.

I would like to extend my gratitude to **Rozanne Adams**, for her inputs regarding flow cytometry and for running the samples and her assistance in editing of this thesis.

I am grateful for the assistance of staff members at the Department of Physiological Sciences, especially **Noel Markgraff**, **Judy Faroe**, **Grazelda**, **Katrina** and **Johnifer**.

To my **parents** – I thank God for you. Thank you for all your love and unconditional support throughout my studies. I am grateful for this opportunity to further my career and I can only dream of repaying you for all that you have sacrificed for me. To my siblings, (**Rozan** and **Sidney**) niece **Christina** thank you for all the support and encouragement.

Thank you to **CMRG**, for the friendships, sense of humor and valuable critical discussions.

Lastly I would like to thank **Oppenheimer Trust**, the **Medical Research Council**, **Stellenbosch University** and the **National Research Foundation** for financial assistance.

TABLE OF CONTENTS

LIST OF FIGURES

LIST OF TABLES

LIST OF ABBREVIATIONS

A

ACC	Acetyl-CoA carboxylase
ACE	Angiotensin converting enzyme
ADP	Adenosine diphosphate
AGEs	Advanced glycation end products
AHF	Acute heart failure
AMP	Adenosine monophosphate
AMPK	Adenosine monophosphate activated kinase
ANOVA	Analysis of variance
AR	Aldose reductase
ATP	Adenosine triphosphate

B

1,3-BPG	1,3-bisphosphoglycerate
BAD	Bcl-2 associated death promoter
BHT	Butylated hydroxytolene
BSA	Bovine serum albumin

C

Ca^{2+}	Calcium
cAMP	cyclic adenosine monophosphate
CAT	Carnitine acyl transferase
CDs	Conjugated dienes

CoA	Co-enzyme A
CPT-I	Carnitine palmitoyltransferase-I
CPT-II	Carnitine palmitoyltransferase-II
CVD	Cardiovascular disease
D	
DCCT	Diabetes Control and Complications Trial
DCF	Dichloro fluorescein
DHAP	Dihydroxylacetone phosphate
DMEM	Dulbecco's Modified Eagle's Medium
DNA	Deoxyribonucleic acid
E	
ECL	Enhanced chemiluminescence
EDTA	Ethylenediaminetetraacetic acid
ELISA	Enzyme-linked immunoadsorbent assay
ETC	Electron transport chain
ESC	European Society of Cardiology
F	
F-1,6-BP	Fructose-1,6-bisphosphate
F-2,6-BP	Fructose-2,6-bisphosphate
F-6-P	Fructose-6-phosphate
FA	Fatty acid
FABPm	Plasma membrane fatty acid binding protein

FACS	Fatty acyl-CoA synthase
$FADH_2$	Flavin adenine dinucleotide reduced
FAs	Fatty acids
FAT	Fatty acid translocase
FBS	Fetal bovine serum
FFAs	Free fatty acids
FN3K	Fructosamine-3-kinase

G

G-3-P	Glyceraldehyde-3-phosphate
GAPDH	Glyceraldehyde-3-phosphate dehydrogenase
GIK	Glucose-insulin-potassium
G-6-P	Glucose-6-phosphate
GLO-1	Glyoxalase-1
GLUT	Glucose transporter protein
GLUT1	Glucose transporter 1
GLUT4	Glucose transporter 4
GSH	Reduced glutathione
GSSG	Oxidized glutathione
GTP	Guanidine triphosphate

H

HbA1c	Glycosylated hemoglobin
HBP	Hexosamine biosynthetic pathway

HF	Heart failure
I	
IR	Immediate release
K	
3-KAT	3-ketoacyl-coenzyme A thiolase
L	
LCAD	Long-chain acyl-coenzyme A dehydrogenase
LDH	Lactate dehydrogenase
LPL	Lipoprotein lipase
LVDP	Left ventricular developed pressure
LVEDP	Left ventricular end diastolic pressure
LVESP	Left ventricular end systolic pressure
M	
MCAD	Medium-chain acyl-CoA dehydrogenase
MCD	Malonyl-CoA decarboxylase
MCT-1	Monocarboxylic acid transporter 1
Mg^{2+}	Magnesium
MG	Methylglyoxal
MG-BSA	Methylglyoxal-Bovine serum albumin
MPC	Mitochondrial pyruvate carrier
MR	Modified release

N

NAD^+	Oxidized nicotinamide dinucleotide
NADH	Nicotinamide adenine dinucleotide reduced
NADPH	Nicotinamide adenine dinucleotide phosphate
NF-κB	Nuclear factor κBr
NOGPs	Non-oxidative glucose pathways

O

ORAC	Oxygen radical absorbance capacity

P

PARP	Poly (ADP ribose) polymerase
PBS	Phosphate buffered saline
PDH	Pyruvate dehydrogenase
PDK	Pyruvate dehydrogenase kinase
PDK4	Pyruvate dehydrogenase kinase 4
PDP	Pyruvate dehydrogenase phosphatase
PKA	Protein kinase A
PFK1	Phosphofructokinase 1
PFK2	Phosphofructokinase 2
PI3K	Phosphatidylinositol 3-kinase
PKC	Protein kinase C
PPAR-α	Peroxisome proliferator activated receptor alpha

R

RAGE	Receptor for advanced glycation end products
RLU	Reflective light units
ROS	Reactive oxygen species
RNS	Reactive nitrogen species
RPP	Rate pressure product
RyR	Ryanodine receptor

S

SDH	Sorbitol dehydrogenase
SDS-PAGE	Sodium dodecyl sulfate poly-acrylamide gel electrophoresis
SDS	Sodium dodecyl sulfate
SEM	Standard error of the mean
SOD	Superoxide dismutase
SR	Sarcoplasmic reticulum
SSA	sub-Saharan Africa

T

TBARS	Thiobarbituric acid reactive substances
TMB	3,3’,5,5’-tetramethylbenzidine
THESUS-HF	The Sub-Saharan Africa Survey of Heart Failure
TIM	Triose phosphate isomerase
TMZ	Trimetazidine

U

UCPs	Uncoupling proteins
UKPDS	United Kingdom Prospective Diabetes Study

V

VMAC	Vasodilation in the Management of Acute Congestive Heart Failure

W

WHO	World Health Organization

UNITS OF MEASUREMENT

%	percentage
AU	arbitrary units
°C	degree celsius
cm H_2O	centimeter of water
g	grams
kDa	kilodalton
L	litre
M	molar
mg	milligram
mg/kg	milligram per kilogram
mg/mL	milligram per millilitre
min	minutes
ml	millilitres
mM	millimolar
mmHg	millimeter of mercury
mmHg/sec	millimeter of mercury per second
mmol/L	millimolar per litre
ng/mL	nanogram per millilitre
nmol/well	nanomolar per well
nm	nanometer
sec	second

V	volt
µg	microgram
µM	micromolar

1 CHAPTER 1

1.1 Prelude

According to the European Society of Cardiology (ESC) acute heart failure (AHF) can be defined as the "rapid changes in signs and symptoms of heart failure (HF)"

(McMurray *et al.*, 2013). AHF is the major cause of mortality and loss of quality of life according to the guidelines described by international heart associations such as the ESC and the American Heart Association. It is a life-threatening syndrome that results in the urgent need for therapy (McMurray *et al.*, 2013). Management of AHF is difficult as it does not have an universally accepted definition, nor is the pathophysiology properly understood (Nieminen, 2005). A reason for this situation is the lack of focused research that subsequently limits the foundation of rational treatment strategies (Nieminen, 2005). AHF affects individuals in all age groups and is a major reason for re-hospitalization and post discharge mortality rates. Most AHF occurs over existing chronic HF and also within the context of diabetes. It is also the most common primary diagnosis in patients admitted for heart diseases in Africa (Sliwa and Mayosi, 2013). It is therefore essential to develop/study therapeutic agents and the metabolic pathways involved as this will help alleviate the growing global burden of HF.

As the focus of this study is on metabolic modulation as a therapy for AHF, it is important to note that high circulating levels of free fatty acids (FFAs) can elicit damaging effects on myocardial function by "oxygen wastage" and diminished mitochondrial adenosine triphosphate

(ATP) generation (Essop and Opie, 2004). By contrast, glucose is proposed to be beneficial to the failing heart and here drugs like trimetazidine (TMZ) - shifts metabolism from fatty acid (FA) oxidation to glucose metabolism - showed promising results (Quinlan *et al*., 2008). Moreover, glucose-insulin-potassium administration (GIK) can also trigger this metabolic switch with resultant cardioprotection (Kloner and Nesto, 2008). However, despite such progress there is a limited understanding of the role of metabolic fuel selection (FFAs versus glucose) within the context of AHF. Of note, diabetic individuals exhibit an increased risk for developing cardiovascular complications and it is therefore considered as one of the leading causes of diabetes-related morbidity and mortality (Kengne *et al*., 2010) The current study therefore investigated this research question as an increased understanding may result in the utilization of novel metabolic therapies for AHF. Here we hypothesized that the metabolic agent TMZ aids the recovery of diabetic hearts after an episode of AHF by shifting substrate utilization away from FA. We initially set out to establish an *ex vivo* rat AHF model in the diabetic heart (developmental component of this study) and thereafter evaluated the efficacy of TMZ within this context. Heart tissues were also collected and various molecular analyses performed to delineate underlying mechanisms driving the onset of AHF in diabetic versus non-diabetic hearts. Here our rationale was that an improved understanding of mechanisms involved in AHF ± TMZ treatment may eventually lead to improved care and well-being of patients within the clinical setting.

2 CHAPTER 2

Cardiac metabolism under physiological conditions

2.1 Substrate utilization

The cardiovascular system requires a continuous supply of oxygen and energy providing substrates to sustain rhythmic contractions (Taegtmeyer *et al*., 1980). When the homeostatic balance is disturbed in response to severe lack of oxygen this leads to cardiac damage and maladaptive responses (Essop, 2007). ATP is the main energy currency in the heart with a turnover of 6 to 8 times per minute (Lopaschuk and Ussher, 2010). To meet its energetic demands, the heart utilizes various energy substrates namely FFAs, glucose, lactate, ketone bodies and pyruvate (Lopaschuk and Ussher, 2010). The efficiency of ATP production is dependent on the energy substrate used, where FFAs are a major energy source for the mammalian adult heart, contributing approximately 60 – 80% of the energy requirements. Under physiological conditions approximately 95% of ATP formation in the myocardium is derived from oxidative phosphorylation in mitochondria, while the remainder is generated from glycolysis and guanidine triphosphate (GTP) formation in the citric acid cycle (Stanley *et al*., 2005).

Myocardial ATP content is moderate under physiological conditions where ATP hydrolysis has a turnover approximately every 10 seconds (Opie, 1991). ATP is broken down at a high rate, and re-synthesized by utilizing energy from FAs, glucose and lactate in the mitochondrion (Stanley,

2001). An average of 60 – 70% of ATP hydrolysis is utilized for contractile shortening, with the remainder mainly employed for the sarcoplasmic reticulum and ionic modulators such as the Ca^{2+} pump (Figure 2.1). Energy required for mitochondrial oxidative phosphorylation derives from electrons that are transferred from carbon fuels (FAs, glucose and lactate) by dehydrogenation reactions that produce reducing equivalents, i.e. nicotinamide adenine dinucleotide reduced (NADH) and flavin adenine dinucleotide reduced ($FADH_2$) (Figure 2.1) (reviewed in Stanley *et al*., 2005). FA β-oxidation and the citric acid cycle are primary contributors to electrons utilized in mitochondrial oxidative phosphorylation, with pyruvate dehydrogenase (PDH) and glycolysis contributing to a lesser extent (Stanley *et al*., 2005).

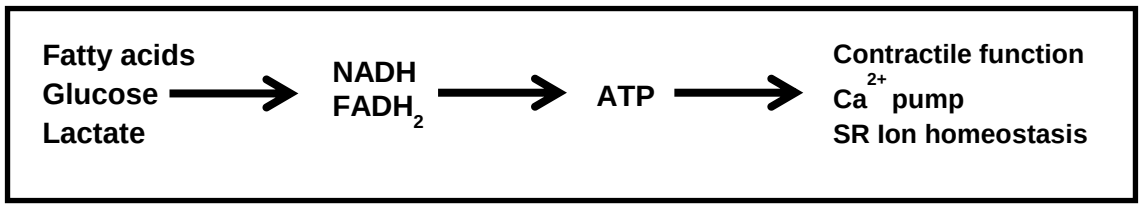

Figure 2.1. Myocardial substrate utilization: Metabolic fuel substrates are converted to reducing equivalents NADH and $FADH_2$ to produce mitochondrial ATP that is utilized for optimal cardiac function. NADH: nicotinamide adenine dinucleotide reduced; $FADH_2$: flavin adenine dinucleotide reduced; ATP: adenosine triphosphate; SR: sarcoplasmic reticulum.

The majority of the ATP produced requires O_2 for mitochondrial oxidative metabolism and the efficiency of this reaction is dependent on the type of substrate used (Weiss and Maslov, 2004). For example, one molecule of glucose can produce 31 ATP molecules through glycolysis and glucose oxidation and this requires 6 O_2. However, the production of 105 ATP molecules by palmitate oxidation requires 23 O_2 – FAs therefore need more O_2 per molecule ATP generated.

Thus FAs are a less efficient energy substrate under stressful conditions, e.g. the failing or ischemic heart (Lopaschuk and Ussher, 2010).

2.2 Regulation of glucose uptake

Glucose is one of the major fuel substrates that contribute to myocardial metabolism. Glycolytic substrates are derived by dietary intake and/or exogenous glucose and endogenous (glycogen) stores (Stanley *et al*., 2005). Moreover, during the fed state it becomes the primary energy substrate by intake of dietary carbohydrates. Various triggers may stimulate glycogenolysis e.g. ischemia, adrenergic stimulation, reduced myocardial ATP levels and intense exercise (Goldfarb *et al*., 1986; Hue and Taegtmeyer, 2009; Stanley *et al*., 1997a).

Myocardial glucose transport is dependent on plasma glucose concentrations and the availability of glucose transporters (GLUT) within the plasma membrane (Santalucia, 1999). Two main glucose transporters have thus been identified in the heart, i.e. GLUT1 and GLUT4 (Doria-Medina *et al*., 1993; James *et al*., 1989). GLUT1 and GLUT4 are the predominant glucose transporters in the fetal and adult heart, respectively (Postic *et al*., 1994; Santalucía *et al*., 1992). Although GLUT1 is the predominant fetal transporter, it can also contribute to constitutive glucose uptake in the adult heart. However, GLUT4 facilitates the majority of basal glucose uptake in the adult heart (Bergman *et al*., 1980; Bersin and Stacpoole, 1997). Insulin availability leads to the translocation of GLUT1 and GLUT4 from intracellular locations to the plasma membrane to thereby increase glucose uptake by the heart (Russell *et al*., 1999; Young *et al*., 1997). GLUT1 is more profound in the intracellular pool under conditions that favor basal

cardiac glucose uptake (Luiken *et al*., 2004), while GLUT4 is the insulin-responsive transporter (Laybutt *et al*., 1997; Olson and Pessin, 1996). Glucose transporters can be stimulated in response to ischemia and/or increased work demand by the myocardium (Stanley *et al*., 1997a; Young *et al*., 2000, 1997). Moreover, other regulators can also impact on the role of glucose transporters, e.g. increased availability of citrate and malate can inhibit its translocation and subsequent glucose uptake (Beauloye *et al*., 2002).

2.3 Glycolysis

Glycolysis is a cytosolic process where glucose is converted to lactate under anaerobic conditions, or to pyruvate under aerobic conditions. The initial step is the uptake of glucose by the cardiac myocyte whereafter it is rapidly phosphorylated to glucose-6-phosphate (G-6-P) by hexokinase II enzyme (Figure 2.2), forming a carbon skeleton of glucose impermeable to cell membrane. For the fetal heart GLUT1 (Postic *et al*., 1994; Santalucía *et al*., 1992) and hexokinase I are predominant, however, following birth expression of these modulators decrease while GLUT 4 and hexokinase II are upregulated (Postic *et al*., 1994; Santalucía *et al*., 1992). G-6-P can either be converted to glycogen or enter the glycolytic pathway. For the latter process, isomerase converts G-6-P to fructose-6-phosphate (F-6-P), followed by phosphofructokinase-1 (PFK1) leading to fructose-1,6-bisphosphate (F-1,6-BP) formation (Jaswal *et al*., 2011) with utilization of one ATP molecule (Hue and Rider, 1987). This is the rate-limiting enzyme of the glycolytic pathway (Depre *et al*., 1993; Rider *et al*., 2004). PFK1 may be inhibited by low pH, high intracellular citrate or ATP levels - stimulated by adenosine diphosphate (ADP), adenosine

monophosphate (AMP), phosphatase and fructose 2,6-bisphosphate (F-2,6-BP) (Depre *et al*., 1993; Rider *et al*., 2004; Stanley *et al*., 2005).

When glycolysis is coupled to glucose oxidation, pyruvate is translocated into the mitochondrion by the mitochondrial pyruvate carrier (MPC). PDH subsequently converts pyruvate to acetyl-CoA that enters the citric acid cycle, leading to the production of 31 ATP molecules per glucose molecule (Herzig *et al*., 2012; Panchal *et al*., 2001, 2000). However, if pyruvate does not undergo further oxidation (anaerobic conditions) then it is converted to lactate by lactate dehydrogenase. The latter step is crucial as it enables the conversion of NADH back to oxidized nicotinamide dinucleotide (NAD^+) allowing glycolysis to proceed. Phosphofructokinase-2 (PFK2) catalyzes the conversion of F-1,6-BP to F-2,6-BP (Hue and Rider, 1987). PFK2 can be inhibited by citrate and subsequently increase F-2,6-BP levels to ultimately inhibit PFK1 activity (Kantor *et al*., 2001). PFK2 activity can also be stimulated by protein kinase C (PKC) and phosphatidylinositol 3-kinase (PI3K) (An and Rodrigues, 2006; Depre *et al*., 1998; Marsin *et al*., 2000).

The next step in the glycolytic pathway is the conversion of F-1,6-BP by aldolase into triose phosphates, i.e. dihydroxylacetone phosphate (DHAP) and glyceraldehyde-3-phosphate (G-3-P). In addition, the rate-limiting enzyme glyceraldehyde-3-phosphate dehydrogenase (GAPDH) catalyzes the conversion of G-3-P to 1,3-diphosphoglycerate producing glycolytically-derived NADH (Ceriello *et al*., 2002). This is an important step during conditions such as ischemia (Stanley *et al*., 2005). The accumulation of cytosolic NADH also leads to the inhibition of GAPDH activity while upregulation of NAD^+ activates GAPDH activity (Stanley *et al*., 2005).

Increased lactate concentrations can also lead to the inhibition of NADH to NAD^+ conversion and therefore in a reduction of GAPDH activity. Subsequent to this step, phosphoglycerokinase transfers a phosphate between 1,3-bisphosphoglycerate (1,3-BPG) to ADP to form ATP and glycolytic flux thus yields two ATP molecules per glucose metabolized. During aerobic conditions glycolysis typically contributes approximately 10% towards ATP production (Opie and Knuuti, 2009).

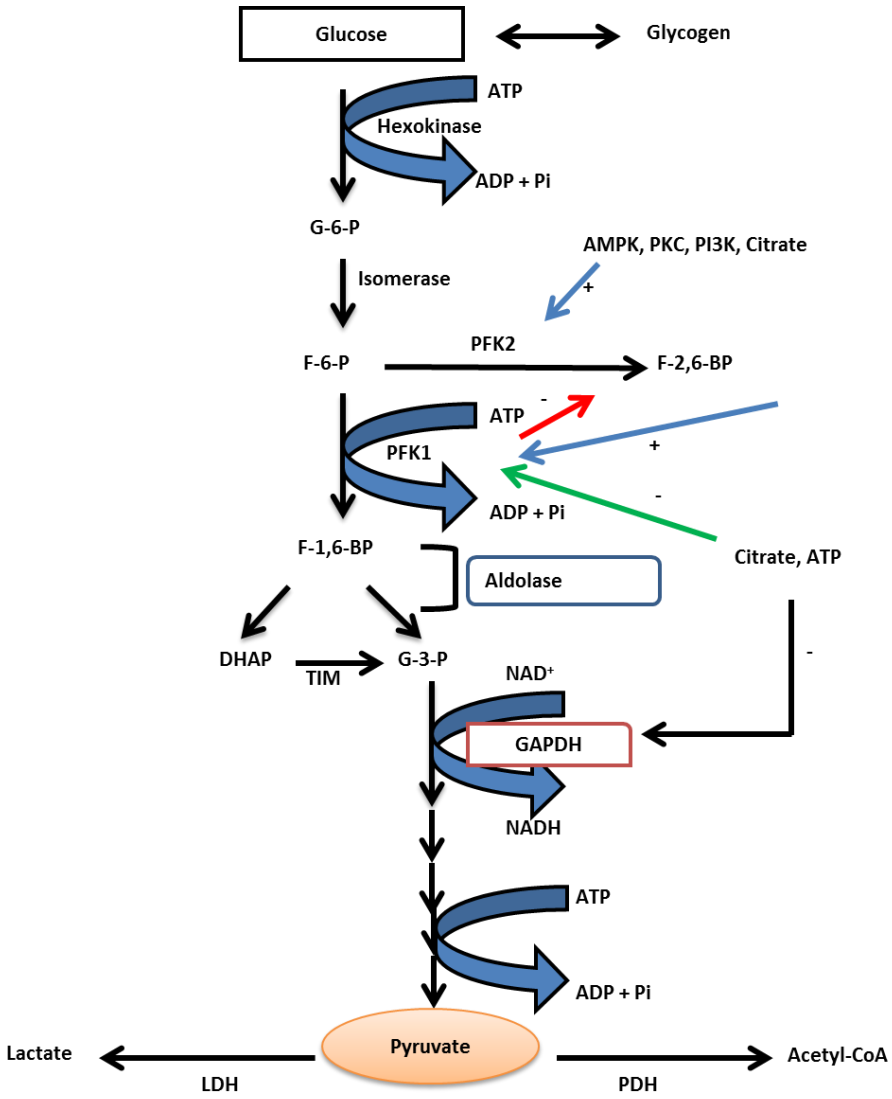

Figure 2.2. Regulation of the glycolytic pathway: Glucose is metabolized to pyruvate through several steps. GAPDH and PFK1 are stimulated in response to various stimuli. AMPK: adenosine monophosphate activated kinase; 1,3-BPG: 1,3-bisphosphoglycerate; DHAP: dihidroxylacetone phosphate; F-6-P: fructose-6-phosphate; F-1,6-BP: fructose 1,6-bisphosphate; F-2,6-BP: fructose 2,6 bisphosphate; G-6-P: glucose-6-phosphate; G-3-P: glyceraldehyde-3-phosphate; LDH: lactate dehydrogenase; PFK1: phosphofructokinase 1; PFK2: phosphofructokinase 2; PDH: pyruvate dehydrogenase; PKC: protein kinase C; PKA: protein kinase A; PI3K: phosphoinositide-3-kinase; TIM: triose phosphate isomerase.

Glycolytic end-products formed (NADH, pyruvate) can be transported into the mitochondrial matrix and utilized for energy production by oxidative metabolic processes. However, when oxygen availability is limited (e.g. during ischemia) pyruvate is converted to lactate by lactate dehydrogenase and subsequently this leads to the oxidation of NADH to NAD^+. Lactate is taken up into the myocardium via monocarboxylic acid transporter 1 (MCT-1) (Garcia *et al*., 2015; Johannsson *et al*., 1997). An impairment in pyruvate oxidation and increased glycolysis can lead to increased lactate production during disease states such as diabetes (Avogaro *et al*., 1990; Hall *et al*., 1996; Stanley *et al*., 1997b) or ischemia (Depre *et al*., 1998; Opie, 1991; Stanley *et al*., 1997a). Pyruvate formed by glycolysis can either be converted to lactate, decarboxylated to acetyl-CoA or carboxylated to oxaloacetate or malate (Randle, 1986). Pyruvate decarboxylation is the major irreversible step in the oxidation of carbohydrates and it is catalyzed by PDH (Randle, 1986). PDH forms part of a complex that consists of pyruvate dehydrogenase kinase (PDK) and pyruvate dehydrogenase phosphatase (PDP). Here PDK can inhibit PDH through phosphorylation and can alleviate the inhibition by the process of de-phosphorylation (Reviewed in Stanley *et al*., 2005). PDH is inhibited by pyruvate dehydrogenase kinase 4 (PDK4) mediated phosphorylation on the E_1 subunit of the enzyme complex (Randle and Priestman, 1996). PDK4 is the major isoform that is induced in response to starvation, diabetes and peroxisome proliferator activated receptor-α (PPAR-α) (Bowker-Kinley *et al*., 1998; Harris *et al*., 2001). Elevated circulating lipids and the accumulation of intracellular long-chain FAs (e.g. with fasting or diabetes) lead to increased PPAR-α mediated expression of PDK4. The latter results in increased PDH inhibition and a decrease in pyruvate derived from glycolysis and lactate oxidation (Harris *et al*., 2001). Pyruvate can also inhibit PDK by lowering acetyl-CoA, free CoA

and NADH/NAD^+ ratios (Kerbey *et al*., 1976; Randle and Priestman, 1996; Whitehouse *et al*., 1974). The PDH complex also contains a PDH phosphatase that can be increased in response to Ca^{2+} and Mg^{2+} (McCormack and Denton, 1984. This provides a mechanism for adrenergic stimulation's effects on PDH, i.e. it increases cytosolic and mitochondrial Ca^{2+} to activate PDH (McCormack and Denton, 1989). Lastly, increased FFA supply and FA oxidation inhibit PDH activity and pyruvate oxidation (Randle, 1986).

2.4 Fatty acid uptake and metabolism

FAs are the preferred fuel substrate and accounts for approximately 70% of ATP production under basal conditions (Merkel, 2002). The amount of FAs utilized by the heart is dependent on both the source and the presence of competing energy substrates together with the heart's metabolic demand and the contributions/activities of the citric acid cycle and electron transport chain (ETC) (Lopaschuk and Ussher, 2010). The degree of FA uptake is dependent on the concentration of non-esterified FAs present in plasma (Bing *et al*., 1954; Lopaschuk *et al*., 1994; Wisneski *et al*., 1985). Here FAs are transported in plasma being bound to albumin or covalently attached in triglycerides and enclosed with chylomicrons or very low density lipoproteins (Lopaschuk *et al*., 1994). During the fasted state (low insulin, high catecholamines) the systemic FA concentration increases thereby leading to elevated rates of FA uptake (Lopaschuk *et al*., 1994). For example, plasma FFA concentration can increase to 1 mM in the event of metabolic stress situations such as ischemia and diabetes (Lopaschuk *et al*., 1994).

FAs are taken up into the cardiomyocyte by passive diffusion or protein-mediated transport across the sarcolemma (van der Vusse *et al*., 2000) by fatty acid translocase (FAT) and plasma membrane fatty acid binding protein (FABPm) (Glatz *et al*., 2001) (Figure 2.3). The predominant FAT protein is known as CD36 and it is also the main FA uptake regulator found in the heart and skeletal muscle (Schaffer, 2002; van der Vusse *et al*., 2000). Of note, individuals with mutations in CD36 are associated with decreased long-chain FA analog uptake suggesting that CD36 is closely linked to the regulation of myocardial FA uptake (Schaffer, 2002). Once transported FAs bind to FABPm they are converted by fatty acyl-CoA synthetase (FACS) (Schaffer, 2002). This is followed by the addition of a CoA group to the FA by fatty acyl-CoA synthetase that enables long-chain FAs to enter the mitochondrion (Lopaschuk and Ussher, 2010). After uptake and esterification fatty acyl-CoA can be utilized to produce ATP for the triglyceride or the intracellular lipid pools. FABP and FACS associated to CD36 can also be found within the cytoplasm and converts intracellular FFA to fatty acyl-CoA (Schaffer, 2002).

FA β-oxidation mainly occurs in mitochondria and to a lesser extent in peroxisomes (Kunau *et al*., 1995; Schulz, 1994) and primarily leads to the production of NADH, $FADH_2$ and acetyl-CoA. Long-chain fatty acyl-CoA can be esterified by glycerolphosphate acyltransferase to triglyceride or by acylcamitine palmitoyltransferase I (CPT-I) to long-chain fatty acylcamitine in the intermembrane space (Lopaschuk *et al*., 1994).

Long-chain fatty-acyl carnitine is transported across the mitochondrial inner membrane by carnitine translocase and then converted back into long-chain fatty acyl-CoA to subsequently enter the FA β-oxidation spiral (Lopaschuk *et al*., 1994). Acetyl-CoA, NADH and $FADH_2$ are

produced after each FA oxidation cycle and reducing equivalents are employed by the mitochondrial ETC for ATP generation.

The inner mitochondrial membrane is impermeable to long-chain acyl-CoA and it is therefore transferred from the cytosol into the matrix by the carnitine-dependent transport system (Kerner and Hoppel, 2000; Lopaschuk *et al*., 1994). The formation of long-chain acylcarnitine from long-chain acyl-CoA is catalyzed by CPT-I between the inner and outer mitochondrial membrane. CPT-I is the predominant in the regulation of mitochondrial FA uptake (Kerner and Hoppel, 2000; Lopaschuk *et al*., 1994). The long-chain acylcarnitine is subsequently transported across the inner mitochondrial membrane by carnitine acyltranslocase. Various factors influence the regulation of FA oxidation and here especially malonyl-CoA and the glucose-FA cycle play key roles. Malonyl-CoA is a potent inhibitor of CPT-I and hence mitochondrial FA uptake and oxidation (McGarry *et al*., 1978, 1977; Paulson *et al*., 1984). Here malonyl-CoA decarboxylase (MCD) and acetyl-CoA carboxylase (ACC) primarily regulate malonyl-CoA levels as MCD converts malonyl-CoA to acetyl-CoA while ACC catalyzes the reverse reaction. MCD inhibition would thus potentially reduce CPT-I activity and in parallel attenuate FA oxidation while ACC inhibition would release the brake on CPT-I activity and increase FA oxidation (Dyck, 2004; Kolwicz *et al*., 2012; Ussher *et al*., 2012). Carnitine acyl translocase (CAT) transports acylcarnitine across the mitochondrial intermembrane and this leads to free carnitine. Fatty acyl-CoA is restored by carnitine palmitoyl transferase-II (CPT-II) which is then transported back into the intermembrane space by CAT (Kerner and Hoppel, 2000; Lopaschuk *et al*., 1994; Schulz, 1994). Once fatty acyl-CoA enters the mitochondrial lumen it undergoes FA β-oxidation.

The metabolism of long-chain CoA inside the mitochondrial matrix involves the metabolism of acyl-CoA by a) acyl-CoA dehydrogenase, b) enoyl-CoA hydratase, c) L-3-hydroxyacyl-CoA dehydrogenase and d) 3-ketoacyl-CoA thiolase (3-KAT) (Schulz, 2008). These enzymes exist in different isoforms with varying chain lengths and shortens each fatty-acyl by two carbons and in the process generating acetyl-CoA, $FADH_2$ and NADH. Each enzyme has a feedback inhibition mechanism e.g. by NADH and $FADH_2$. For example, the feedback inhibition of 3-KAT can occur as a result of the accumulation of acetyl-CoA. This is vital in the event of low metabolic demand where decreased ETC and citric acid cycle activity leads to the accumulation of acetyl-CoA, $FADH_2$ and NADH and subsequent inhibition of FA β-oxidation enzymes (Fillmore and Lopaschuk, 2011). Therefore flux through FA β-oxidation is dependent on both myocardial demand and the availability of fuel substrates (Lopaschuk *et al*., 2007).

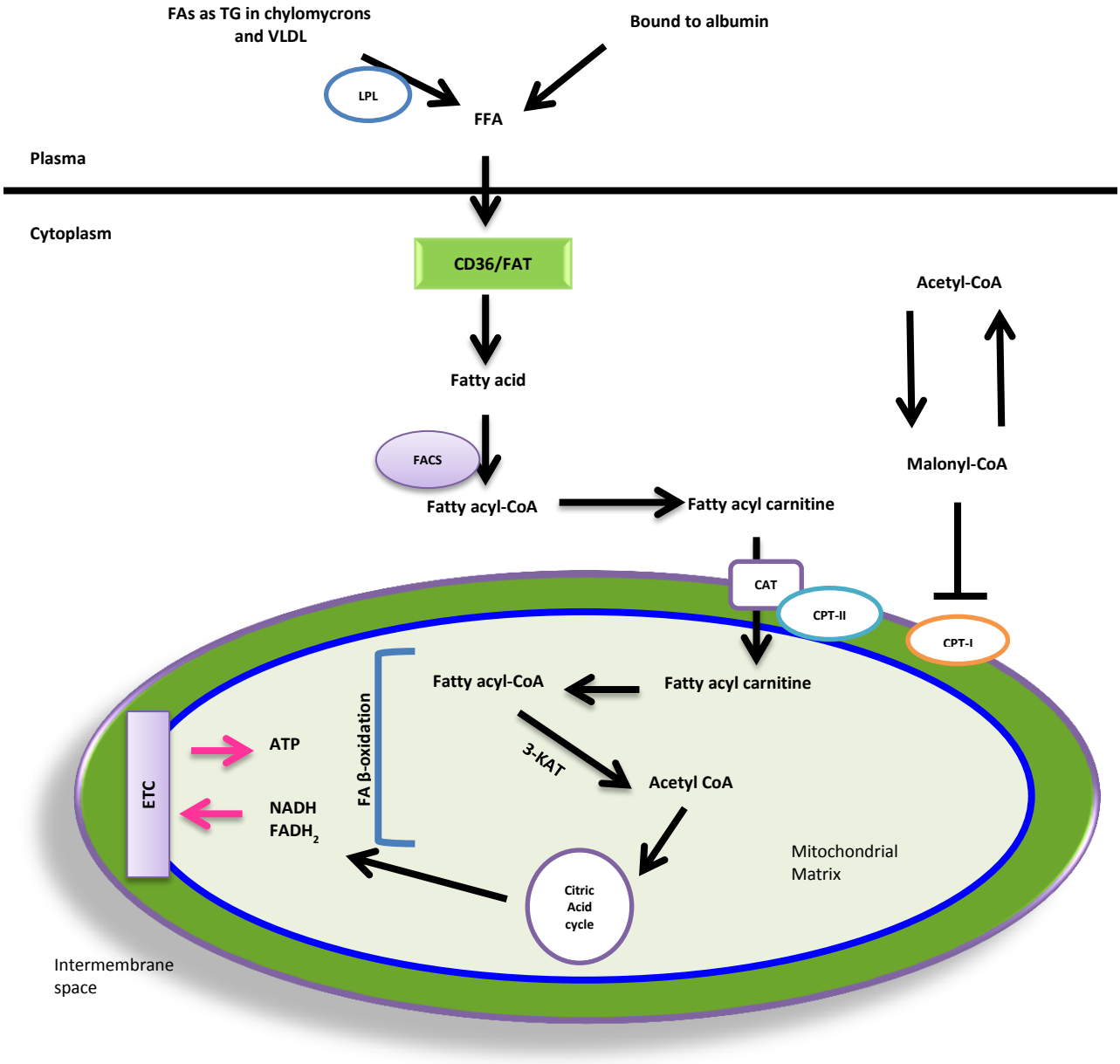

Figure 2.3. Fatty acid metabolism: FAs enter the cell by transporter proteins that are converted to fatty acyl-CoA in the cytosol. CPT-I facilitates transport into the mitochondrion which is inhibited by malonyl-CoA, while CAT removes carnitine groups. Fatty acyl-Co-A is then utilized in the mitochondrial matrix for FA β-oxidation. ACC: acetyl-CoA carboxylase; CAT: carnitine acyltransferase; CPT-I: carnitine palmitoyl transferase; CoA: co-enzyme A; FAs: fatty acids; FACS: fatty acyl-CoA synthase; $FADH_2$: Flavin adenine dinucleotide reduced; AT/CD36: fatty acid translocase; FABPm: fatty acid binding protein; LPL: lipoprotein lipase; MCD: malonyl-CoA decarboxylase; NADH: nicotinamide adenine dinucleotide reduced.

2.5 Mitochondrial energetics

Mitochondria are often referred to as the "powerhouse" of the cell as they are the major sites of ATP production. They have tightly regulated and active pathways that facilitate the conversion of fuel substrates into electrons and finally into ATP. Mitochondria possess its own genome that provides regulatory proteins and enzymes required to operate efficiently. The myocardium is enriched with mitochondria in order to maintain ATP levels and they typically occupy approximately 25 – 35% of the total myocardial volume (Dobson and Himmelreich, 2002). Mitochondria are divided into two populations, i.e. intramyofibrillar and sarcolemmal (Palmer, 1977) and such sub-populations can be distinguished by differences in terms of cristae structure, respiration rates and the expression of distinct metabolic proteins (Palmer, 1977; Roden *et al*., 1996). However, both populations contribute towards optimal cardiac functioning by ATP generation and maintenance of ionic balance (Ishiki and Klip, 2005).

2.6 The citric acid cycle

The citric acid cycle also known as the Krebs or tricarboxylic acid cycle is a primary point of myocardial metabolism (Owen *et al*., 2002). Acetyl-CoA - originating from the oxidation of carbohydrates, FAs and proteins - fuels the citric acid cycle (Gibala *et al*., 2000; Neely *et al*., 1972). This is a crucial process as depletion of the citric acid cycle within the myocardium leads to a decline in contractile function. However, this can be reversed by the addition of anaplerotic substrates such as malate, 2-oxoglutarate, succinyl-CoA, oxaloacetate and fumarate (Gibala *et al*., 2000; Russell and Taegtmeyer, 1991; Taegtmeyer *et al*., 1980). The citric acid cycle enzymes

are located within the mitochondrial matrix, with succinate dehydrogenase found within the inner mitochondrial membrane (Humphries and Szweda, 1998; Kerner and Hoppel, 2000). This cycle also generates reducing equivalents for ATP generation, e.g. α-ketoglutarate catalyzes the conversion of α-ketoglutarate to succinyl-CoA and produces NADH and CO_2 (Cooney *et al*., 1981, Humphries & Szwelda, 1998; Moreno-Sanchez *et al*., 1990). Reducing equivalents generated by the citric acid cycle can then feed into the mitochondrial ETC for ATP generation (Gibala *et al*., 2000).

2.7 The electron transport chain and oxidative phosphorylation

The ETC is composed of five enzymes complexes (I – IV) and V (ATPase synthase) situated within the inner mitochondrial membrane. The adenosine nucleotide translocase functions by transporting ATP to the cytoplasm in exchange for ADP; this collectively referred to as the oxidative phosphorylation system (Casademont and Miro, 2002). Electrons enter the ETC through NADH:ubiquinone oxidoreductase (complex I), a large complex that consists of approximately 45 subunits (Carroll, 2005, 2002; Cecchini, 2003). Complex I functions by transferring electrons from NADH to ubiquinol through various redox centers such as flavin mononucleotide moiety and clusters of seven to nine iron-sulfur and up to three ubisemiquinone species (Friedrich & Scheide, 2000; Koopman *et al*., 2005; Ohnishi, 1998; Yano *et al*., 2000). Energy is preserved in this complex where four protons are transported across the mitochondrial inner membrane coupled to electron transfer; therefore conserving energy. Moreover, complex I contributes towards the proton-motive force and in turn supports ATP synthesis while maintaining the NAD^+/NADH ratio within the mitochondrial matrix and providing ubiquinol to

complex III (Hirst, 2005). A phospholipid cardiolipin may also play a crucial role in the optimal functioning of complex I in the ETC (Dröse *et al*., 2002; Fry and Green, 1981; Paradies *et al*., 2001; Ragan, 1978), although this exact mechanism has not been elucidated thus far.

Complex II, also known as succinate dehydrogenase or succinate:ubiquinone oxidreductase plays a crucial role by coupling the oxidation of succinate to fumarate and subsequently reducing ubiquinone (Cecchini, 2003; Yankovskaya *et al*., 2003). Complex III (cytochrome bc1 complex) oxidizes the ubiquinol generated by complexes I and II and here electrons are transferred from ubiquinol to cytochrome c rendering the proton motive Q cycle (Cecchini, 2003). Complex I and II transfer electrons through cytochrome c to the Q cycle through to complex IV (di Rago *et al*., 1990).

An energy carrier between complexes II and IV is known as cytochrome c (Gupte and Hackenbrock, 1988). Complex IV (also known as cytochrome oxidase) generates a proton gradient that reduces oxygen to water (Belevich *et al*., 2006; Cecchini, 2003; Gupte and Hackenbrock, 1988; Ludwig *et al*., 2001; Yoshikawa, 2003; Yoshikawa *et al*., 2006). Complex V (also known as ATPase or F1F0) is the final step in the mitochondrial ETC and here ATP is produced by pumping protons by the electromagnetic gradient (Cecchini, 2003).

2.8 The Randle cycle: The link between glucose and fatty acid metabolism

The process whereby FAs and glucose regulate each other is referred to as the ‘’Randle cycle’’ (Koonen *et al*., 2005) and was first described by Randle and colleagues during the 1960s

(Garland *et al*., 1963; Randle *et al*., 1964). The preferential utilization of fuel substrates (glucose versus FAs) is regulated by interlinked mechanisms and here the regulation of PDH plays an important role. The rate-limiting step of pyruvate decarboxylation is an irreversible step catalyzed by PDH (Patel and Korotchkina, 2006; Randle, 1986). PDH can be inhibited by phosphorylation on the E_1 subunit on the enzyme complex by PDK and be activated by de-phosphorylation via a PDH phosphatase. However, higher FA β-oxidation leads to increased acetyl-CoA/CoA and NADH/NAD^+ ratios that results in decreased myocardial PDH activity (Clarke, 1996; Higgins *et al*., 1981; Kruszynska *et al*., 1991; Lopaschuk *et al*., 1994; Stanley *et al*., 1997a). Here such byproducts activate PDK which results in the inhibition of PDH. Such changes are also proposed to lead to increased cytosolic citrate levels that in turn can inhibit PFK1 and PFK2 and lower glycolysis (Hue and Taegtmeyer, 2009).

As this chapter summarized the essentials of cardiac metabolism under physiological conditions, it provides a useful foundation to evaluate metabolic dysfunction within the context of cardiovascular complications.

3 CHAPTER 3

The burden of cardiovascular disease

3.1 Introduction

Cardiovascular complications are leading causes of death and disability in the industrialized world (Nichols *et al*., 2014). Currently cardiovascular diseases (CVD) account for 31% global mortality rate according to the World Health Organization (WHO) (http://www.who.int/mediacentre/factsheets/fs317/en/) and major risk factors such as obesity and diabetes further exacerbate this increasing burden of disease (Dimmeler, 2011). Diabetes is robustly associated with CVD and here mortality rate is two to four-fold higher in such individuals (Gu *et al*., 1998). Thus there is a tight inter-linkage between these two debilitating conditions and this will further increase in the next years. For example, projections indicate that by 2030 CVD will be the leading cause of mortality in Africa (Mensah, 2008), while the South African National Department of Health indicated that diabetes is a major risk factor for CVD development (Norman *et al*., 2007). Moreover, diabetic individuals who develop CVD suffer tremendously in comparison to non-diabetic persons with similar conditions (MacDonald *et al*., 2008). There are also other risk factors associated with CVD in sub-Saharan Africa (SSA) such as stroke and hypertension and here hypertension is predicted to be prevalent in approximately 30% of adults in SSA (Dalal *et al*., 2011). Such risk factors further fuel CVD development, e.g. the INTERHEART Africa study found that hypertension and diabetes were most common in black Africans suffering acute myocardial infarction (Steyn *et al*., 2005a).

3.2 Heart failure (HF)

Heart failure (HF) was described by Hippocrates as shortness of breath and peripheral edema (Katz and Katz, 1962) and also as a clinical syndrome that significantly contributes to the burden of CVD in SSA (Cowie *et al*., 1997). A more precise definition for HF is given by Katz as "a clinical syndrome in which heart disease reduces the cardiac output, increases venous pressures and is accompanied by molecular abnormalities that cause progressive deterioration in the failing heart and premature myocardial cell death" (Katz, 2000). Clinical representations of HF are characterized by pulmonary congestion, dyspnea and fatigue. There are two broad HF classifications, i.e. chronic and acute. The chronic state gradually occurs over time while "acute" refers to the more rapid deterioration of heart function. Systolic dysfunction is the most frequently occurring form of HF (Kingue *et al*., 2005) as most of the literature was published prior to the recognition of HF with preserved ejection fraction (Adewole *et al*., 1996).

The main causes of HF in the developing world are due to non-ischemic causes, i.e. hypertensive heart disease, valvular and myocardial damage from rheumatic fever and myocardial damage from infectious agents (Steyn *et al*., 2005b). HF tends to occur frequently at a younger age in SSA and this is possibly due to the significant contribution of rheumatic fever (Doust *et al*., 2005). In agreement, other studies (Damasceno *et al*., 2007; Kingue *et al*., 2005; Oyoo and Ogola, 1999; Sliwa and Mocumbi, 2010) suggested that the primary underlying causes of HF are different within the African context and thus include mediators such as endomyocardial fibrosis and tuberculous pericarditis. Additional risk factors include the so-called Westernized lifestyle that often leads to increased hypertension, obesity and diabetes especially in urban areas

(Mayosi *et al*., 2009). Such complexity within the SSA context may also be responsible for the variation of HF etiologies observed (Bloomfield *et al*., 2013) while sub-optimal healthcare systems and limited resources/research will also further fuel HF prevalence.

3.3 Acute heart failure (AHF)

The ESC describes AHF as "the rapid onset of, or change in, symptoms and signs of HF" (McMurray et al., 2012) resulting in the need for urgent therapy. AHF can be divided into two sub-types namely a new onset known as *de novo* AHF or the acute worsening of an existing, chronic HF condition (Metra *et al*., 2010). It is also a complex clinical syndrome and management of AHF is difficult as it does not have a universally accepted definition, nor is the pathophysiology properly understood. It also varies in it terms of underlying pathophysiology, clinical representations and treatments (Metra *et al*., 2010). AHF accounts for one of the main causes of hospitalization worldwide (McMurray *et al*., 2012). It is the most common diagnosis in individuals >65 years of age, with increased in-hospital mortality and an even higher post-discharge mortality, with an increased chance of re-admission (Metra *et al*., 2010).

Treatment strategies for chronic HF have resulted in improvements in symptoms (Lindenfeld *et al*., 2010; McMurray *et al*., 2012). Here treatment strategies include diuretics, oxygen and vasodilators but fail to reduce mortality rates (Lindenfeld *et al*., 2010; McMurray *et al*., 2012). These symptoms occur predominantly as a consequence of severe pulmonary congestion due to increased left ventricular filling pressure (with or without low cardiac output). CVD such as coronary artery disease, hypertension, atrial arrhythmias and other conditions (e.g. diabetes) are

often present and may contribute to the pathophysiology of AHF (Adams *et al*., 2005; Cleland *et al*., 2003; Fonarow *et al*., 2008). Despite treatments the morbidity and mortality rates for AHF patients are increasing with a 30% chance of re-hospitalization and a 90 day post-discharge mortality rate (Gheorghiade *et al*., 2005). There has been relatively limited research undertaken on AHF in SSA although The Sub-Saharan Africa Survey of Heart Failure (THESUS-HF) trial (Figure 3.1) demonstrated that such patients displayed mean age of 52 years. Here approximately 46% were diagnosed with AHF as consequence of hypertension, while for rheumatic fever and ischemia the figures were 14.3 and 7.7%, respectively (Damasceno *et al*., 2012).

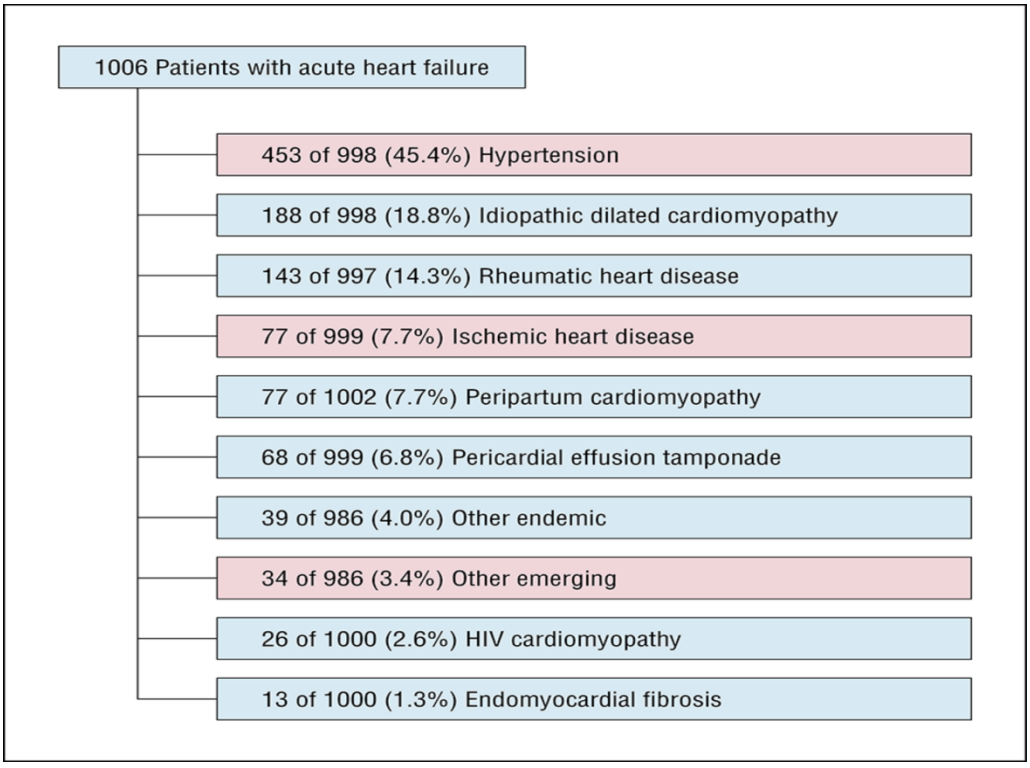

Figure 3.1 Causes of AHF in Africa in The sub-Saharan Africa Survey of Heart Failure (THESUS-HF).

3.4 AHF etiology

AHF can occur with/without previous history of cardiac disease and may be related to systolic or diastolic dysfunction, cardiac rhythm or the incongruity between pre- and afterload (Nieminen, 2005). Moreover, it is the most common primary diagnosis in patients hospitalized with heart disease in Africa (Damasceno *et al*., 2012; Sliwa and Mayosi, 2013). For hospitalized patients with *de novo* AHF, they usually present with acute pulmonary edema and cardiogenic shock together with hypertension and coronary syndrome (Nieminen *et al*., 2006). Underlying causes may also be of ischemic or non-ischemic origin (Drexler *et al*., 2012). Regardless of the cause, AHF patients present with systemic and pulmonary congestion as a consequence of left ventricular filling with/without reduced cardiac output (Gheorghiade *et al*., 2005). Numerous cardiovascular conditions such as coronary heart disease, hypertension, valvular heart disease and non-cardiac related conditions such as renal failure contribute towards the pathophysiology of AHF (Adams *et al*., 2005; Cleland *et al*., 2003; Fonarow *et al*., 2008).

The etiology of HF can be divided into two subtypes, i.e. individuals with CVD history (e.g. myocardial ischemia, coronary artery disease) and patients without such a history (Katz, 2000). The early stages of HF are usually asymptomatic due to compensatory mechanisms that include the renin-angiotension system, sympathetic nervous system and the progression of myocardial hypertrophy. Such mechanisms also play a role in HF onset by advancing ventricular remodeling (Casademont and Miro, 2002; Goldenthal and Marín-García, 2002; Henry *et al*., 1981; Kelly and Strauss, 1994). Due to the diverse etiology of HF various pharmacotherapies are utilized for treatment, especially in individuals with complicated disorders like diabetes, insulin resistance

and obesity. HF with an ischemic origin progresses slowly post-myocardial infarction and subsequently affects ventricles with alterations in both infarct and non-infarct regions of the myocardium. Thus it is clear that AHF is a complex syndrome that is difficult to treat and hence requires the development of novel and effective therapies.

3.5 Experimental models of AHF

AHF is linked to a relatively high in-hospital mortality rate, especially in patients which have reduced systolic blood pressure. As summarized in the prelude in chapter 1 of this review, it is pivotal to find novel therapeutic strategies to counteract this effect.

Our model of *de novo* AHF has been modified from an existing *ex vivo* model of *de novo* AHF setup by Deshpande *et al*. (Deshpande *et al*., 2010; Opie and Deshpande, 2016; Opie *et al*., 2010). Their AHF model consisted of 3 phases i.e. 30' Stabilization, 35' AHF and 30' Recovery. The model is a representation of cardiogenic shock where its perfusion pressure governs the external mechanical work in the rat heart which is suddenly decreased. This is similarly observed when contractility is reduced in the myocardium and hypotension occurs. This model also employs hypotension accompanied by a decreased heart rate and alterations in concentration of substrates (calcium, fatty acids and glucose) (Deshpande *et al*., 2010; Opie and Deshpande, 2016; Opie *et al*., 2010). It has similarities and differences to AHF within the clinical setting that is typically accompanied by relatively low blood pressure (also evident in patients with Takotsubo cardiomyopathy) (Wittstein, 2012; Wittstein *et al*., 2005) and possibly accompanied by a reduced systolic pressure that ranges between 50 – 104 mmHg (Gheorghiade *et al*., 2006).

In Deshpande's *de novo* AHF model they focused on increased adrenaline levels during the AHF phase and also by altering calcium, glucose and fatty acid levels (Opie *et al*., 2010). Of note, catecholamines are increased in response to high adrenaline levels and in turn leads to the upregulation of FA oxidation. This model of AHF was in fact a modified version of a Langendorff underperfused ischemic model that was originally established by Bricknell and Opie (Bricknell and Opie, 1978). The original model utilized the same perfusion pressures as found in Deshpande's work. What about ischemia in this instance? Ischemia is defined as the reduction in arterial blood flow (Jennings, 1970). However, in isolated ischemic rat hearts perfused with oxygenated nutrients, it can be defined as when the flow of oxygenated nutrients is either reduced or completely cut off from the isolated heart (Sakai *et al*., 2016). The latter is one of the key factors that distinguishes Deshpande's AHF model to a classical ischemic isolated heart model.

In our AHF model we solely concentrated on the metabolic effects (supra-physiological fatty acids and reduced glucose) during AHF whereas Deshpande *et al*. (2010) focused more on specific molecular alternations.

3.6 Metabolic alterations in the failing heart

Research focusing on the expression of metabolism during HF predominantly concentrated on the end-stage of this condition. For example, under such circumstances there is a down-regulation of FA oxidation enzymes and this correlates with a switch towards increased glucose oxidation (Stanley *et al*., 2005). In agreement, analysis of hearts from transplant recipients

showed a marked decrease in the activity of FA β-oxidation enzymes versus donor hearts (Sack and Kelly, 1998). Further, these hearts displayed attenuated long-chain acyl-CoA dehydrogenase (LCAD) and medium-chain acyl-CoA dehydrogenase (MCAD) gene expression, with no changes in MCAD protein expression (Karbowska *et al*., 2003). However, others found contrarian results with HF where higher FA β-oxidation and lower glucose oxidation (Murray *et al*., 2012; Opie, 2004). This probably depends on the stage of HF and the higher FA utilization likely occurs during the earlier stages of HF progression. Here Opie (Opie, 2004) described a ‘’metabolic vicious cycle’’ where the lower cardiac output found with HF results in a compensatory hyperadrenergic state that hyperphosphorylates the sarcoplasmic reticulum to lower cardiac output. In parallel, supraphysiological, circulating FFA concentrations are taken up by the cardiomyocyte and metabolized by heart mitochondria. However, this can lead to uncoupling of mitochondrial respiration and result in an energy-depleted state thereby causing further contractile dysfunction in the failing heart. For example, Murray *et al*. (Murray, Anderson, Watson, Radda & Clarke, 2004; http://dx.doi.org/10.1016/S0140-6736(04)17402-3) showed that supraphysiological plasma FFA concentrations with HF manifest in parallel with decreased and increased levels of GLUT4 and uncoupling proteins (UCPs), respectively. Moreover, increased mitochondrial reactive oxygen species (ROS) (due to higher FA oxidation) can also activate UCPs and thereby promoting uncoupling, dissipation of membrane potential and eventually decreased mitochondrial ATP production (Figure 3.3) (Essop and Opie, 2004).

Increased FA oxidation can also lead to PDH inhibition as discussed and thereby further exacerbate cardiac metabolic function (Figure 3.2) (Opie, 2004). Moreover, the FA-mediated

decrease in glycolysis leads to lower ATP availability for the sodium pump (Cross *et al*., 1996) that will fuel cardiac dysfunction.

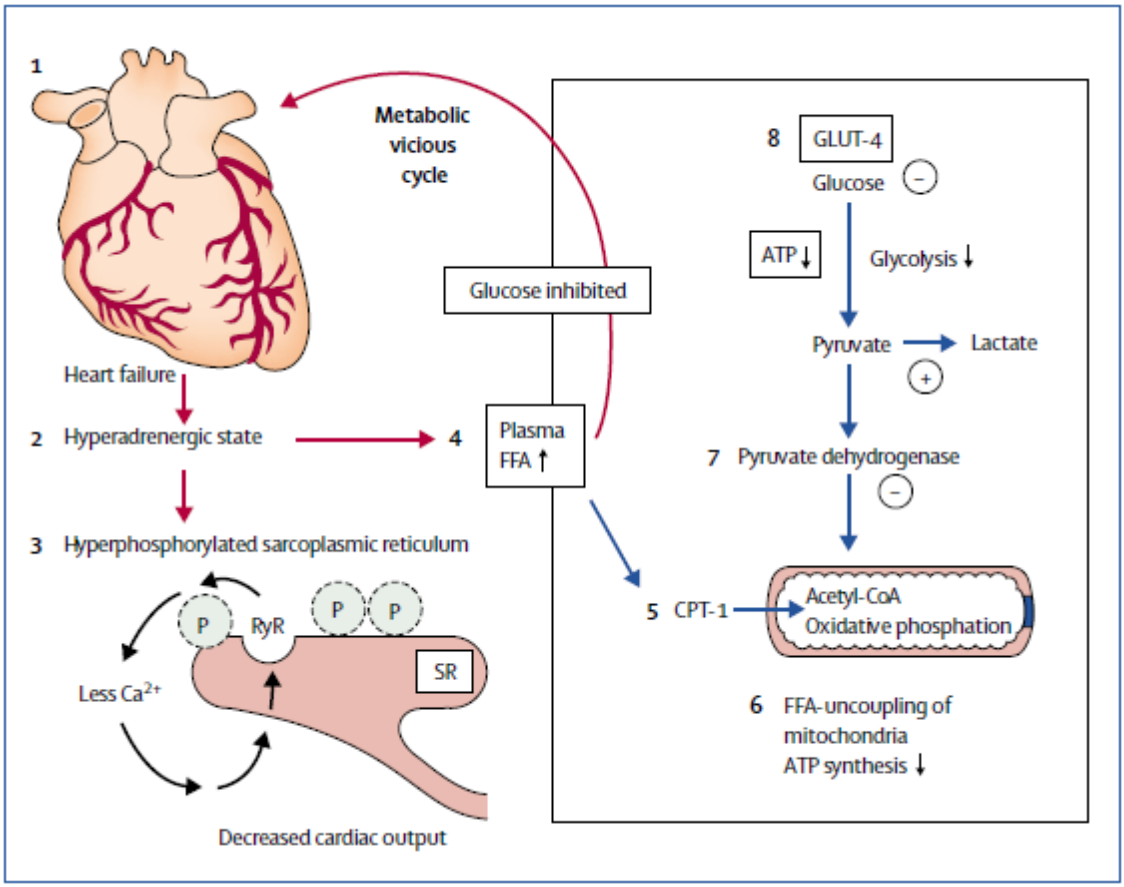

Figure 3.2. Metabolic dysfunction with heart failure. Free fatty acids (FFA), ryanodine receptor (RyR), sarcoplasmic reticulum (SR) (reproduced from Opie, 2004).

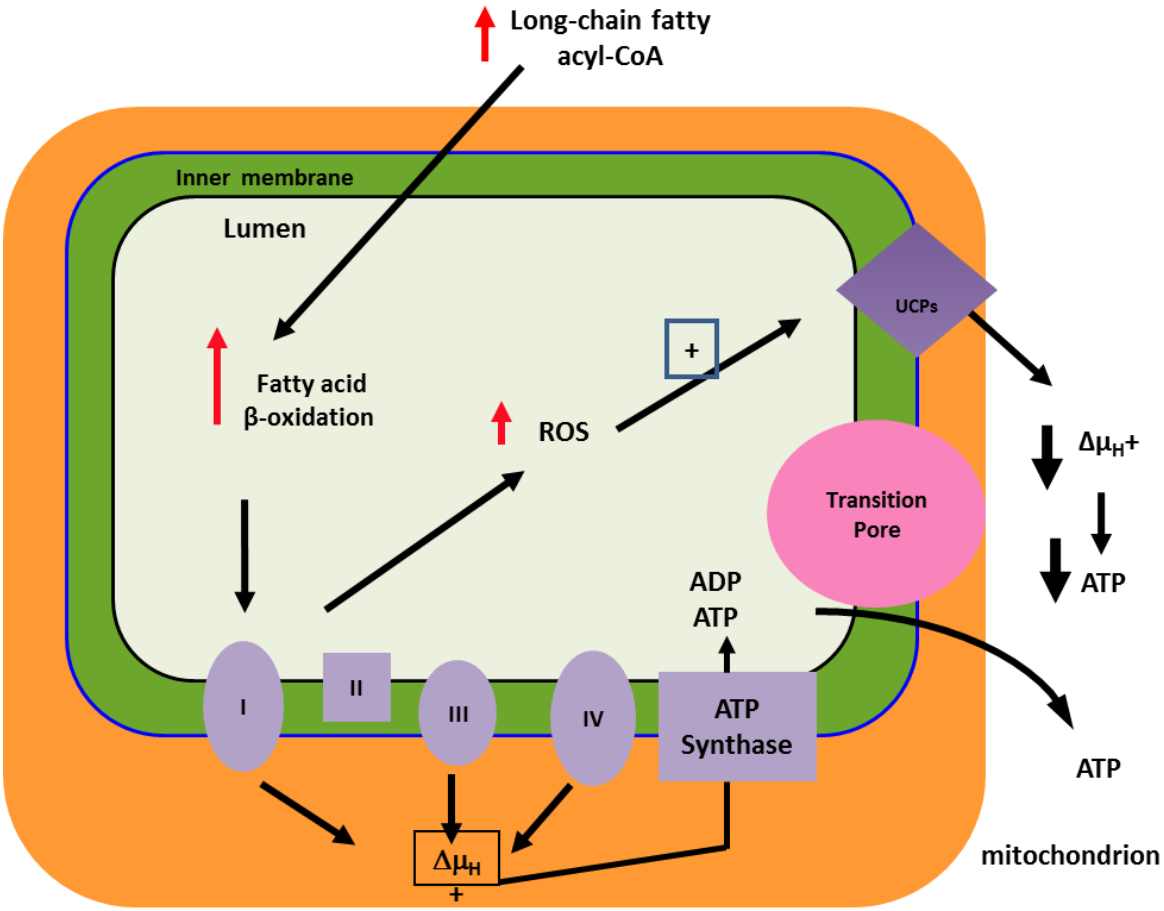

Figure 3.3. Mitochondrial dysfunction in the failing heart **(reproduced from Essop and Opie, 2004).**

This vicious metabolic cycle offers an argument favorable to a metabolic approach for the treatment of HF (Opie, 2004), i.e. by decreasing FA metabolism and/or enhancing glucose metabolism. Here approaches that can be employed include the anabolic hormone insulin that can interrupt this cycle by promoting glycolysis, enhance glycolytic ATP generation and also inhibit hormone-sensitive lipase to lower FFA release from adipose tissue (Randle *et al*., 1963). By contrast, the anti-anginal drug TMZ also offers cardioprotection as it acts as a FA utilization inhibitor.

4 CHAPTER 4

Exploring links between diabetes and heart failure – metabolic focus

4.1 Diabetes mellitus and hyperglycemia

Diabetes is defined as a metabolic disorder characterized by chronic hyperglycemia accompanied with disturbances in carbohydrate, fat and protein metabolism as a result of impairment in the regulation of either insulin secretion, action or both (Alberti and Zimmet, 1998). Type 1 diabetes (insulin-dependent) is an autoimmune disease that occurs as a result of the selective destruction of β-pancreatic cells that subsequently leads to loss of insulin secretion. Type 2 diabetes (insulin resistance) is associated with diminished insulin function. Although diabetes types display different etiologies, they result in similar complications such as oxidative stress, organ failure and CVD complications (Alberti and Zimmet, 1998; Liu *et al*., 2013; Roglic *et al*., 2005). For example, diabetic individuals exhibit an increased risk for developing cardiovascular complications and the latter is one of the leading causes of diabetic-related morbidity and mortality (Kengne *et al*., 2010). Here the mortality rate is two to four-fold higher in individuals with diabetes (Gu *et al*., 1998) and it is also a known risk factor for HF onset. For example, the Framingham study demonstrated that HF incidence was 2x and 5x higher in diabetic men and women, respectively, compared to control subjects (Kannel and McGee, 1979).

The diabetic heart is associated with diastolic and systolic dysfunction, left ventricular hypertrophy and enhanced myocardial fibrosis (Marwick, 2008). Several risk factors are involved in the pathogenesis of diabetic complications, e.g. glycemic control, hypertension, dyslipidemia, diet and smoking (Chiarelli and Marcovecchio, 2013). Here hyperglycemia is a vital factor contributing to vascular complications and studies found damaging effects can occur in response to both acute and chronic hyperglycemia (Chiarelli and Marcovecchio, 2013). The role of hyperglycemia has been shown to be directly associated with vascular complications by studies such as the Diabetes Control and Complications Trial (DCCT) and UK Prospective Diabetes Study (UKPDS) (Blumenkranz, 1993).

The diabetic heart is characterized by significant disruptions of metabolic pathways and molecular mechanisms needed for physiological cardiac function, e.g. impairment of calcium signaling that leads to changes in cardiac contraction and relaxation (Golfman *et al*., 1996). In addition, increased oxidative stress can activate a plethora of signaling cascades that can result in impaired cardiac function, e.g. NF-κB and c-Jun N-terminal kinases by oxidative modifications of certain residues (Bayeva *et al*., 2013). The accumulation of misfolded proteins and endoplasmic reticulum stress can also contribute and lead to pathophysiologic outcomes such as cardiac apoptosis (Xu *et al*., 2013). On the metabolic front, diabetic individuals typically display reduced myocardial glucose uptake and increased FA utilization (Ungar *et al*., 2015), with the latter fuel known to be detrimental to the myocardium when available in excess (Opie, 1970). For example, the diabetic cardiomyopathy is associated with increased reliance on FAs as an energy source for the myocardium (Bayeva *et al*., 2013) that can result in the loss of metabolic flexibility (Sharma *et al*., 2004). Moreover, patients burdened with both type 2 diabetes and HF

displayed a significant accumulation of lipids within the myocardium together with a perturbed profile of lipid metabolic genes (Sharma *et al*., 2004).

4.2 Oxidative stress in diabetes and heart failure

Oxidative stress can be defined as the imbalance between the generation of ROS/reactive nitrogen species (RNS) and intracellular antioxidant capacity (Wang *et al*., 1998). With diabetes the sources of oxidative stress include for e.g. auto-oxidation of glucose, shifts in redox balance and attenuated activation of antioxidants such as reduced glutathione (GSH), vitamin E_1 and antioxidant defense enzymes such as superoxide dismutase (SOD) (Brownlee and Cerami, 1981). Moreover, the mitochondrial ETC is an important source of ROS (Chance *et al*., 1979), while NADPH oxidase and uncoupled nitric oxide also make significant contributions to diabetes-related oxidative stress (Tsutsui *et al*., 2011).

4.2.1 The non-oxidative glucose pathways (NOGPs)

The mechanisms of hyperglycemia-mediated tissue damage are complex but a well-known hypothesis posits that ROS plays a central role in this process by activation of downstream, damaging metabolic circuits (Brownlee and Cerami, 1981; Nishikawa *et al*., 2000a, 2000b). Here the concept emerges that hyperglycemia leads to mitochondrial superoxide production and excess superoxide. This in turn results in DNA damage and the activation of poly (ADP ribose) polymerase (PARP) that initiates ribosylation and inhibition of GAPDH. As a result of this blockage, upstream glycolytic metabolites are diverted into non-oxidative glucose pathways

(NOGPs) with damaging outcomes (Brownlee, 2005). It is proposed that there is interplay between NOGPs and that contribute to detrimental effects to the myocardium such as oxidative stress, ROS and cellular dysfunction that are further fueled by hyperglycemia-induced NOGP activation (Mapanga and Essop, 2015). These pathways include the polyol pathway, advanced glycation end products (AGEs), the hexosamine biosynthetic pathway and the activation of PKC. The polyol pathway and AGEs will now be briefly introduced as this was part of the focus of this thesis.

4.2.2 Polyol pathway

Under physiological conditions in mammalian cells, glucose is phosphorylated by hexokinase to G-6-P and enters the glycolytic pathway, while a relatively small proportion enters the polyol pathway (Morrison *et al.*, 1970). However, with hyperglycemia flux through the polyol pathway accounts for a much higher proportion of glucose metabolism (Cheng and González, 1986). The rate-limiting step in the pathway is the reduction of glucose to sorbitol by the enzyme aldose reductase (AR) at the expense of nicotinamide adenine dinucleotide phosphate (NADPH) (Yabe-Nishimura, 1998). Thus higher activation of this pathway will deplete NADPH (Lee and Chung, 1999). Sorbitol is subsequently converted to fructose by enzyme sorbitol dehydrogenase (SDH) with NAD^+ utilized as a co-factor (Figure 4.1). As NADPH is a critical co-factor in the regeneration of the intracellular antioxidant reduced glutathione (GSH), lower availability will contribute to an increase in oxidative stress (Brownlee, 2005). Thus hyperglycemia-induction of the polyol pathway can increase oxidative stress and thus contribute to downstream effects that will impact on cardiac function (Mapanga and Essop, 2015).

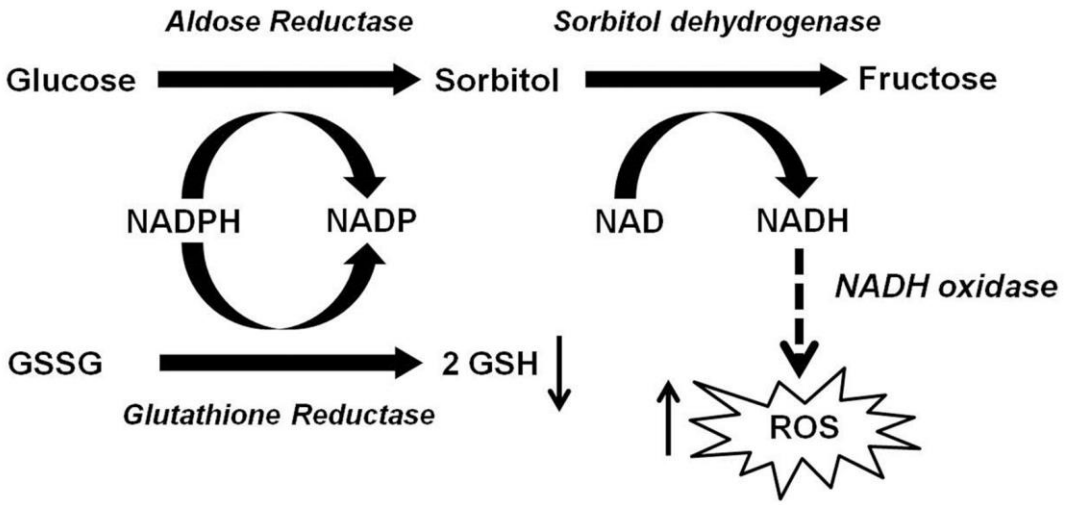

Figure 4.1. The role of the polyol pathway in triggering hyperglycemia-induced oxidative stress (reproduced from Tang *et al*., 2012).

4.2.3 AGEs

AGEs are formed during a Maillard reaction which involves the non-enzymatic reaction between sugar residues with a protein amino group to form a Schiff-base (Figure 4.2). This is a rapid reaction and can be reversed depending on the concentration of substrate. The Schiff-base is subsequently converted into a more stable Amadori product (examples of this reaction include glycosylated hemoglobin [HbA1c]). This can be further metabolized to lead to stable and irreversible AGE compounds (Miyata *et al*., 2001a). Hyperglycemia may directly increase AGE precursors as a result of the accumulation of G-3-P in the glycolytic pathway which is then diverted to form the AGE precursor, methylglyoxal.

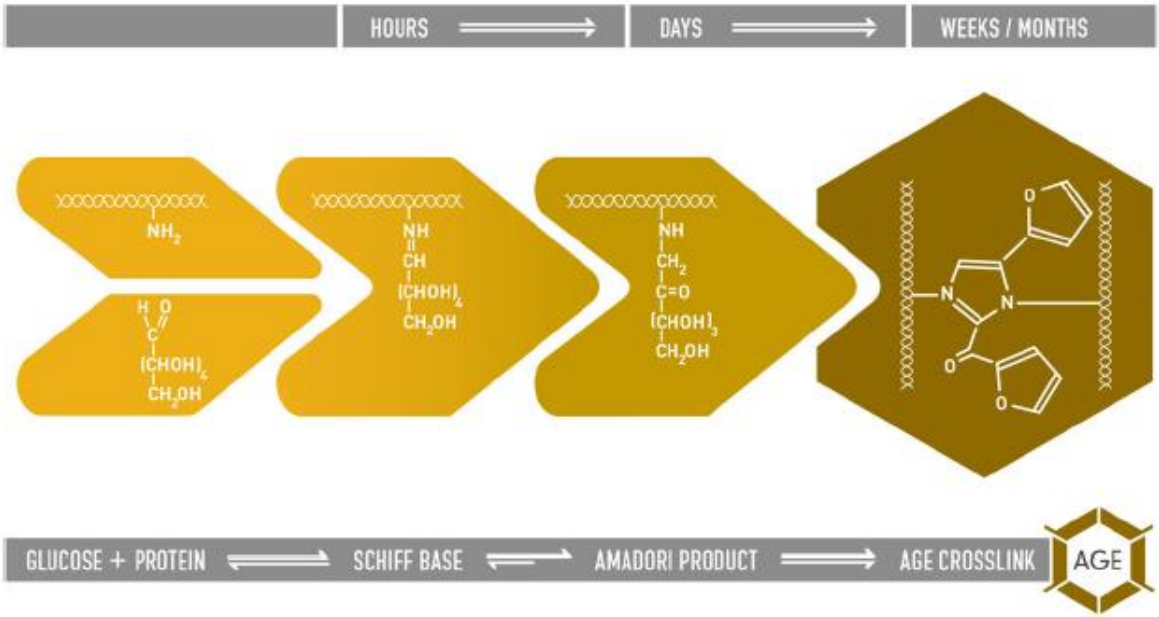

Figure 4.2. The formation of AGEs **(reproduced from Hartog *et al*., 2007).**

AGEs accumulate with aging and such accrual is also accelerated in diabetic individuals associated with detrimental effects (Meerwaldt *et al*., 2007; Monnier *et al*., 1999). In addition, accelerated dietary intake of AGEs may contribute to pathophysiologic outcomes (Brownlee, 2001) and thus its effects may not only be limited to diabetic individuals. For example, some found an association between non-diabetics and AGEs together with the development and progression of HF (Hartog *et al*., 2007). However, with diabetes the AGEs are also implicated in the progression of HF by two key pathways, i.e. 1) affecting physiological components of proteins in the extracellular matrix via cross-links and 2) resulting in vascular and cardiac changes through its interaction with AGE receptors thereby causing diastolic and systolic perturbations (Hartog *et al*., 2007). Another pivotal precursor of AGEs is known as fructosamine (Popova *et al*., 2010). Of note, the human body is also exposed to exogenous AGEs that are present in various foodstuffs (Cai *et al*., 2012). Therefore, the mechanism of deglycation is an important factor in the deceleration of the progression of vascular damage, i.e. there are two enzymatic protective systems known as fructosamine 3-kinase (FN3K) and the glyoxalase

system involved in decreasing the production of AGEs. An increased expression of FN3K was observed in tissues prone to glycation, e.g. heart, nerves and kidneys (Mohas *et al*., 2010). Fructosamine can be phosphorylated by FN3K which leads to the production of the more unstable fructosamine-3-phosphate (Delpierre and Van Schaftingen, 2003). The latter can in turn form 3-deoxyglucoasone and phosphate that leads to deglycation of proteins (Delpierre and Van Schaftingen, 2003). 3-deoxyglucosone is also a potent precursor for AGE formation (Kusunoki *et al*., 2003). Fructosamines are formed as a result of condensation between glucose and primary amines, after which an Amadori product is, produced. The glycation of proteins in diabetes is of particular importance for two reasons, i.e. a) the reaction rate is low and directly proportionally to glucose concentration (Day *et al*., 1979; Higgins and Bunn, 1981), and b) levels of glycated hemoglobin and serum fructosamines are used to measure blood glucose levels over relatively longer time periods. Therefore the latter is commonly utilized to assess the efficacy of treatment of diabetic individuals (Armbruster, 1987; Goldstein *et al*., 1986; Johnson *et al*., 1983). Fructosamines and AGEs are also involved in the development of diabetic complications (Cohen *et al*., 1996).

Glyoxylase-1 (GLO-1) is an enzyme that catalyzes acyclic alphaoxoaldehydes to derivatives of hydroxyacylglutathione. This results in the inhibition of glycation of methylglyoxal, glyoxal and other alphaoxoaldehydes. Oxidative stress and ageing result in an attenuation in GLO-1 levels that in turn can lead to an increase in glycation and tissue damage. A deficiency in GLO-1 is also linked to abnormal AGE levels in hemodialysis patients (Miyata *et al*., 2001b). Moreover, GLO-1 knockdown mimics diabetic nephropathy in non-diabetic mice (Giacco *et al*., 2014). It has been recognized that glyoxalase requires glutathione as a cofactor - however glutathione has

no effect on glycolysis (Jowett and Quastel, 1933). The GLO system produces D-lactate that is converted to pyruvate by D-lactate dehydrogenase. Methylglyoxal and the GLO pathway remain one of the most mysterious challenges in modern biochemistry. Methylglyoxal is toxic and the GLO pathway therefore serves as a protective mechanism that comprises GLO-1 (lactoylglutathione methylglyoxallyase) and GLO-2 (hydroxyacylglutathione hydrolase) that are responsible for the formation of D-lactate from the hemithioacetal formed from methylglyoxal and glutathione (Thornalley, 1990).

The diabetic heart's signature is thus characterized by damaging effects mediated by FAs (e.g. uncoupling of mitochondrial respiration) and also hyperglycemia-mediated effects by pathways such as AGEs. Although the diabetic heart takes up lower amounts of glucose, the AGE pathway can still be activated by oxidative stress and by poor nutritional intake (e.g. enriched with AGEs). These pathways are all relevant within the context of HF and thus provide unique targets to test as therapeutic agents – the focus of this thesis. However, we will first provide some insights regarding existing treatment options for HF and thereafter shift the focus to metabolic modulators such as TMZ.

5 CHAPTER 5

5.1 Current treatments for AHF

AHF is a major global burden on public health and research. Current therapeutic strategies are - unlike for chronic HF - mainly based on clinical practice instead of evidence generated from randomized clinical trials (Murray *et al*., 2012). Here primary goals involve the stabilization of hemodynamics and symptomatic relief (Nieminen, 2005), e.g. stabilizing the patient by improving signs and symptoms, correcting volume overload, increasing hemodynamic status and counteracting neurohormonal hyperactivation (Nieminen, 2005).

AHF treatment remains a challenge due to heterogeneity in terms of its presentation and it is therefore unlikely that a single treatment modality will be employed for all patients (Onay-Besikci and Ozkan, 2008). Current treatment modalities include oxygen, diuretics, vasodilators and positive inotropic agents - all with clinical limitations (Nieminen, 2005). For example, oxygen is employed to treat hypoxemia (SpO_2<90%) but is associated with increased risk of short term mortality and it should not be used routinely as it can lead to vasoconstriction and decreased cardiac output (Park *et al*., 2010). Non-invasive ventilations are also frequently employed by AHF treatment sites, while invasive ventilation procedures are used in very few cases.

Diuretics (e.g. furosemide) are well established as a cornerstone of therapeutic strategies in this instance and result in prompt symptomatic relief. The reliance on diuretics can be understood as

the majority of AHF patients present with volume overload and thus this therapeutic strategy provides rapid relief of symptoms such as breathlessness. However, some studies demonstrated that the use of diuretics can lead to increased mortality (Cooper *et al*., 1999; Philbin *et al*., 1997) and activation of the neurohormonal response that can in turn trigger cardiac arrhythmias. In addition, diuretics may be detrimental to AHF patients who suffer from with acute renal failure (Mehta *et al*., 2002). Vasodilators assist in improving hemodynamics but side-effects include tachyphylaxis and dose-related outcomes (Nieminen, 2005). For example, the Vasodilation in the Management of Acute Congestive heart failure (VMAC) study found that tachyphylaxis can start within 1 to 2 hours post-therapy (Cuffe *et al*., 2002). Positive inotropic agents such as dobutamine and milrinone are beneficial to increase cardiac index in patients with low output HF, but inotrope usage can also lead to a sub-optimal prognosis (Nieminen, 2005). Such drugs act by exerting a positive inotropic action by increasing cyclic adenosine monophosphate (cAMP) levels and calcium handling within the myocardium. However, there are insufficient studies addressing the safety and efficiency of such drugs employed in AHF management. For example, although several studies have focused on the efficacy of dobutamine these have had several limitations that include lack of properly controlled studies and relatively small sample sizes (Nieminen, 2005). Inotropic drugs are also associated with an increased proarrhythmic risk versus other AHF therapeutic agents, e.g. dobutamine can trigger increased ventricular tachycardia compared to nesiritide (Burger *et al*., 2015b). Moreover, there is mounting evidence that positive inotropic agent usage in AHF patients is associated with increased mortality (Burger *et al*., 2015a; Silver *et al*., 2002) and impacting on lengths of hospital stays (Burger *et al*., 2015b; Siostrzonek *et al*., 2000).

Thus to sum up it is clear that conventional treatments for HF are focused on modifying hemodynamic effects. Here many agents function by lowering myocardial oxygen consumption, increasing coronary blood supply or by improving ventricular relaxation by redistributing blood flow (Marzilli, 2003). However, the efficacy of hemodynamic therapeutic interventions is limiting due to the occurrence of a plateau effect in diminishing heart rate and contractility of the myocardium. This leads to a failure to control cardiovascular dysfunction and often such patients are referred for cardiac re-vascularization (Pepine *et al*., 1994). According to the ESC (McMurray *et al*., 2013) neurohormonal agents (β-blockers, ACE inhibitors and mineralcorticoids) are used to prevent the progression of systolic dysfunction in chronic HF. Diuretic agents are often used as combination treatment to relieve symptoms of congestion. Thus it is clear that the limitations of current therapies for AHF necessitate the development of novel therapeutic agents that will improve both the patient's prognosis and quality of life.

Metabolic agents are a new class of drugs that act by optimizing myocardial substrate metabolism and hence do not target hemodynamic parameters (Rosano *et al*., 2015). For example, Kantor *et al*. (Kantor *et al*., 2000) demonstrated TMZ elicited no significant effects on heart rate, systolic pressure, developed pressure and cardiac output. This study also demonstrated that TMZ had no significant effects on oxygen consumption (Kantor *et al*., 2000). Thus the hope remains that such agents should result in improved care of AHF patients and we predict this will include less side-effects as typically found with existing treatment modalities. As earlier discussed, the failing heart is associated with impaired energy metabolism (Rosano *et al*., 2015) that includes mitochondrial dysfunction (Van Bilsen *et al*., 2009) and damaging effects of increased FA utilization (Essop and Opie, 2004) (discussed in Chapter 3). Thus the lowering

FA utilization and the concomitant increase in glucose metabolism is a feasible paradigm to strive for when trying to improve cardiovascular complications in AHF patients (Piatti *et al*., 2015). As the focus of this study is on TMZ as a novel therapy for AHF, the next section will further provide background on this unique drug.

5.2 The ABCs of TMZ

Trimetazidine (1-[2,3,4-trimethozybenzyl] piperazine (TMZ) is a clinically efficient metabolic modulator and a well-tolerated anti-anginal drug (Figure 5.1). It has several cytoprotective effects that are beneficial to patients without changing myocardial oxygen consumption or blood supply (Chierchia and Fragasso, 1993). TMZ selectively inhibits the long chain isoform of 3-KAT, the final enzyme of the mitochondrial FA β-oxidation spiral. This results in partial inhibition of cardiac FA β-oxidation and the concomitant increase in glucose oxidation (thus reversing the Randle effect). Here TMZ treatment helps ‘’couple’’ glycolysis to glucose oxidation by increasing PDH activity due to an attenuation of the Randle cycle (Kantor *et al*., 2000). Finally, the lowering of such effects will also improve mitochondrial function by attenuating FA-mediated uncoupling and ATP depletion.

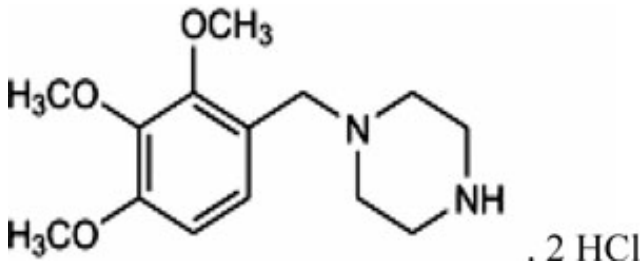

Figure 5.1. The chemical structure of TMZ (Onay-Besikci & Ozkan, 2008).

The two main forms of TMZ available on the market are the immediate release (IR) 20 mg tablet taken three times a day and the modified release (MR) 35 mg taken twice daily (Servier, Suresnes, France). The IR is designed to sustain plasma TMZ levels (Dézsi, 2015), while the 35 mg dosage allows the drug to maintain anti-anginal efficiency by providing 12 hours of cardioprotection (Sellier and Broustet, 2003). It can be administered as monotherapy or combination treatment with other anti-anginal agents and is rapidly absorbed by the intestinal tract, with the patients fast or fed state having no effect on its bioavailability (Ozbay *et al*., 2012). TMZ has a half-life of approximately 6 hours (Harpey *et al*., 1988) and is generally well-tolerated with few side-effects (mainly gastrointestinal disturbances, vomiting and nausea) (Massó *et al*., 2005).

Metabolic agents may be a more effective approach when used as monotherapy or in combination with standard therapies as they act by shifting cardiac substrate metabolism without inducing any negative hemodynamic effects (Stanley *et al*., 2005). Since the early 1970s there has been increasing evidence of TMZ's protective effects. This is especially the case within the context myocardial ischemia, e.g. it increased cardiac efficiency in pre-clinical (Ikizler *et al*., 2006; Kantor *et al*., 2000; Khan *et al*., 2010; Lopaschuk *et al*., 2003) and clinical studies (Brottier *et al*., 1990; Fragasso *et al*., 2013, 2011, 2006a, 2003; Lu *et al*., 2015; Marzilli and Klein, 2003; Szwed *et al*., 2001; Vitale *et al*., 2015, 2004). Clinical trials also demonstrated that combination therapy (hemodynamic together with metabolic modulation) to be effective and also that it is well tolerated (no significant changes in heart rate, blood pressure and rate pressure product) (Detry *et al*., 1994). Treatment with TMZ for HF and ischemic heart disease patients are well documented and its beneficial effects have also been demonstrated in other ischemic organs

(Onay-Besikci and Ozkan, 2008). The beneficial effects of TMZ were demonstrated in several *in vitro* and *in vivo* studies using various models of ischemia and also in clinical trials. There is increasing evidence that TMZ improves ischemic injury and cardiac function in animal models (Ikizler *et al*., 2006; Kantor *et al*., 2000) and in humans (Bui *et al*., 2011). For example, elderly chronic HF patients that were treated with TMZ displayed improved cardiac output and quality of life (Vitale *et al*., 2004). Additional cytoprotective effects of TMZ may potentially include diminished mitochondrial ATP production and a reduction in apoptosis, although further studies are required to verify this. Here TMZ could potentially reduce the FA-mediated uncoupling of respiration and thereby increase cardiac output (Chandler *et al*., 2002).

The efficiency of TMZ to improve HF can be attributed to its modulation of FA metabolism, lowering of ROS and subsequent improvement in contractile function (Gambert *et al*., 2006). A randomized clinical trial also demonstrated that TMZ in combination with conventional pharmacological agents resulted in improved left ventricular end-systolic volume and ejection fraction in HF patients (Fragasso *et al*., 2006b). Together the data strongly supports a beneficial role for TMZ for CVD treatment, with limited side-effects. However, whether TMZ can offer cardioprotection within the context of AHF and with diabetes as a co-existent risk factor remains poorly understood. **In light of this, for the current study we hypothesized that TMZ offers cardioprotection to diabetic rat hearts subjected to *ex vivo* AHF.**

The objectives of this study are to 1) establish an experimental diabetic *ex vivo* rodent model of AHF; 2) assess whether the metabolic agent TMZ can improve myocardial contractile function with AHF (non-diabetic and diabetic hearts); and 3) determine underlying mechanisms (focusing

on polyol pathway and AGEs) driving the onset of AHF in normal and diabetic hearts and establish how this altered with TMZ treatment.

6 CHAPTER 6

Materials and Methods

6.1 Hypothesis

We hypothesize that metabolic modulation using TMZ protects the myocardium with onset of AHF by improving contractile function of the diabetic heart.

6.2 Aims

1. Establish an experimental, *ex vivo* rat model of experimental AHF and evaluate the impact of diabetes within this context.
2. Assess whether the metabolic agent TMZ is able to improve contractile function with AHF with and without diabetes.
3. Determine underlying mechanisms driving the onset of AHF in normal and diabetic hearts and assess how this can be altered by TMZ treatment.

6.3 Methodology for model of acute heart failure

6.3.1 Animals and ethics statement

All animals were treated in accordance with the Guide for the Care and the Use of Laboratory Animals of the National Academy of Sciences (NIH publication No. 85-23, revised 1996). Studies were performed with the approval of the Animal Ethics Committee of Stellenbosch University (SU_ACUM13-00020) (Appendix A) and (SU_ACUM13-00030) (Appendix B).

6.3.2 Induction of experimental diabetes Type 1

Male Wistar rats (180 – 220 g) were injected intraperitoneally (i.p) with a single dose of streptozotocin (STZ) (60 mg/kg) as routinely performed in our laboratory (Mapanga *et al*., 2014) to induce experimental diabetes. Control animals were divided into untreated and vehicle groups; the latter injected with citrate buffer (0.1 M) (Appendix C). Blood glucose levels were determined with the use of an ACCU-CHEK® glucometer (Roche, Basel, Switzerland) a week after STZ injection and values > 20 mmol/L indicated the successful induction of diabetes (Mapanga *et al*., 2014). Body weights were recorded prior to Langendorff heart perfusion experiments.

6.3.3 Conjugation of bovine serum albumin to palmitate for retrograde heart perfusions

Dialysis tubing (Spectra/Por® dialysis tubing, Fisher Scientific, Waltham MA) was placed into a beaker of distilled water to allow the tubing to soften up prior to the addition of conjugated solution.

The fatty acid content of bovine serum albumin fraction V (BSA) (Roche Ltd., Basel, Switzerland) (2 x 15 mg) was sent for gas chromotography analysis prior to conjugation. This was performed in conjunction with Prof. Wentzel Gelderblom (SA MRC, Tygerberg, South Africa). Here results indicated that the amount of C16 fatty acid was 0.3 mM. We therefore dissolved 3% BSA (Roche Ltd., Basel, Switzerland) in 400 ml of Krebs-Henseleit buffer at 37°C while stirring. Separately, palmitic acid (1.2 mM) and sodium carbonate (1.4 mM) were added to a solution containing 15 ml distilled water and 10 ml 95% ethanol (Lopaschuk and Barr, 1997). To dissolve the palmitate and sodium carbonate this solution was heated to 60°C until all the ethanol had evaporated. Once the ethanol was boiled off the palmitate solution was quickly added to the warm BSA solution stirred. Upon the addition of palmitate to BSA, the solution initially became cloudy thereafter it cleared (resembling a brown beer-type color) indicating the successful conjugation of palmitate to BSA. The conjugated BSA:palmitate solution was poured into dialysis tubing and the ends of the tubing tied off and placed in a beaker of Krebs-Henseleit buffer (without glucose) and stirred at 4°C overnight. The final concentration of palmitate was 1.5 mM. The following day the dialysis tubing was removed from the Krebs-Henseleit buffer and the conjugated solution poured into a glass beaker. The solution was adjusted to final volume of 1 L with Krebs-Henseleit buffer.

6.3.4 Langendorff retrograde heart perfusions

Non-diabetic and diabetic rats were anesthetized using sodium pentobarbitone (100 mg/kg, i.p injection) and hearts rapidly excised and immersed in ice cold Krebs-Henseleit buffer which contained 11 mM glucose, 118.5 mM NaCl, 25 mM $NaHCO_3$, 4.75 mM KCl, 1.19 mM MgSO4.7H_2O, 1.18 mM KH2PO4, 1.36 mM CaCl dehydrate for non-diabetics and 30 mM glucose, 118.5 mM NaCl, 25 mM $NaHCO_3$, 4.75 mM KCl, 1.19 mM MgSO4.7H_2O, 1.18 mM KH2PO4, 1.36 mM CaCl dehydrate for diabetic hearts (refer to Appendix D). The aorta was rapidly mounted on a cannula connected to our modified Langendorff retrograde perfusion model of *de novo* AHF and perfused with Krebs-Henseleit buffer. A 2.0 silk suture was used to tie the heart to the cannula and thereafter a pressure transducer (Stratham MLT 0380/D, AD Instruments Inc., Bella Vista, New South Wales, Australia) connected to a balloon (made from cling wrap) was inserted into the left ventricle of the heart. The pulmonary artery was cut to expel Krebs buffer from the right ventricle. The balloon was inflated with distilled water inside the left ventricle and the diastolic pressure was set between 5 – 12 mmHg. The left ventricular pressure was maintained between 80 – 120 mmHg for the duration of the stabilization phase. Hearts were maintained at 37°C throughout the protocol and monitored with a temperature probe. The PowerLab System (AD Instruments Bella Vista, New South Wales, Australia) was used and connected to the pressure transducer (Stratham MLT 0380/D, AD Instruments Inc., Bella Vista, New South Wales, Australia) and the electrical signaling of the beating heart was converted to an electrical signal that was read by the PowerLab System ML410/W (AD Instruments Inc., Bella Vista, New South Wales, Australia). The following parameters were recorded: heart rate, left ventricular end diastolic pressure (LVEDP), left ventricular end systolic

pressure (LVESP), left ventricular developed pressure (LVDP, the difference between LVESP and LVEDP, rate pressure product (RPP) (heart rate x LVDP) and maximum velocity of contraction (dP/dt_{max}) that is calculated as the pressure difference in mmHg/sec. The perfusion protocol consisted of 3 phases, i.e. stabilization (30 min), AHF (35 min) and the recovery phase (30 min). Here non-diabetic and diabetic hearts were perfused with 11 mM and 30 mM glucose, respectively, during the stabilization phase at 100 cmH_2O and during the recovery phases, ± 1.5 mM palmitate, at 100 cm H_2O perfusion pressure (refer to Figure 6.1). During the AHF phase hearts were perfused with Krebs-Henseleit buffer that contained 1.5 mM palmitate and 2.5 mM glucose, where the perfusion pressure was reduced to 20 cm H_2O. For the control no-AHF, hearts (non-diabetic and diabetic) were perfused for 95 min in the stabilization phase. The non-diabetic and diabetic end-AHF groups were perfused until the end of the AHF phase.

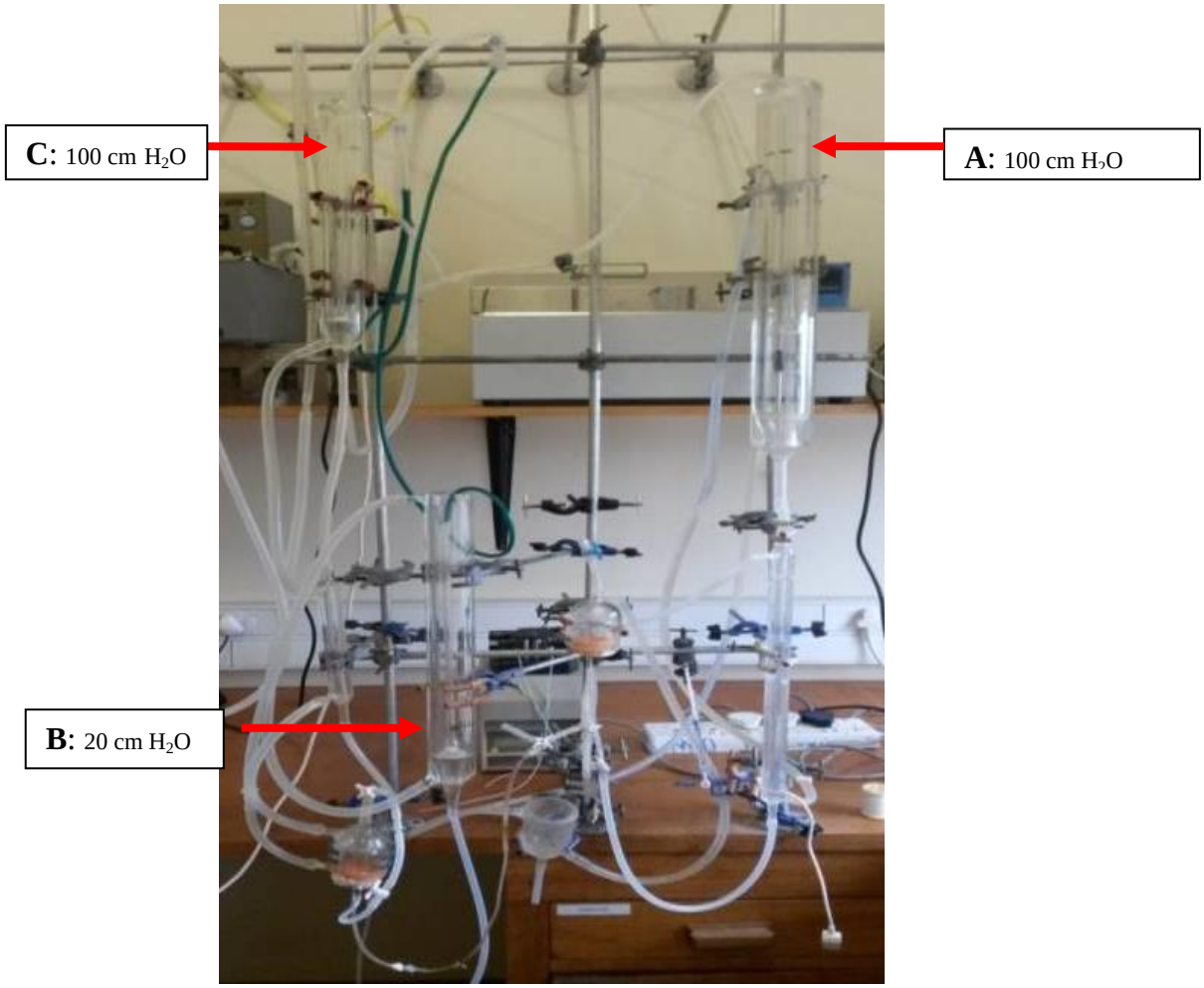

Figure 6.1. Langendorff retrograde perfusion system, modified to an experimental acute heart failure system. The system consists of 3 phases: Stabilization, AHF and Recovery.

6.3.5 Our AHF model

An *ex vivo* diabetic rat heart Langendorff perfusion model of *de novo* AHF (Figure 6.1) was adapted from a previously established non-diabetic rat heart model of AHF (Deshpande *et al*., 2010; Opie and Deshpande, 2016; Opie *et al*., 2010). The *de novo* AHF model consists of 3 phases: stabilization, AHF and recovery. Each phase can be independently activated between

reservoirs by opening the stop cocks. Hearts are under-perfused in order to stimulate systolic failure which impairs the hearts ejection (Opie *et al*., 2010). In each phase buffers were gassed with 95% O_2/5% CO_2 (#801068-RC-A, AFROX, Gauteng, South Africa) prior to and for the duration of heart perfusions.

A: Stabilization

The stabilization phase took place over a 30 min period at a perfusion pressure of 100 cm H_2O, constituted with glucose (either 11 mM [non-diabetic] or [30 mM diabetic]) as the sole substrate in Krebs-Henseleit buffer. Since *ex vivo* Langendoff perfusions are typically performed with 11 mM glucose we used this as baseline glucose concentration in our non-diabetic hearts, where diabetic hearts were perfused with high glucose 30 mM to mimic high concentration of circulating glucose in diabetic heart. The purpose of this phase is to wash out any metabolites and to assess basal functional parameters (heart rate, left ventricular developed pressure (LVDP), rate pressure product and maximum velocity of contraction (dP/dt_{max}). All hearts that had an LVDP < 80 mmHg were excluded from the study.

B: AHF phase

This phase took place over a 35 min period where the perfusion pressure was reduced to 20 cm H_2O to stimulate AHF associated with systolic dysfunction (Opie *et al*., 2010) and glucose reduced to 2.5 mM with the addition of supraphysiological levels of FAs (1.5 mM palmitate). In this phase glucose is reduced to decrease the delivery of glucose and diminish its protective

effect at low coronary flow rates and to increase circulating FA uptake. Here the premise is employed that increased FAs are associated with detrimental effects in the failing heart (Opie *et al*., 2010). Moreover, Hamilton and Saggerson (1997) indicated that 2.5 mM glucose in myocytes is associated with reduced concentrations of malonyl-CoA compared to physiological glucose (5 mM) as malonyl-CoA inhibits carnitine palmitoylytransferase-1 (CPT1) activity that in turn regulates fatty acid uptake into mitochondria (Lopaschuk *et al*., 1994) - will increase FA metabolism. It has also been demonstrated that hearts perfused with 1.2 mM palmitate display ventricular dysfunction and impaired calcium homeostasis (Aasum and Larsen, 1997). In addition a global ischemic model of low-flow perfusion was previously established where the perfusion pressure was reduced from 100 cm H_2O to 20 cm H_2O in order to stimulate ischemia (Bricknell and Opie, 1978). Thus our AHF model was based on the same principle where the perfusion pressure was reduced to 20 cm H_2O to mimic hypotension often associated with AHF patients (Deshpande *et al*., 2010).

C: Recovery phase

The duration of this phase was 30 min, where the perfusion pressure is restored to 100 cm H_2O without altering the palmitate (1.5 mM) concentration, while glucose availability is restored, i.e. 11 mM and 30 mM (non-diabetic and diabetic hearts respectively). We employed a 1 µM TMZ dose as it was previously associated with optimal functional recovery after ischemia-reperfusion (Di Napoli *et al*., 2007). Therefore in our model we perfused hearts ± 1 µM TMZ for the entire recovery period. At the end of recovery phase hearts were collected and freeze-clamped in liquid nitrogen and stored at -80°C for further analysis.

6.3.5.1 Determination of infarct sizes (tetrazolium staining) -hearts exposed to AHF protocol

Male Wistar rats (180 – 220 g) were anesthetized using sodium pentobarbitone (100 mg/kg) and by i.p injection. Hearts were subsequently excised, cannulated and perfused on our modified Langendorff retrograde perfusion model of *de novo* AHF. Hearts (non-diabetic and diabetic) were perfused for the stabilization and AHF phase. At the end of the AHF phase, hearts were removed and 2.0 suture was placed through the heart and stored suspended in a tube at -20°C for 24 hours in preparation for tetrazolium staining (TTC) (Sigma-Aldrich, St Louis MO). The TTC salt staining method involves the use of dehydrogenase enzymes and cofactors in tissues to react with TTC salts to form a formazan pigment.

The following day, hearts were removed from the freezer and allowed to partially thaw. Thereafter, hearts were sliced into four even pieces with the use of a scalpel blade. Heart slices were placed on paper towel to further defrost. Two buffers, i.e. 100 mM NaH_2PO_4 (Solution 1) and 100 mM Na_2HPO_4 (Solution 2) were separately prepared. Thereafter, 1% TTC was dissolved in 2 parts of Solution 1, and 8 parts of Solution 2 to make up the TTC solution. Heart slices were transferred into the TTC solution and placed in a 37°C waterbath for a total of 20 min. After the first 10 min, hearts were agitated and thereafter left for a further 10 min at 37°C (a total of 20 min). Following the 20 min period, heart slices were removed and placed onto paper towel to dry. Heart slices were then placed in a dark cupboard in 10% formalin solution for 24 hours. Thereafter, hearts were analyzed for infarct size using Image J software (v1.46p; National Institutes of Health, Bethesda MD).

6.3.6 Mitochondrial protein isolation

Mitochondria were isolated from frozen tissue with the use of a tissue extraction kit (Abcam, Cambridge MA). The appropriate amount of heart tissue was weighed out (0.2 – 0.4 g) and the tissue washed twice with the wash buffer provided in the kit. The tissue was homogenized in a pre-chilled Dounce homogenizer (Thomas Scientific, United States). Thereafter 1 ml of isolation buffer (Appendix E) was added to the homogenizer and 40 strokes were employed to homogenize the tissue. The homogenate was successfully transferred to a 2 ml microfuge tube and centrifuged at 1,000 g for 10 min at 4°C. The supernatant (crude mitochondria) was collected and transferred into a fresh 2 ml microfuge tube and the pellet discarded. Thereafter the crude mitochondria was centrifuged a second time at 12,000 g for 15 min at 4°C and placed in a new microfuge tube for further analysis. Mitochondrial proteins were used for Western blot analysis of SOD2, PDH, 3-KAT and UCP2.

6.3.7 Western blot analysis

Hearts were thawed on ice and proteins were isolated by homogenizing heart tissue in modified Radio-Immunoprecipitation (RIPA) buffer (Appendix F). Thereafter the homogenates were transferred to pre-chilled microfuge tubes and kept on ice. The samples were sonicated for 15 sec each, and centrifuged at 4,300 g for 15 min at 4°C. The isolated protein were transferred into a microfuge tube and stored at –80°C until needed. Protein samples were quantified using the Bradford method (refer Appendix F) and 20 µg protein was used for each sample. Expression was evaluated using both total and mitochondrial protein extracts for the following antibodies:

BAD, phosphorylated-BAD (Ser 136), PDH (Cell Signaling, Danvers MA), UCP2 (uncoupling protein 2), ACCA1 (acetyl-Coenzyme A acyltransferase 1) for long-chain 3-KAT and SOD2 (superoxide dismutase 2) (Abcam, Cambridge MA) and RAGE (receptor of advanced glycation end products) (Abcam, Cambridge MA). Samples were subjected to 10% SDS-PAGE and a semi-dry transfer using the Trans-blot® turbo transfer system (Bio-Rad, Hercules CA) (refer full protocol in Appendix G). Membranes were blocked with 5% non-fat milk in TBS-T and incubated with the appropriate primary antibody at 4°C overnight (Appendix H). This was followed by washing of the membrane with TBS-T (20 mM Tris-HCl and 150 mM NaCl, pH7.4 and 0.1% Tween 20) (3 x 5 min washes) and incubated with the appropriate horseradish peroxidase (HRP)-conjugated secondary antibody (1:5000) for an hour at room temperature. Membranes were detected with enhanced chemiluminescence (ECL) (Bio-Rad, Hercules CA) and visualized using Bio-Rad Chemidoc imaging system (Bio-Rad, Hercules CA). Total protein was used as a loading control (Appendix H) and Western blots were analyzed using the Image Analysis software (Bio-Rad, Hercules CA).

6.3.8 Evaluation of oxidative stress

Frozen heart tissue was used for the evaluation of oxidative stress. We employed four measurements of oxidative stress, i.e. conjugated dienes (CDs), thiobarbituric acid reactive substances (TBARS), reduced/oxidized glutathione (GSH/GSSG) and the oxygen radical absorbance capacity (ORAC) assay. These assays were conducted in conjunction with the Oxidative Stress Research Centre at the Cape Peninsula University of Technology (under supervision of Dr. Dirk Bester).

6.3.8.1 Conjugated dienes (CDs)

CDs assay is the measurement of early signs of oxidative stress. Hearts (100 mg) were homogenized with choloroform:methanol mixture (2:1) followed by vortexing and centrifugation (Eppendorf 5810R, Eppendorf, Hamburg, Germany) at 3,000 g for 10 min. The upper layer was discarded and the bottom layer transferred into a clean centrifuge tube with the addition of 100 µl NaCl until completely separated. Thereafter, samples were allowed to dry overnight in the fridge. The following day, 700 µl of cyclohexane was added to each sample and vortexed. An amount of 200 µl of sample was added to each well in a 96-well plate and read in a Multiskan spectrum platereader (Thermo Electron corporation, Waltham, MA) the absorbance taken at 233 nm against a cyclohexane standard (standard 1 O.D. = 37.5 nmoles) using a platereader (The concentration of CDs are expressed as µmol/g protein. The concentration of CDs was determined by the use of the following equation:

Concentration calculation (CDs)

Beer Lamberts Law

$A = \varepsilon \times C$

$C = A/\varepsilon$

With the extinction co-effienct (ε) being 29500

6.3.8.2 Evaluation of thiobarbituric acid reactive substances (TBARS)

Hearts (100 mg) were homogenized in 6.25 µl (4 mM) cold butylated hydroxytolene (BHT) and 0.2 mM ortho-phosphoric acid. Thereafter, samples were vortexed for 10 seconds followed by the addition of TBA reagent (0.11 M in 0.1 M NaOH). Samples were briefly vortexed and heated at 90°C for 45 min. Subsequently, 1000 µl butanol and 50 µl saturated of NaCl was added, vortexed and centrifuged (Boeco M240, Boeco, Hamburg, Germany) at 13,700 for 2 min. Samples were read immediately (absorbance $A_{532} - A_{572}$) and the concentration of TBARS expressed as µmol/g. The concentration of TBARS was measure with the following equation: Beer Lamberts Law

$$A = \varepsilon \times C$$

$$C = A/\varepsilon$$

With the extinction coeffcient (ε) being 240.98

6.3.8.3 Glutathione redox analysis (GSH/GSSG) assay

The glutathione assay was adapted from Asensi *et al*. 1999 (Asensi *et al*., 1999). The ratio of reduced (GSH) to oxidized glutathione (GSSG) was also evaluated as a measurement of oxidative stress. For the glutathione (GSH) assay, 100 mg heart tissue was homogenized in ice cold 15% trichloroacetic acid (2 ml) (TCA) that contained 1 mM EDTA. Thereafter, samples

were centrifuged at 15,000 g for 5 min at 4°C and 500 µl of the supernatant used for analyses. For the glutathione (GSSG) assay, 100 mg of heart tissue was homogenized in ice cold 6% perchloric acid (PCA) (2 ml) containing 3 mM 1-methyl-2-vinyl-pyridinium trifluoromethane sulfonate (M2VP) and 1 mM EDTA. The homogenates were centrifuged at 15,000 g for 5 min at 4°C. Thereafter, 500 µl of acidic supernatant was used for analyses and samples diluted in Buffer A (500 mM $NaPO_4$, 1 mM EDTA). Samples for the GSH and GSSG assays were prepared in triplicates in separate 96-well plates. An amount of 50 µl of the standards, blank or samples were added in a microtiter plate, followed by the addition of 50 µl 5,5' Dithiobis-(2-nitrobenzoic acid) solution (DTNB). We then added 50 µl of the enzyme solution (glutathione reductase), mixed and incubated the plate for 5 min at room temperature. The reaction is started by the addition of 50 µl NADPH to each well and the absorbance was measured at 412 nm for 5 min using a Multiskan spectrum platereader (Thermo Electron corporation, Waltham, MA). The linear slope of the standards was used to calculate concentrations according to the following formula:

GSHt = µM x dilution factor (488) (GSH= GSHt – 2GSSG)

GSSG = µM x dilution factor (60)

Ratio = (GSHt – 2GSSG)/GSSG = GSH.

6.3.8.4 Evaluation of oxygen radical absorbance capacity (ORAC) assay

Heart tissue (100 mg) was homogenized in 1 ml (7.5 mM) phosphate buffer pH 7.0 using a Potter Elvenhjem Telfon pestle and glass tube tissue homogenizer (10 strokes). The homogenate was centrifuged at 12, 000 g at 4°C for 10 min. The supernatant of the samples was then de-proteinized with 0.25 M perchloric acid and centrifuged at 14, 000 g for 15 min. Trolox (500 µM stock) was used for the standards (0, 83, 167, 250, 333 and 417 µM). For the Trolox standard series we took six centrifuge tubes (marked A – F) and added the appropriate amount of standard stock solution and diluents to each tube (refer Appendix J). To the wells, we added 12 µl of standards per well into a 96-well plate. For the sample well an amount of 12 µl was added in triplicates. From the fluorescein stock solution (Appendix J), 10 µl was added to 2 ml phosphate buffer in a centrifuge tube. Next 240 µl of this solution was added to 15 ml phosphate buffer into a 15 ml centrifuge tube. An amount of 138 µl of this solution was added to each well. Next we added 6 ml phosphate buffer to the AAPH solution (preparation in Appendix J), mixed it properly and then 50 µl was added to each well. The plate was then placed into fluorescence spectrometer - the ORAC method is performed by using the Fluoroskan Ascent platereader (Thermo Fisher Scientific Inc., Waltham MA) until zero fluorescence occurs. The results obtained were expressed as the ORAC value which refers to the area under the curve of β-PE (fluorescein) in the presence of an antioxidant. The ORAC value is calculated by dividing by the area under the sample curve by the area under the curve for Trolox (TE). Values were expressed as µmol TE/g

6.3.9 Evaluation of non-oxidative glucose pathways (NOGPs)

We employed two commercial kits to evaluate markers of NOGPs. For the polyol pathway we used the D-sorbitol colorimetric assay kit (Biovision, Mountain View CA), while AGE precursors were evaluated using the OxiSelect™ Methylglyoxal (MG) competitive ELISA kit (Cell Biolabs, San Diego CA). To evaluate two pivotal enzymes fructosamine-3-kinase (FN3K) and glyoxylase I (GLO-I) involved in deglycation of AGEs we employed two commercial kits Human fructosamine-3-kinase (FN3K) ELISA kit (Cusabio Biotech, Baltimore MD) and the Glyoxalase I assay kit (Abnova, Taipei City, Taiwan).

6.3.9.1 Sorbitol levels (polyol pathway marker)

A 1 mM working solution of the sorbitol standard was prepared using the stock provided in the kit. Fifty µl standards (including reaction blanks) were pipetted in duplicate into 96-well plate to generate 0, 2, 4, 6, 8, 10 nmol/well in assay buffer. Proteins were isolated from heart tissue as described in section 6.3.7 (Appendix E). Protein samples were pipetted in duplicates. Thereafter 50 µl of reaction mix (assay buffer, enzyme mix, developer and probe) was added to both protein and standard wells and incubated at 37°C for 30 min. Absorbance was read at 560 nm using a microplate reader (EL 600 KC Junior Universal Microplate reader, Bio-Tek Instruments, Winooski VT). The concentration of sorbitol (C) was determined from the standard curve (S_a) in nmol, sample volume (S_v) and the dilution factor D in the following equation: $C=S_a/S_v*D$. The concentration of D-sorbitol was expressed as µM protein.

6.3.9.2 Methylglyoxal levels (AGE marker)

Immediately before use, 500 ng/mL of methylglyoxal (MG) conjugate was prepared by diluting 1 mg/mL MG conjugate in 1x conjugate diluent (provided in the kit). A volume of 100 µl of 500 ng/mL MG conjugate was added to each well to be tested and incubated at 4°C overnight. The following day the MG conjugate solution was removed and wells washed twice with 1x phosphate-buffered saline (PBS) (13 mM $NaCl_2$, 2.7 mM KCl, 8 mM Na_2HPO_4 and 1.5 mM KH_2PO_4, pH 7.4.). The plate was blotted on paper to remove excess fluid. The wells were blocked on an orbital shaker for an hour at room temperature by the addition of 200 µl assay buffer. Methylglyoxal-BSA (MG-BSA) standards and blanks were prepared in duplicate by dilution series in the concentration range of 0 to 25 µg/mL with assay diluent. Proteins were isolated from heart tissue as described in section 6.3.7 (Appendix E). Fifty µl of standard or protein samples were added in duplicate to wells of the plate and incubated at room temperature on an orbital shaker for 10 min. Thereafter, 50 µl of diluted anti-MG antibody (1:1000) was added to each well and incubated on an orbital shaker for an hour at room temperature. The primary antibody was removed and the wells washed 3x with 250 µl 1x wash buffer. A volume of 100 µl secondary HRP-conjugated antibody (1:1000) was added to each well and incubated for an hour at room temperature. The wells were washed 5x with 250 µl 1x wash buffer. The substrate solution was warmed to room temperature and 100 µl added to each well. The plate was incubated on an orbital shaker for 20 min at room temperature and the enzyme reaction stopped by the addition of 100 µl stop solution to each well. Absorbance was read immediately at 450 nm using a microplate reader (EL 800 KC Junior Universal Microplate reader, Bio-Tek Instruments, Winooski VT). Optical densities were normalized by subtracting the value of the

blank from both the standard and sample wells. The concentration of methylglyoxal was expressed as µmol/µg protein.

6.3.9.2.1 Fructosamine-3-kinase (FN3K) ELISA assay

The human FN3K ELISA kit (Cusabio Biotech, Baltimore MD) was used to measure levels of FN3K. An amount of 100 mg heart tissue was weighed out for all treatment groups, rinsed with 1x PBS and homogenized in 1 ml PBS. Thereafter, the homogenates were transferred to pre-chilled microfuge tubes and kept on ice. The samples were sonicated for 15 sec each, and centrifuged at 5,000 g for 5 min at 4°C. Proteins were quantified using the Bradford assay**.** A 20 ng/ml working solution of the FN3K standard was prepared using the stock provided in the kit, thereafter a dilution series was performed. 100 µl standards (including reaction blanks) were pipetted in duplicate into a 96-well plate to generate 0, 0.312, 0.625, 1.25, 2.5, 5, 10, and 20 ng/ml/well. Protein samples were pipetted in duplicates. Thereafter, the plate was covered with the adhesion strip provided and incubated for 2 hours at 37°C. Liquid from the plate was discarded and 100x biotin antibody was added to each well. The plate was covered with a new adhesive strip and incubated for 1 hour at 37°C. Thereafter, each well was aspirated and washed three times with 200 µl wash buffer. After the third wash the plate was inverted and blotted onto paper towel. A 100 µl HRP-avidin (1x) was added to each well and covered with a new adhesive strip and incubated for an hour at 37°C. This was followed by five aspiration and wash steps with 1x wash buffer. Ninety µl of 3,3',5,'-tetramethylbenzidine (TMB) substrate was added to each well, incubated and the plate covered (protect from light) for 15 – 20 min at 37°C. We next added 50 µl of stop solution to each well. The absorbance was read at 450 nm using a microplate reader (EL 600 KC Junior Universal Microplate reader, Bio-Tek Instruments, Winooski VT).

The concentration of FN3K (C) was determined from the standard curve (S_a) in ng/ml, sample volume (S_v) and the dilution factor D in the following equation: $C=S_a/S_v*D$. Fn3K was expressed as µg/µl protein.

6.3.9.2.1.1 Glyoxylase-I (GLO-I)

The glyoxylase I assay kit (Abnova, Taipei City, Taiwan) was used to measure GLO-I. The protein concentration was initially determined using the Bradford method. For each sample two tubes were required: one for the GLO-I reaction and another for the sample blank; thus each sample served as its own blank. An amount of 40 µl of each sample was added to 2 separate microfuge tubes. A working solution was prepared for each tube by adding 160 µl Assay Buffer with 8 µl Substrate and 8 µl Cosubstrate. For the GLO-1 reaction, we added 160 µl working reagent to the GLO-1 reaction tubes and thereafter incubated for 20 min at room temperature. After this 70 µl of 4 M perchloric acid was added to each GLO-1 reaction tube, vortexed and put on ice for 15 min. Thereafter, samples were centrifuged at 4,300 g and 200 µl of the supernatant was transferred to separate wells of the 96-well UV titer plate. For the sample blanks, 70 µl of 4M perchloric acid was added to each sample blank tube. The tubes were then vortexed and put on ice for 15 min. Following the 15 min period, 160 µl working reagent was added to each sample blank tube, vortexed and put on ice for 15 min. Thereafter, sample blanks were centrifuged for 5 min at 4,300 g and 200 µl of supernatant was transferred to separate wells of the 96-well UV titer plate. Optical density was read at 240 nm and the concentration of GLO-1 was expressed as µg/µl protein.GLO-1 activity was calculated with the use of the following equation:

$$GLO\text{-}1 = 175 \times (OD_{sample} - OD_{blank}) \times (1.35 \times n)$$

where OD_{sample} and OD_{blank} are the optical density values of the sample and blank, respectively. The dilution factor for de-proteination is 1.35 and n is the dilution factor if a sample dilution is required.

6.4 Methodology for *in vitro* studies

Previous studies demonstrated that TMZ can display antioxidant properties after ischemia/ reperfusion (Ruiz-Meana, 2005). Therefore we aimed to evaluate the effects of TMZ in an *in vitro* setting.

6.4.1 Cell culture

The rat cardiomyoblast cell line, H9c2, was cultured in Dulbecco's Modified Eagle's Medium (DMEM) media containing GlutaMAX^{TM} and 25 mM glucose (Invitrogen, Carlsbad CA).

Media was supplemented with 10% fetal bovine serum (FBS) and 1% penicillin-streptomycin solution (Invitrogen, Carlsbad CA). Cells were cultured as monolayers at 37°C in a humidified atmosphere of 95% air and 5% CO_2. Culturing was done in T75 flasks and subcultured once confluency was reached and cells thereafter trypsinized. The DMEM media in the flask was discarded and the cell monolayer was washed with warm (37°C) PBS. PBS was removed and cells incubated with 4 ml of 0.25 % trypsin-EDTA (Invitrogen, Carlsbad CA) for 4 mins at 37°C

until cells were detached. DMEM was added to the flask to stop trypsinization and followed by centrifugation for 3 min at 1,358 g in a Digicen 20-R Ortoalresa centrifuge (Ortoalresa, Spain). Cells were counted with the use of a hemocytometer (Lasec, Cape Town, South Africa). Cell pellets were resuspended in the appropriate amount of DMEM media and seeded in cell culture flasks, or plates or dishes for experimental passaging. DMEM was refreshed every 48 hours or 24 hours after seeding cells.

6.4.2 Evaluation of oxidative stress in H9c2 cells by flow cytometry

We aimed to evaluate oxidative stress in H9c2 cells treated with or without palmitate and trimetazidine. H9c2 cardiomyoblasts were cultured as described in section 6.4.1, until 80% confluency was reached. Cells were treated for 24 hour period as demonstrated below:

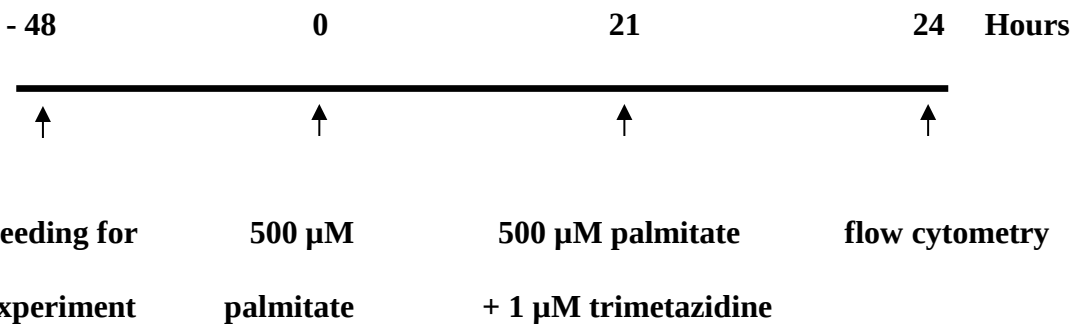

Figure 6.2. Experimental Timeline: H9c2 cells were seeded and allowed to plate 48 hours prior to palmitate treatment for 21 hours. TMZ was added for the final 3 hours of the protocol, followed by flow cytometry analysis

As a study by Shi (2009) showed that cardiomyocytes treated with 500 µM palmitate was associated with severe mitochondrial damage and apoptosis, we treated the H9c2 cells with this dosage.

6.4.3 Evaluation of intracellular ROS levels by flow cytometry- DCF fluorescence

H9c2 cells was seeded in T25 flasks and treated as demonstrated in Figure 6.2. Cells were washed with warm PBS and trypsinized with 3 ml Trypsin-EDTA (Invitrogen, Carlsbad CA) and incubated at 37°C for 4 min to dislodge cells. Five ml warm DMEM media was added to the cell suspension and transferred to a 15 ml tube, and centrifuged at 1,358 g for 3 min in a Digicen 20-R Ortoalresa centrifuge (Ortoalresa, Spain). The pelleted cells were washed with PBS and centrifuged for 3 min. Freshly prepared DCF working solution was added to the cells and incubated for 10 min at 37°C as before. Five hundred µl PBS was added to the pellet before flow cytometry analysis was performed (BD FACSAria™, Becton Dickinson, San Jose CA). Hundred µM H_2O_2 was used as a positive control and a 488 nm laser and 502LP 530/30 BP emission filters were used. A minimum of 10,000 events were analyzed per sample and fluorescence intensity was determined by using the geometric mean. Experiments were repeated 6 – 8 times.

6.4.4 Evaluation of mitochondrial ROS by flow cytometry

Cells were cultured and treated as demonstrated in figure 6.2. MitoSOX™ Red mitochondrial superoxide indicator (MitoSOX) (Molecular Probes, Eugene OR) was used to detect sources of

mitochondrial ROS. MitoSOX™ Red mitochondrial superoxide indicator is a fluorogenic dye used for highly sensitive detection of superoxide in live cells. The dye is a live cell permeant which rapidly and selectively targets the mitochondria. Upon entry to the mitochondria the dye is oxidized by superoxide and exhibits red fluorescence, and has excitation/emission maximum of 510/580 nm.

Stock solutions were prepared by dissolving the contents (50 µg) of one vial of MitoSOX™ mitochondrial superoxide indicator in dimethylsulfoxide (DMSO) to a final concentration of 5 mM. Single use aliquots were stored at – 20°C to protect and wrapped in foil to protect from light. Fresh working MitoSOX™ (5 µM) solution was prepared in PBS and working solution added to the cells followed by 10 min at 37°C.

Thereafter cells were centrifuged at 1,358 g for 2 min. Five hundred µl PBS was added to the pellet before flow cytometry analysis (BD FACSAria™, Becton Dickinson, San Jose CA) and 100 µM H_2O_2 was used for positive control sample.

6.5 Evaluation of fatty acid β-oxidation enzymes

Since we did not find any changes in PDH and 3-KAT the marker for glucose oxidation and TMZ target respectively, we aimed to explore implications of the fatty acid β-oxidation enzymes: HADHA/HADHB for medium-chain specific acyl-CoA dehydrogenase and ACAVDL for the long-chain specific acyl-CoA dehydrogenase.

Experiments were conducted with the use of the fatty acid oxidation human flow cytometry kit (Abcam, Cambridge, MA). H9c2 cells were treated as described in section 6.4.2. Cells were harvested as a single suspension and fixed with 4% paraformaldehyde for 15 mins and centrifuged at 1,358 g for 3 min. The pellet was permeabilized with 1X permeabilization buffer (provided in the kit) for 15 mins and centrifuged at 1,358 g for 3 min. Cells were then blocked with blocking buffer (provided in the kit) for 15 min and centrifuged at 1,358 g for 3 min. Primary antibody (2X) was diluted in blocking/incubation buffer and overlayed onto the pellet for 1 hour. Thereafter, the pellet was washed with washing buffer provided in the kit, followed by the addition of secondary antibody (diluted in blocking/incubation buffer) for an hour. Samples were read with flow cytometry analysis (BD FACSAria™, Becton Dickinson, San Jose CA).

6.6 Evaluation of cell death

Next we aimed to further investigate apoptosis in our *in vitro* model. The caspase-GLO® assay (Promega, Madison, United States) was used according to the manufacturer's instructions. H9c2 cells were treated as described in section 6.4.2. To prepare the caspase-GLO® reagent, caspase-GLO® substrate was added to caspase-GLO® buffer. Equal caspase-GLO® reagent was added to each sample, mixed and incubate for 30 min. Thereafter, the plate was read with the use of the luminometer (Promega, Madison,United States). Data was expressed as reflective light units (RLU).

6.7 Statistical analysis

Data are presented as mean ± standard error of the mean (SEM). Differences between treatment groups and time-points were analyzed using one way analysis of variance (ANOVA). Mann-Whitney unpaired t-test was done when comparisons were made between two groups. Significance was assessed by means of the Tukey-Kramer post hoc. All statistical analysis was performed with the use of GraphPad Prism version 5.01 (GraphPad Software, Inc., La Jolla CA). Values were considered significant $p<0.05$.

7 CHAPTER 7

Results

Validation of *ex vivo* perfusion *de novo* AHF rodent model in non-diabetic and diabetic hearts

7.1 Introduction

We initially aimed to validate our *ex vivo* perfusion AHF rodent model in non-diabetic and diabetic hearts. Control (i.e. no AHF) hearts were perfused in the stabilization phase for 95 min and compared to counterparts subjected to AHF (Section 6.3.5). Our results demonstrate a robust decrease in function in the AHF phase for both non-diabetic ($p<0.001$ *vs.* non-diabetic control) and diabetic hearts ($p<0.001$ *vs.* diabetic control) (Figures 7.1 and 7.2).

This decrease in function is shown by a robust fall ($p<0.001$) in LVDP, i.e. for non-diabetic control hearts LVDP ranged between 77.7 mmHg ± 6 mmHg and 92 mmHg ± 4.8 mmHg *vs.* non-diabetic AHF where it ranged between 8 mmHg ± 2.5 mmHg and 9.8 mmHg ± 6.6 mmHg, respectively. During the same period (AHF phase) RPP and dP/dt_{max} showed a similar pattern (Figure 7.1). This was also the case for heart rate.

During the stabilization phase coronary flow for non-diabetic control hearts ranged between 11 ml/min ± 0.6 ml/min and 8.5 ml/min ± 0.9 ml/min *vs.* non-diabetic AHF hearts (10 ml/min ±

0.6 ml/min). Of note, coronary flow (non-diabetic hearts) significantly decreased during the AHF phase to 3 ml/min ± 0.1 ml/min for both non-diabetic and diabetic hearts and remained like this until the end of the AHF period.

A similar decrease in function was observed in AHF diabetic hearts for all the four parameters (Figure 7.2 A – D, $p<0.001$ *vs.* diabetic control). RPP for AHF diabetic hearts were also reduced, ranging from 195 mmHg/sec ± 52 mmHg/sec to 237 mmHg/sec ± 62 mmHg/sec (Figure 7.2 C, $p<0.001$). We also completed additional experiments where hearts were perfused until the end of AHF phase and evaluated for necrosis using TTC staining as described. Here our data reveal no visible evidence of infarction (Figure 7.3).

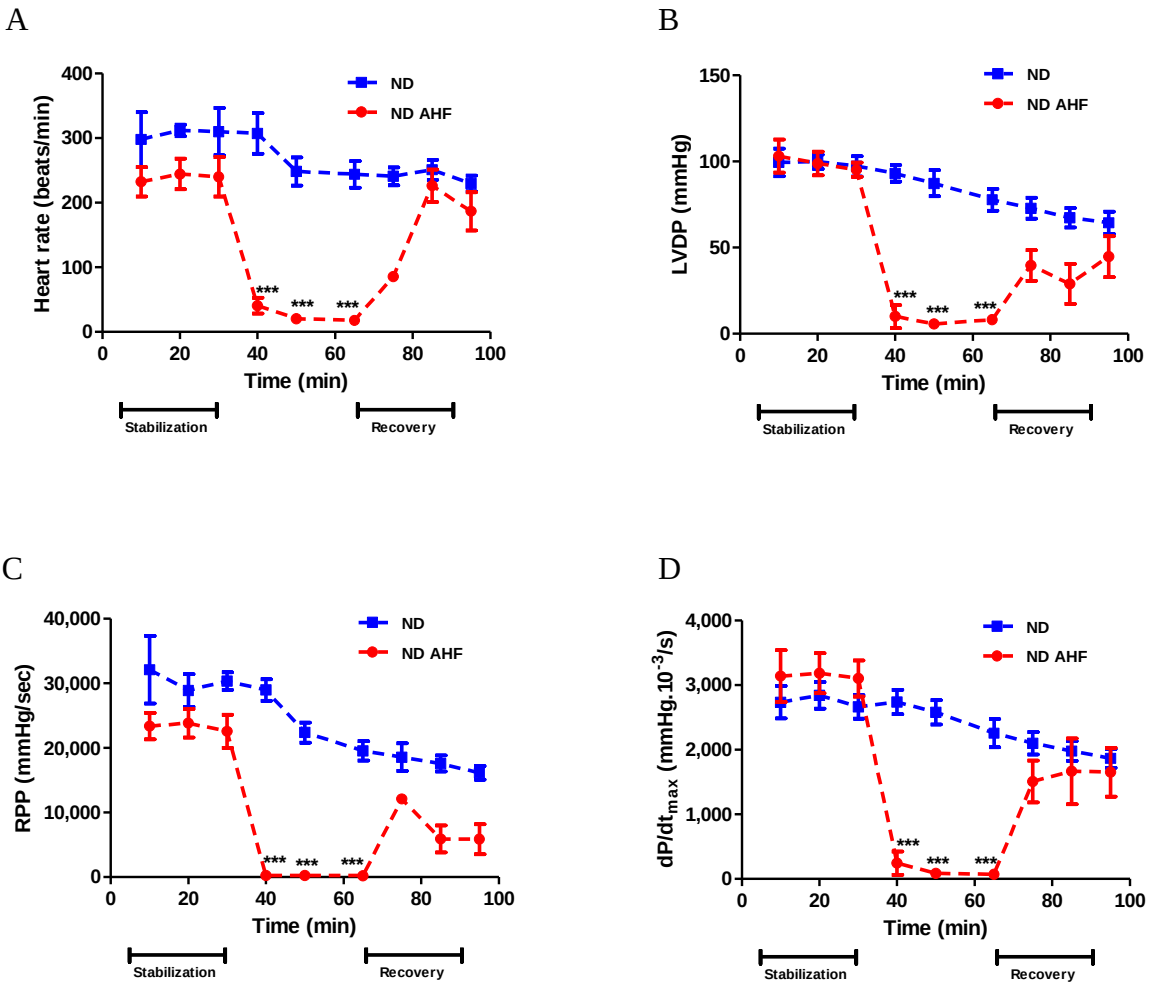

Figure 7.1. Non-diabetic hearts subjected to simulated AHF display a reduction in heart rate, LVDP, RPP and dP/dt during the AHF phase versus non-diabetic control hearts. Isolated non-diabetic rat hearts were perfused under baseline conditions (11 mM glucose) for 95 min stabilization. The second group was subjected to simulated AHF conditions i.e. 30 min stabilization (11 mM glucose), 35 min AHF (2.5 mM glucose, 1.5 mM palmitate) and 30 min of recovery (11 mM glucose, 1.5 mM palmitate). (A) heart rate, (B) left ventricular developed pressure (LVDP), (C) rate pressure product (RPP), (D) maximal velocity of contraction (dP/dt_{max}). Values are expressed as mean ± SEM ($n \geq 6$). ***$p<0.001$ *vs.* non-diabetic control.

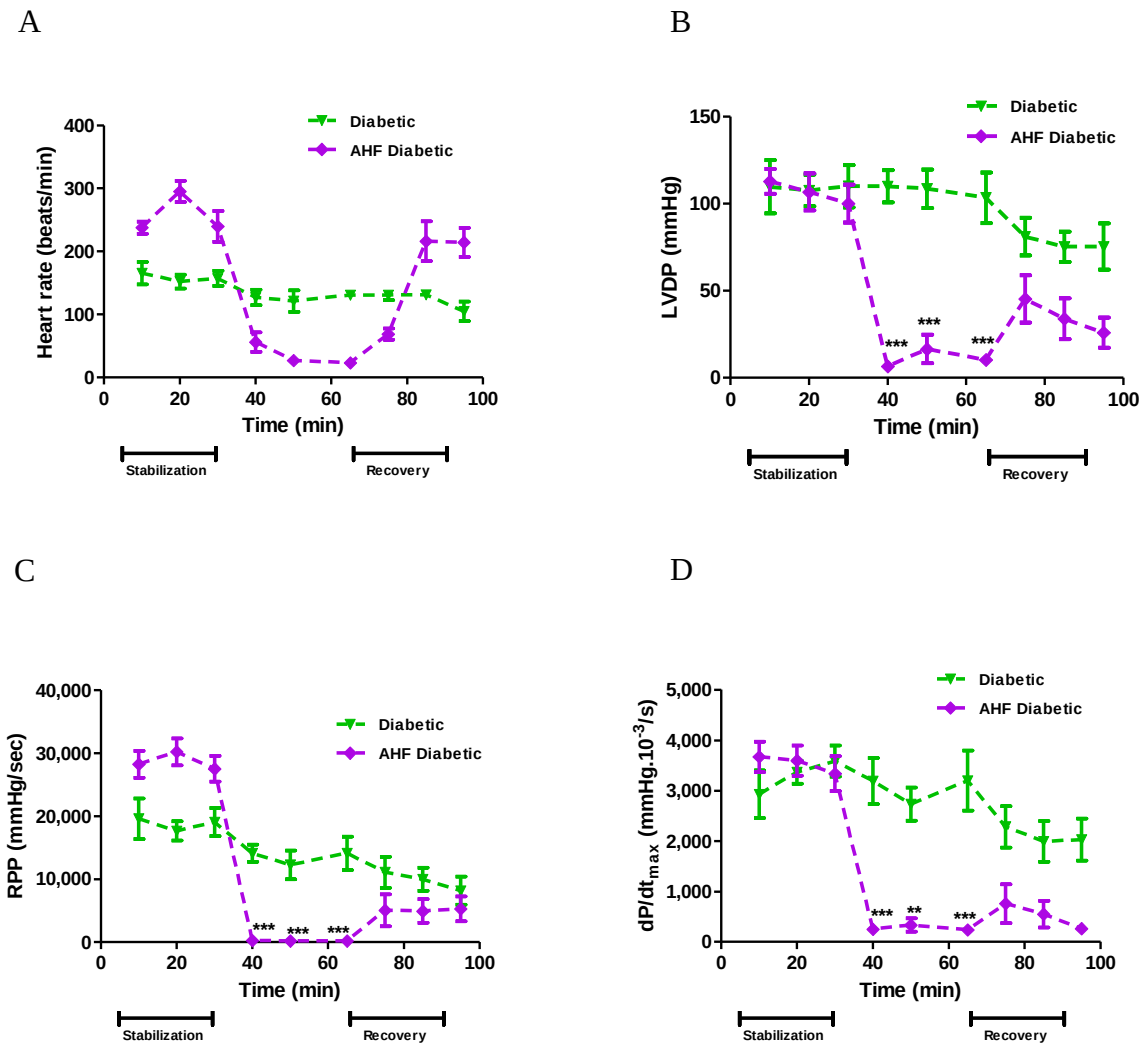

Figure 7.2. Diabetic rat hearts subjected to simulated AHF showed a decrease in contractile function during the AHF phase compared to control diabetic hearts. Isolated diabetic control rat hearts were perfused (30 mM glucose) for 95 min stabilization. The second group was subjected to simulated AHF conditions i.e. 30 min stabilization (30 mM glucose), 35 min AHF (2.5 mM glucose, 1.5 mM palmitate) and 30 min of recovery (30 mM glucose, 1.5 mM palmitate). (A) heart rate, (B) left ventricular developed pressure (LVDP), (C) rate pressure product (RPP), (D) maximal velocity of contraction (dP/dt_{max}). Values are expressed as mean ± SEM ($n \geq 6$). **p<0.01 *vs.* diabetic control; ***p<0.001 *vs.* diabetic control.

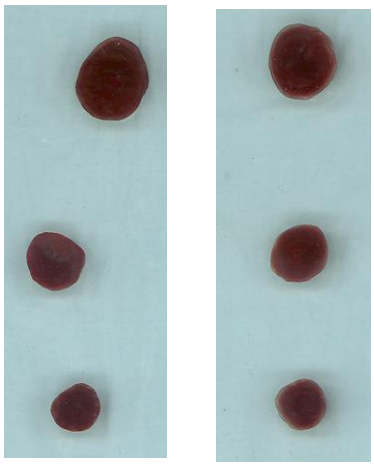

Figure 7.3. Non-diabetic and diabetic rat hearts exposed to the stabilization and AHF phase only. Isolated non-diabetic and diabetic rat hearts were subjected to two phases only, i.e. 30 min stabilization (11mM or 30 mM glucose, non-diabetic and diabetic respectively), followed by 35 min of AHF (2.5 mM glucose, 1.5 mM palmitate). At the end of the AHF phase, hearts were stained by the TTC method (n=6).

These data demonstrate that we successfully validated our *ex vivo* AHF rodent model which shows a significant decrease in function in both non-diabetic and diabetic hearts subjected to AHF compared to respective controls. Furthermore, our TTC staining results show no visible evidence of infarct/necrosis providing additional insights regarding the nature and outcomes of the AHF model here employed. We next proceeded to test the effect of TMZ administration in response to AHF in non-diabetic and diabetic hearts and whether such treatment can serve as a therapeutic agent.

7.2 The effect of TMZ treatment on non-diabetic and diabetic hearts subjected to AHF

Our findings revealed no significant differences in contractile functional parameters for AHF non-diabetic hearts treated with TMZ compared to untreated AHF non-diabetic hearts (Figure 7.5 A – D).

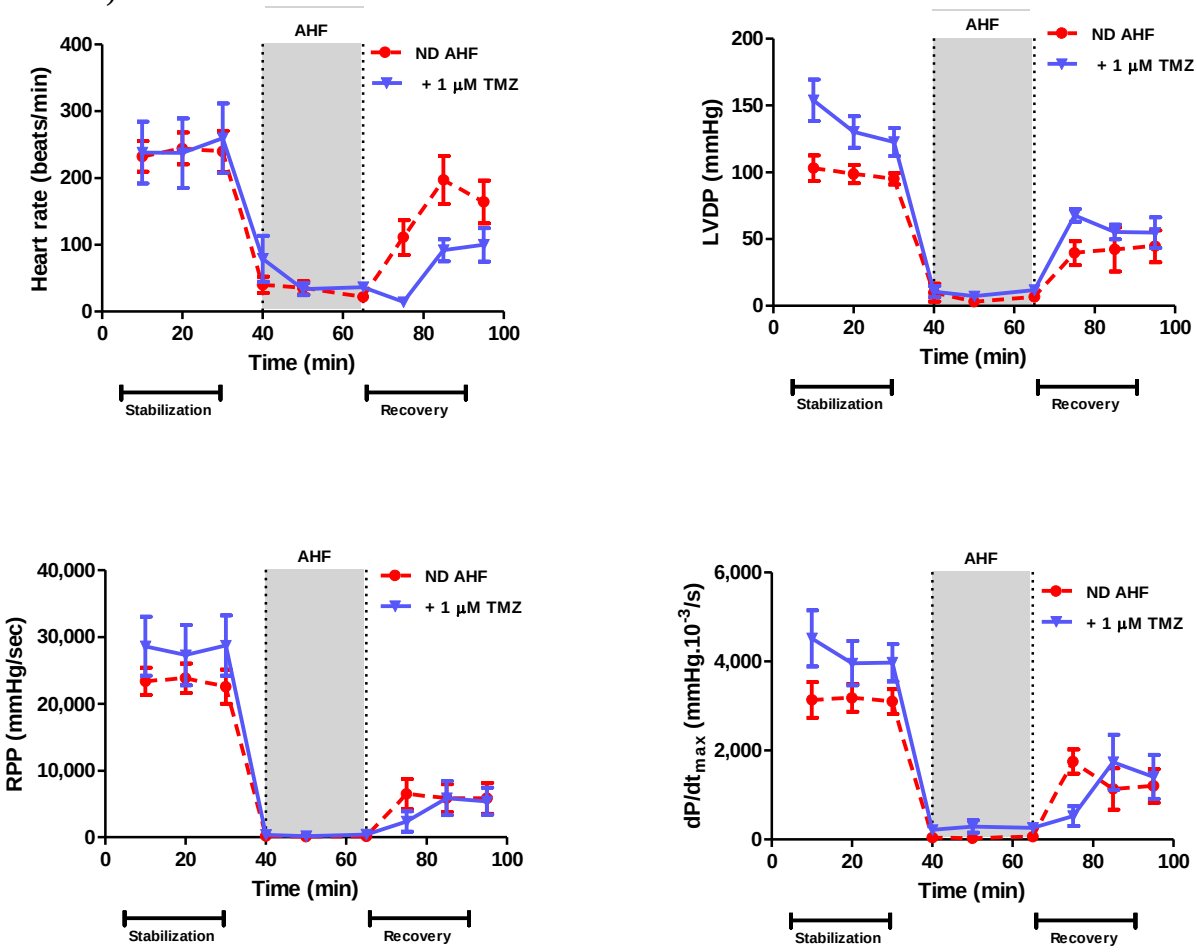

Figure 7.4. TMZ administration does not affect contractile function and heart rate of non-diabetic hearts exposedd to the AHF protocol. Isolated rat hearts were perfused under simulated AHF conditions and subjected to 30 min stabilization (11 mM glucose), 35 min AHF (2.5 mM glucose, 1.5 mM palmitate) and 30 min of recovery (11 mM glucose, 1.5 mM palmitate ± 1 µM TMZ added during the recovery period. (A) heart rate, (B) left ventricular developed pressure (LVDP), (C) rate pressure product (RPP) and (D) maximal velocity of contraction (dP/dt_{max}). Values are expressed as mean ± SEM (n = 6).

However, our findings demonstrate that TMZ treatment markedly improved contractile function in the AHF diabetic hearts as indicated by the increase in LVDP during the recovery phase (Figure 7.5, $p<0.01$ *vs.* untreated AHF diabetic hearts). Untreated AHF diabetic hearts exhibit poor recovery as indicated by the LVDP data (21.8 mmHg ± 8 mmHg and 38 mmHg ± 13 mmHg) compared to TMZ-treated AHF diabetic hearts (76 mmHg ± 6 mmHg and 128 mmHg ± 24 mmHg) during the recovery phase. No significant changes were observed for heart rate, RPP and dP/dt_{max} (Figure 7.6). We also found that AHF diabetic hearts displayed a decrease in functional recovery compared to non-diabetic AHF hearts (Figure 7.6A, $p<0.05$) where it improved from 30.7% ± 5 in AHF diabetic hearts to 86.2% ± 11.2 in counterparts treated with TMZ (Figure 7.6 and Table 7.1). The dP/dt_{max} was also significantly decreased in AHF diabetic hearts (10 ± 3.9%) *vs.* ND AHF hearts (50 ± 9%) (Figure 7.6C), followed by an improvement in AHF diabetic hearts treated with TMZ (69 ± 8.4%).

For systolic and diastolic pressures we found no significant changes (Figure 7.7). Our findings also revealed an improved coronary flow in AHF diabetic hearts treated with TMZ ($p<0.001$) *vs.* untreated AHF diabetic hearts (Figure 7.8).

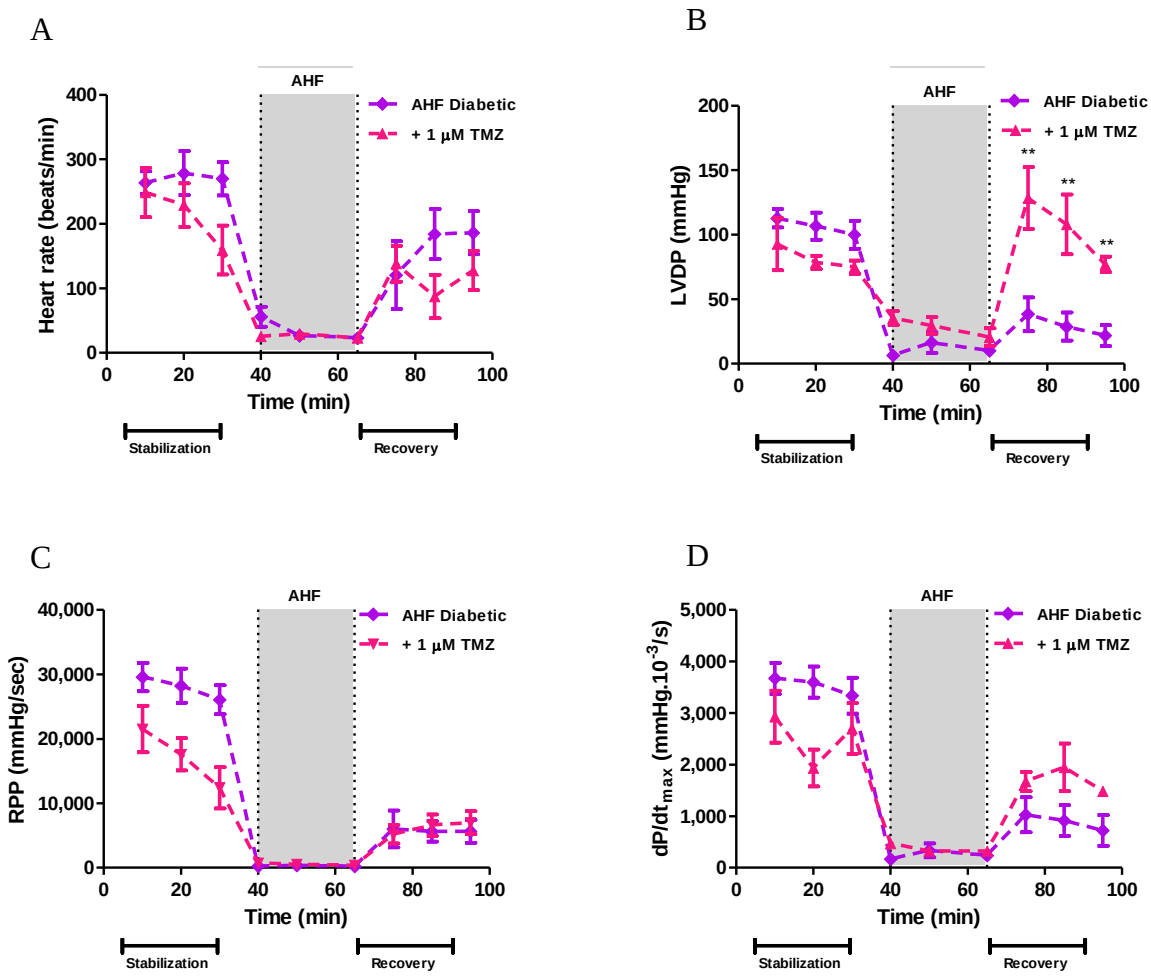

Figure 7.5. TMZ administration blunts cardiac dysfunction in diabetic rat hearts following AHF. Isolated diabetic rat hearts were perfused under simulated AHF conditions and subjected to 30 min stabilization (30 mM glucose), 35 min AHF (2.5 mM glucose, 1.5 mM palmitate) and 30 min recovery (30 mM glucose, 1.5 mM palmitate) ± 1µM TMZ added during the recovery phase. (A) heart rate, (B) left ventricular developed pressure (LVDP), (C) rate pressure product (RPP), (D) maximal velocity of contraction (dP/dt_{max}). Values are expressed as mean ± SEM (n≥5). **p<0.01 *vs.* AHF diabetic.

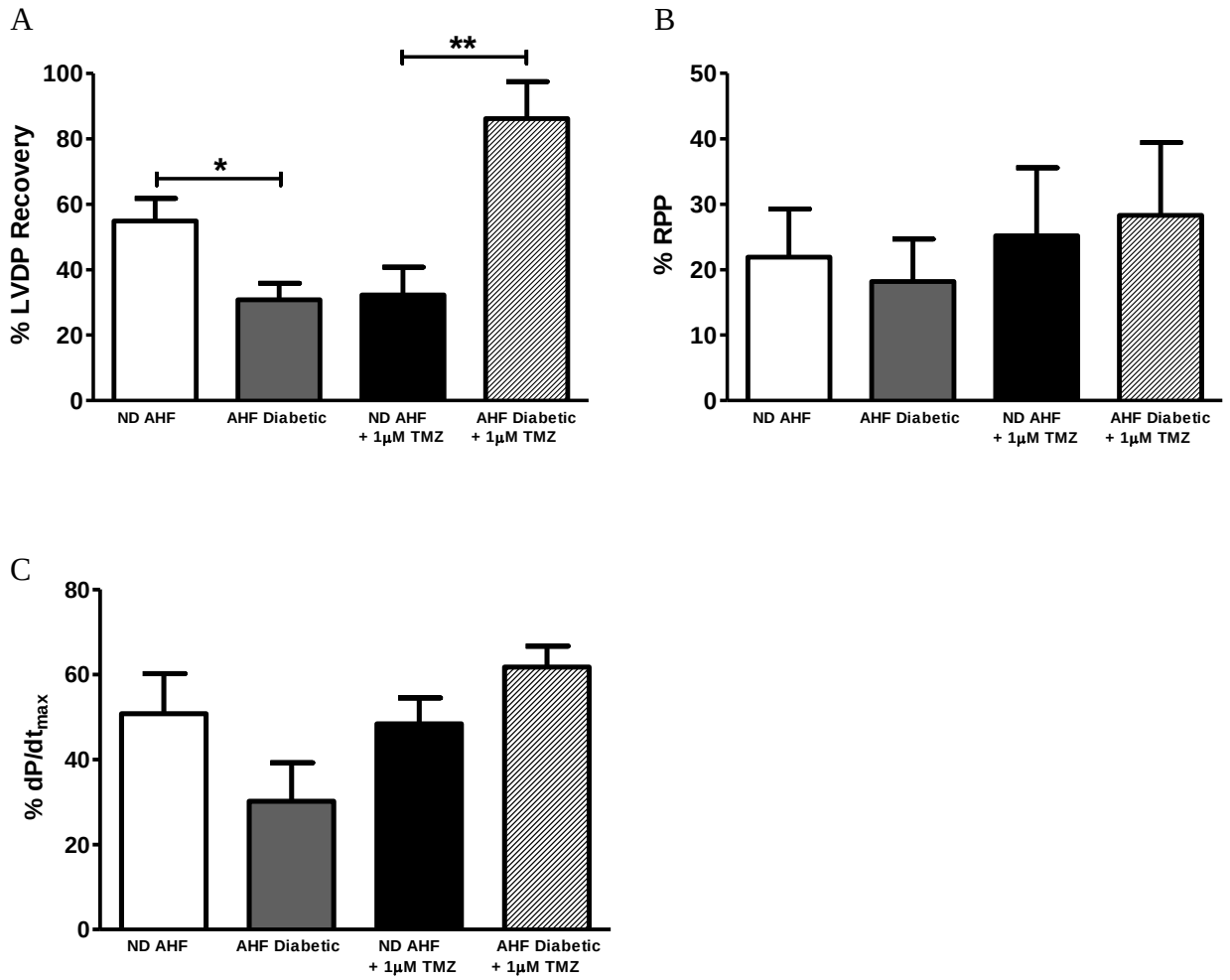

Figure 7.6. Non-diabetic and diabetic rat hearts subjected to simulated AHF showed a significant decrease in contractile function compared to non-diabetic AHF hearts demonstrated by the (A) % LVDP, (B) % RPP and % dP/dt_{max} at the 30 min time-point during the recovery phase. Isolated non-diabetic and diabetic rat hearts were subjected to simulated AHF conditions i.e. 30 min stabilization (11 mM or 30 mM glucose, non-diabetic and diabetic hearts respectively), 35 min AHF (2.5 mM glucose, 1.5 mM palmitate) and 30 min of recovery (11 mM or 30 mM glucose, 1.5 mM palmitate). *$p<0.05$ *vs.* AHF diabetic; **$p<0.01$ *vs.* AHF diabetic. Values are expressed as mean ± SEM (n = 6)

Non-diabetic and diabetic rat hearts during recovery phase (30 min)			
Treatment Group	**% LVDP**	**% RPP**	**% dP/dt_{max}**
ND AHF	54.3 ± 6.9	21 ± 7	50 ± 9
AHF Diabetic	30.7 ± 5 *	18 ± 6	30 ± 8.9
ND AHF + 1µM TMZ	32.8 ± 8.4 **	25 ± 10	48 ± 6
AHF Diabetic +1µM TMZ	86.2 ± 11.22	28 ± 11	61.7 ± 4.8

Table 7.1. The effect of TMZ in non-diabetic and diabetic hearts subjected to simulated AHF. Isolated non-diabetic and diabetic rat hearts were subjected to simulated AHF conditions, i.e. 30 min stabilization (11 mM or 30 mM glucose, non-diabetic and diabetic respectively, 35 min AHF (2.5 mM glucose, 1.5 mM palmitate) and 30 min of recovery (11 mM or 30 mM glucose, 1.5 mM palmitate). Data are shown for the 30 min recovery timepoint. *p<0.05 *vs.* ND AHF;**p<0.01 *vs.* AHF diabetic, **p<0.01 vs. AHF + 1µM TMZ. Values are expressed as % mean ± SEM (n=6).

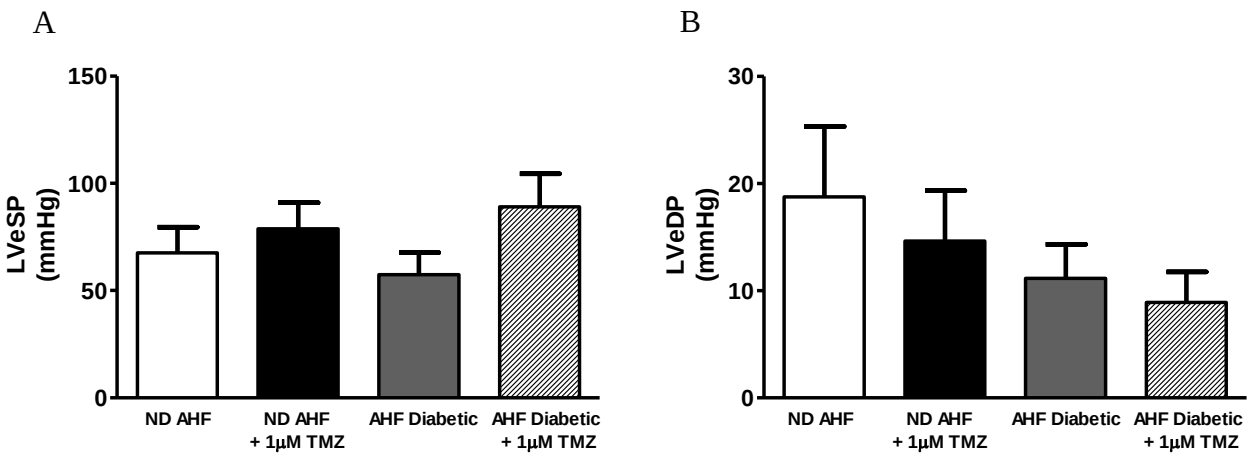

Figure 7.7. TMZ administration leads to no significant changes in systolic or diastolic pressure. Isolated non-diabetic and diabetic rat hearts were perfused under simulated AHF conditions and subjected to 30 min stabilization (11 mM or 30 mM glucose, non-diabetic or diabetic respectively), 35 min AHF (2.5 mM glucose, 1.5 mM palmitate) and 30 min recovery (11 mM or 30 mM glucose, non-diabetic or diabetic respectively, 1.5 mM palmitate) ± 1µM TMZ added during the recovery phase. (A) Left ventricular end systolic pressure (LVeSP) and (B) Left ventricular end diastolic pressure (LVeDP). Values are expressed as mean ± SEM (n=6).

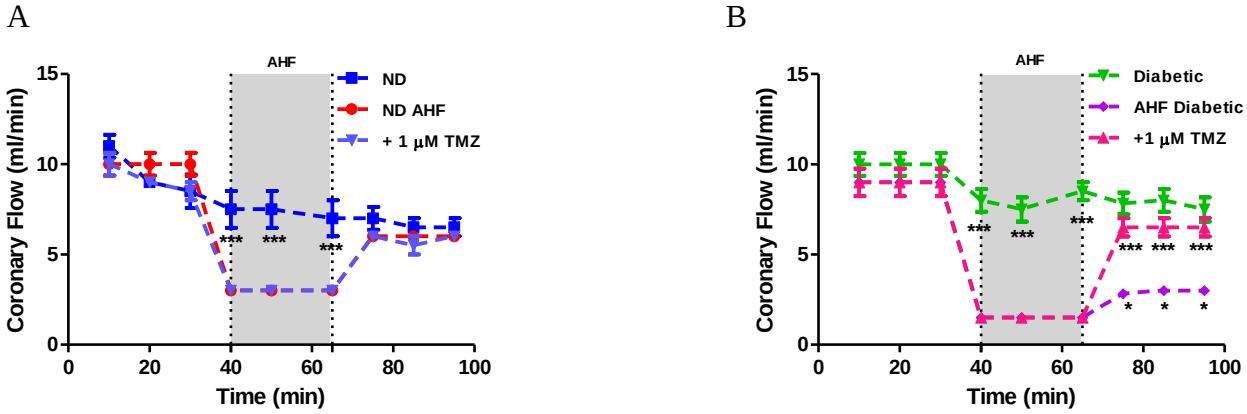

Figure 7.8. TMZ administration leads to an improved coronary flow in the diabetic heart. Isolated non-diabetic and diabetic rat hearts were perfused under simulated AHF conditions and subjected to 30 min stabilization (11 mM or 30 mM glucose, non-diabetic or diabetic respectively), 35 min AHF (2.5 mM glucose, 1.5 mM palmitate) and 30 min recovery (11 mM or 30 mM glucose, non-diabetic or diabetic respectively, 1.5 mM palmitate) ± 1µM TMZ added during the recovery phase. *p<0.05 *vs.* diabetic;***p<0.001 *vs.* AHF diabetic. Values are expressed as mean ± SEM (n=6).

Thus these data demonstrate that TMZ administration significantly improved the contractile function and coronary flow in diabetic hearts subjected to AHF. We therefore next aimed to elucidate possible mechanisms whereby TMZ may exert such cardioprotective effects.

7.3 The effect of TMZ administration on 3-KAT and PDH expression in non-diabetic and diabetic AHF hearts

The best known mechanism of action of TMZ is the inhibition of long-chain 3-KAT activity which subsequently leads to the upregulation of PDH activity to stimulate glucose oxidation (Kantor *et al*., 2000). We employed Western blot analysis to evaluate PDH, long-chain 3-KAT and UCP2 as markers for glucose oxidation, fatty acid β-oxidation and mitochondrial membrane potential respectively. These markers were evaluated in mitochondrial extracts.

Our findings show no significant changes in PDH and UCP2 expression, however, expression of 3-KAT was lower in non-diabetic AHF hearts treated (Figure 7.9) with TMZ ($p<0.05$ *vs.* non-diabetic AHF).

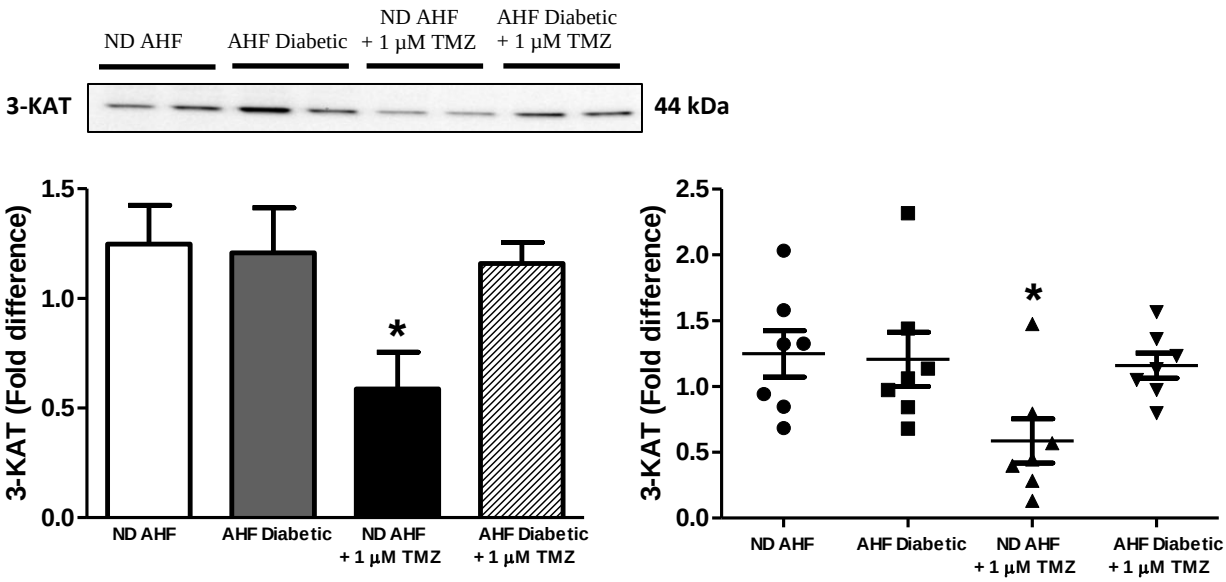

Figure 7.9. TMZ administration downregulated the expression of long chain 3-KAT. Crude mitochondria were isolated from perfused non-diabetic AHF ± TMZ and AHF diabetic ± TMZ for Western blot analysis of pyruvate dehydrogenase and long chain 3-KAT. Values are expressed as mean ± SEM (n=7). *p<0.05 *vs.* non-diabetic AHF.

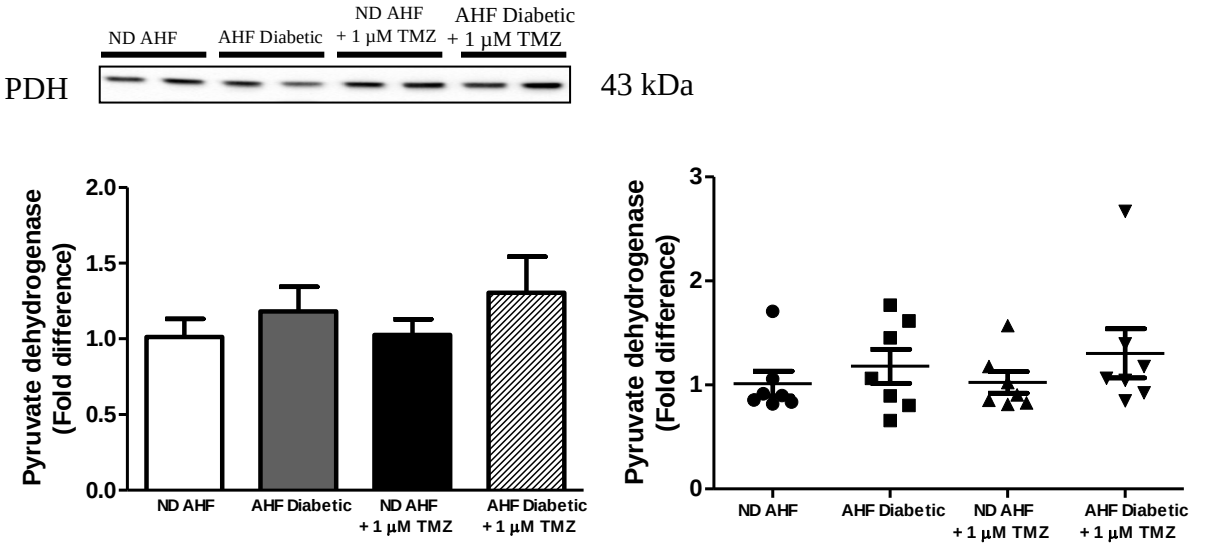

Figure 7.10. TMZ administration resulted in no changes in mitochondrial PDH expression. Crude mitochondria were isolated from perfused hearts and Western blot analysis as described. Values are expressed as mean ± SEM (n=7).

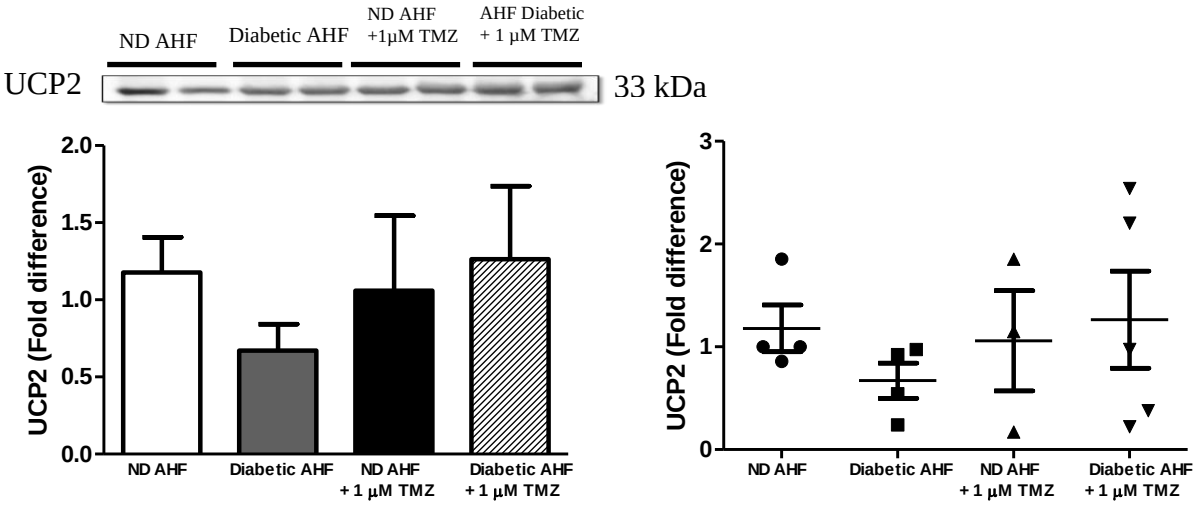

Figure 7.11. TMZ administration did not significantly alter mitochondrial UCP2 protein expression. Crude mitochondria were isolated from perfused hearts for Western blot analysis. Values are expressed as mean ± SEM (n≤5).

These data sets indicate that TMZ has no effect on the mitochondrial protein levels of PDH (Figure 7.10) and UCP2 (Figure 7.11). However, the UCP2 data may not be conclusive as the number of samples used was low and the error in the data was quite high (Figure 7.11). To gain further insights into underlying mechanism in TMZ cardioprotection, we next aimed to look at oxidative stress and apoptosis and how this was altered in our experimental system.

7.4 The effects of TMZ administration on antioxidant capacity and apoptotic regulation

As a study by Ruiz-Meana (2005) demonstrated antioxidant properties of TMZ with ischemia-reperfusion, we investigated potential antioxidant properties. Here we employed Western blot analysis to assess mitochondrial SOD2, CDs, TBARS, GSH/GSSG and ORAC as well as pBAD/BAD levels (for total protein fraction) in order to evaluate intracellular antioxidant capacity and apoptosis, respectively. Results indicate no significant changes in SOD2 expression (Figure 7.12). However, we observed an increase in pBAD/BAD (Figure 7.13) ratio in non-diabetic AHF ($p<0.05$ *vs.* untreated non-diabetic AHF) and AHF diabetic hearts ($p<0.01$ *vs.* AHF untreated diabetic) treated with TMZ versus respective non-diabetic AHF and AHF diabetic controls (Figure 7.13).

Our oxidative stress assessments showed no significant changes for CDs, a sensitive marker for early changes in oxidative stress (Figure 7.14). However, TBARS (longer-term marker for oxidative stress) were significantly higher at the end of the AHF phase (for both non-diabetic and diabetic hearts) suggesting increased oxidative stress at this phase (Figure 7.15). The GSH/GSSG was lower for non-diabetic AHF hearts while ORAC was higher for the same group (Figures 7.16 and 7.17). Of note, the latter changes were not observed for the diabetic AHF experimental group.

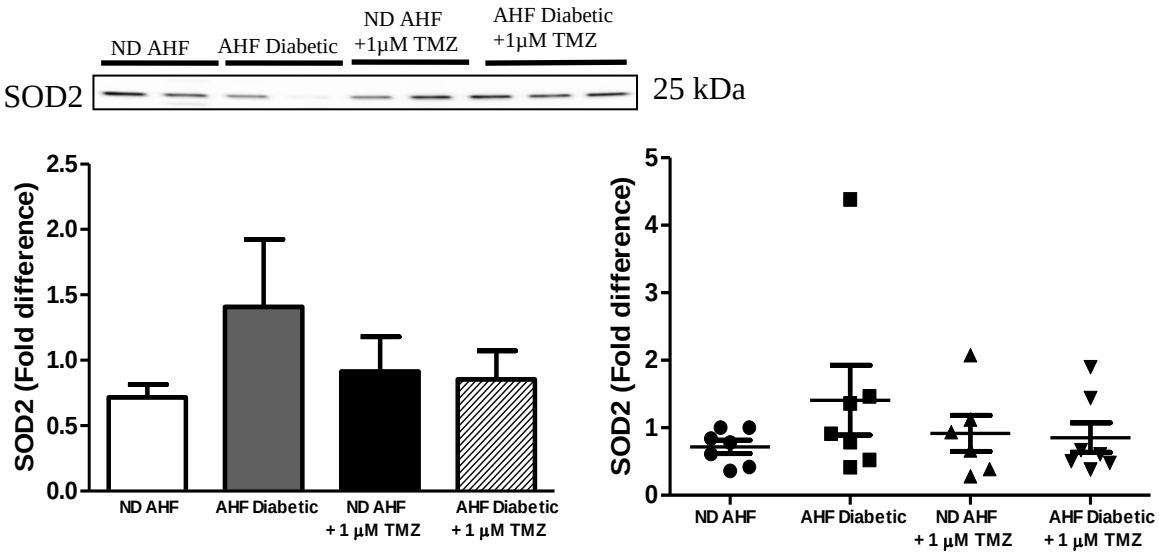

Figure 7.12. TMZ administration resulted in no significant effect on SOD2 expression. Crude mitochondria were isolated from perfused hearts and Western blot analysis as described. Values are expressed as mean ± SEM (n=7).

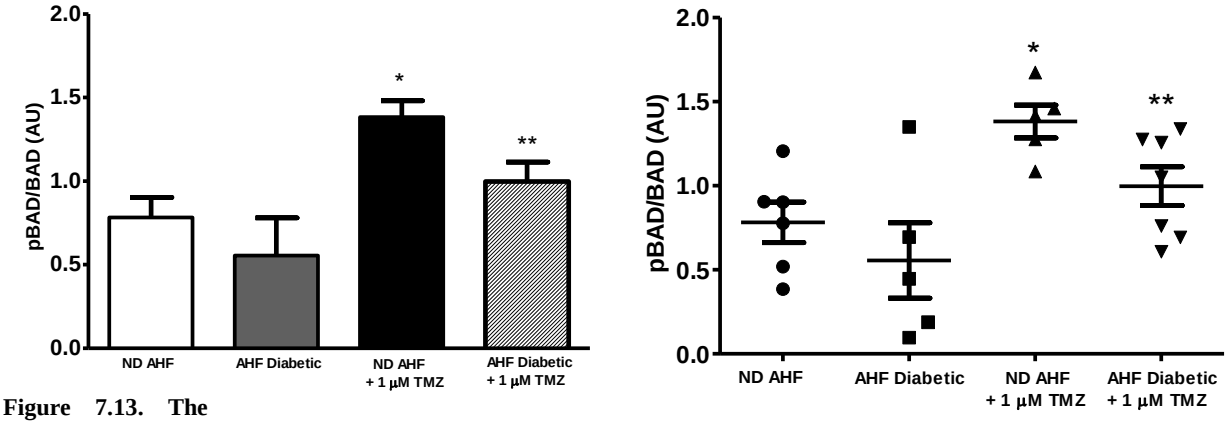

Figure 7.13. The expression of pBAD/BAD is significantly increased in non-diabetic and diabetic AHF hearts treated with TMZ. Total proteins were isolated from perfused hearts and Western blot analysis was used to evaluate the expression of pBAD/BAD. Values are expressed as mean ± SEM (n≤6). *p<0.05 *vs.* ND AHF; **p<0.01 *vs.* AHF diabetic.

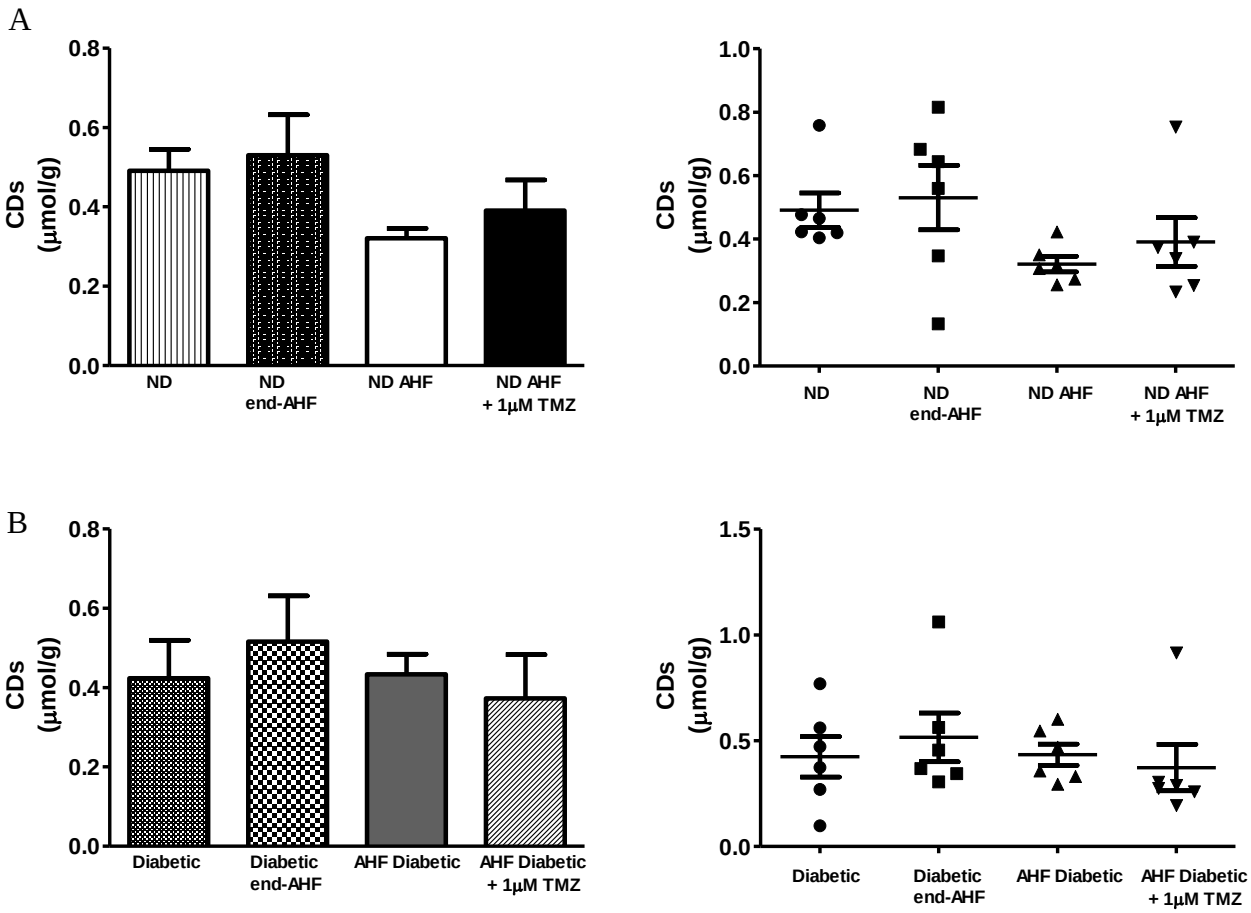

Figure 7.14. TMZ administration resulted in no significant effect on levels of conjugated dienes. Total proteins were isolated from perfused hearts and used to measure conjugated dienes. Isolated non-diabetic and diabetic rat hearts were subjected to simulated AHF conditions, i.e. 30 min stabilization (11 mM or 30 mM glucose, non-diabetic and diabetic respectively, 35 min AHF (2.5 mM glucose, 1.5 mM palmitate) and 30 min of recovery (11 mM or 30 mM glucose, 1.5 mM palmitate). An additional group was added where non-diabetic and diabetic hearts were only perfused until the end of the AHF phase (non-diabetic end-AHF and diabetic end-AHF). Values are expressed as mean ± SEM (n=6). Values were expressed as µmol/g protein.

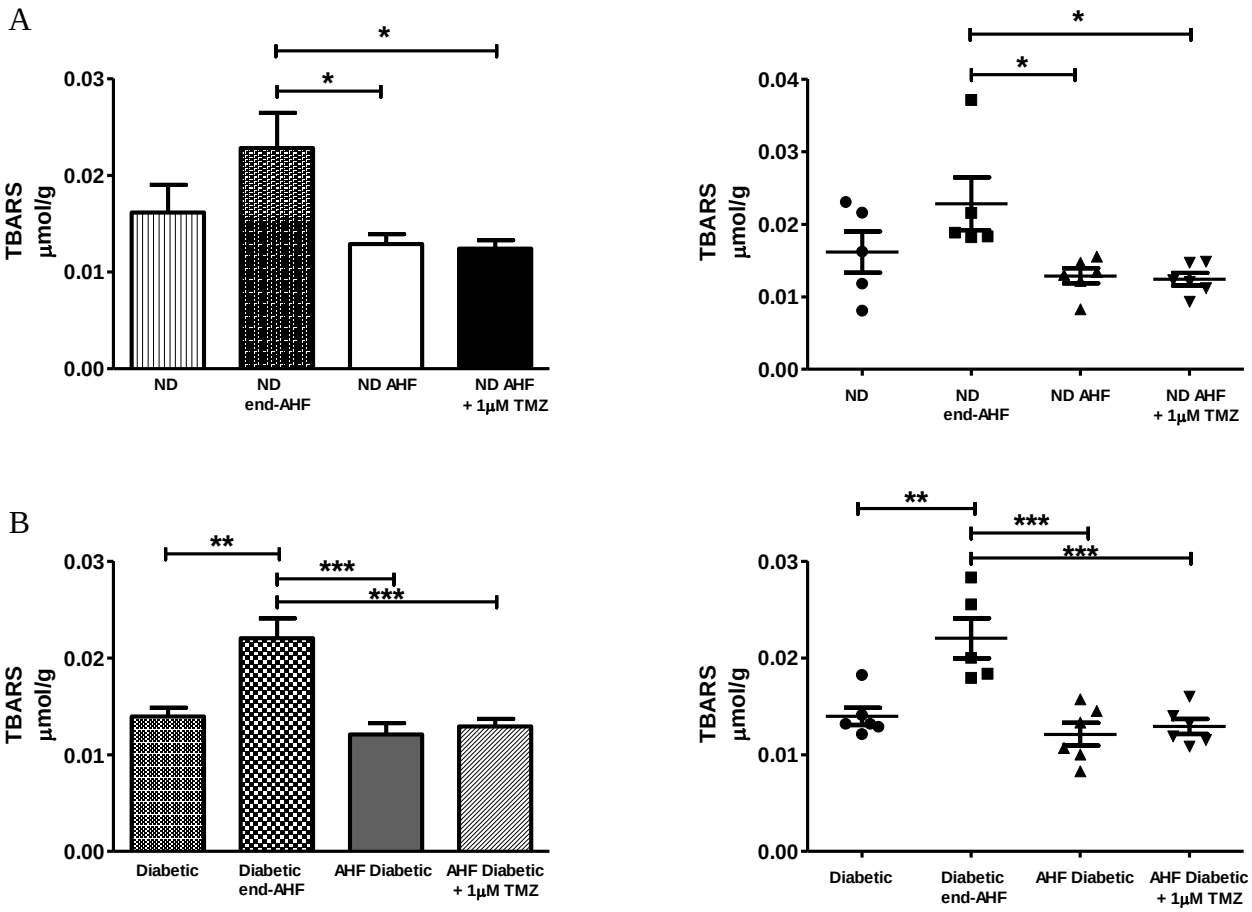

Figure 7.15. TBARS are increased during the AHF phase in non-diabetic and diabetic hearts. Total proteins were isolated from perfused hearts and used to measure TBARS. Isolated non-diabetic and diabetic rat hearts were subjected to simulated AHF conditions, i.e. 30 min stabilization (11 mM or 30 mM glucose, non-diabetic and diabetic respectively, 35 min AHF (2.5 mM glucose, 1.5 mM palmitate) and 30 min of recovery (11 mM or 30 mM glucose, 1.5 mM palmitate). An additional group was added where non-diabetic and diabetic hearts were perfused only until the end of the AHF phase (non-diabetic end-AHF and diabetic end-AHF). Values are expressed as mean ± SEM (n=6).Values were expressed as µmol/g protein. *p<0.05 *vs*. ND AHF + 1µM TMZ;**p<0.01 vs. Diabetic end-AHF; ***p<0.001 vs. AHF Diabetic + 1 µM TMZ.

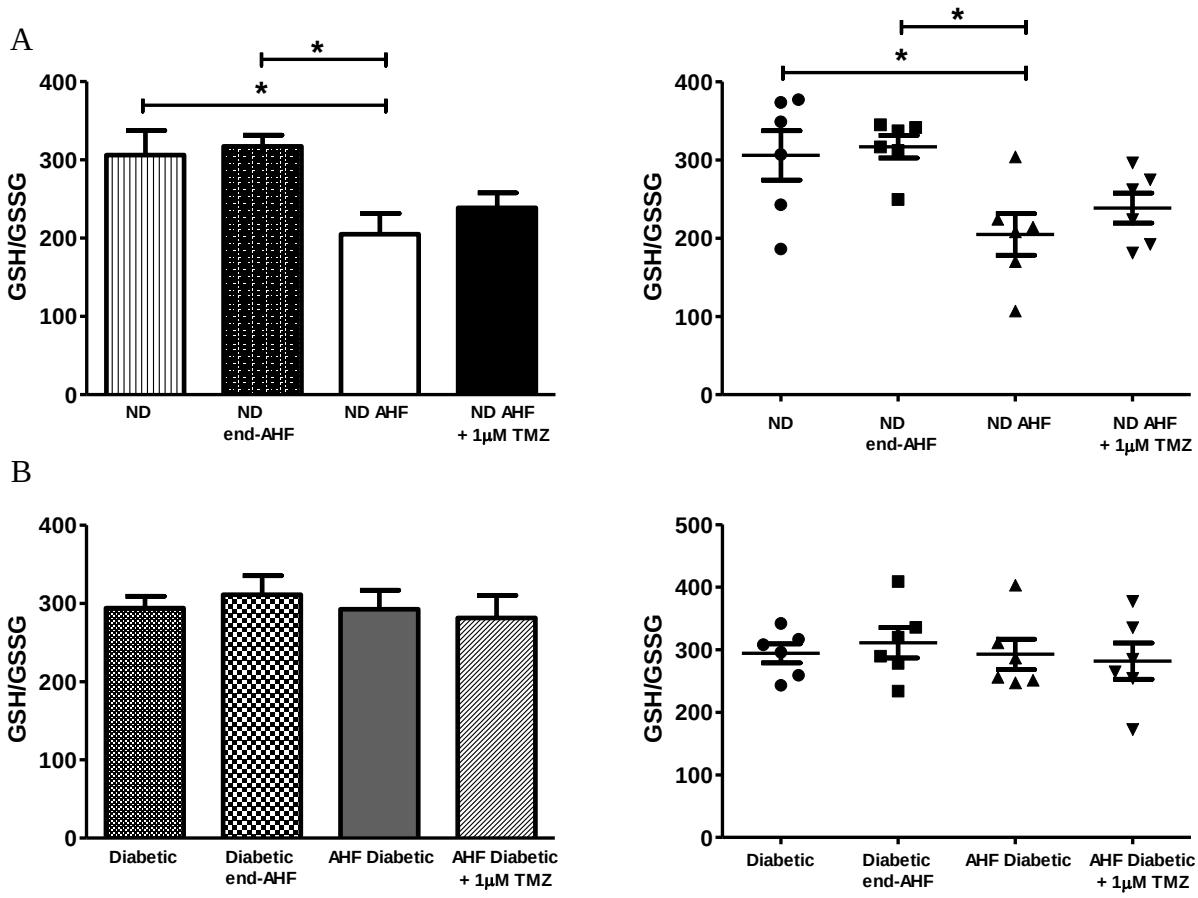

Figure 7.16. TMZ treatment and changes in GSH/GSSG. Total proteins were isolated from perfused hearts and used to measure conjugated dienes. Isolated non-diabetic and diabetic rat hearts were subjected to simulated AHF conditions, i.e. 30 min stabilization (11 mM or 30 mM glucose, non-diabetic and diabetic respectively, 35 min AHF (2.5 mM glucose, 1.5 mM palmitate) and 30 min of recovery (11 mM or 30 mM glucose, 1.5 mM palmitate). An additional group was added in which non-diabetic and diabetic hearts were only perfused until AHF (non-diabetic end-AHF and diabetic end-AHF). Values are expressed as mean ± SEM (n=6).

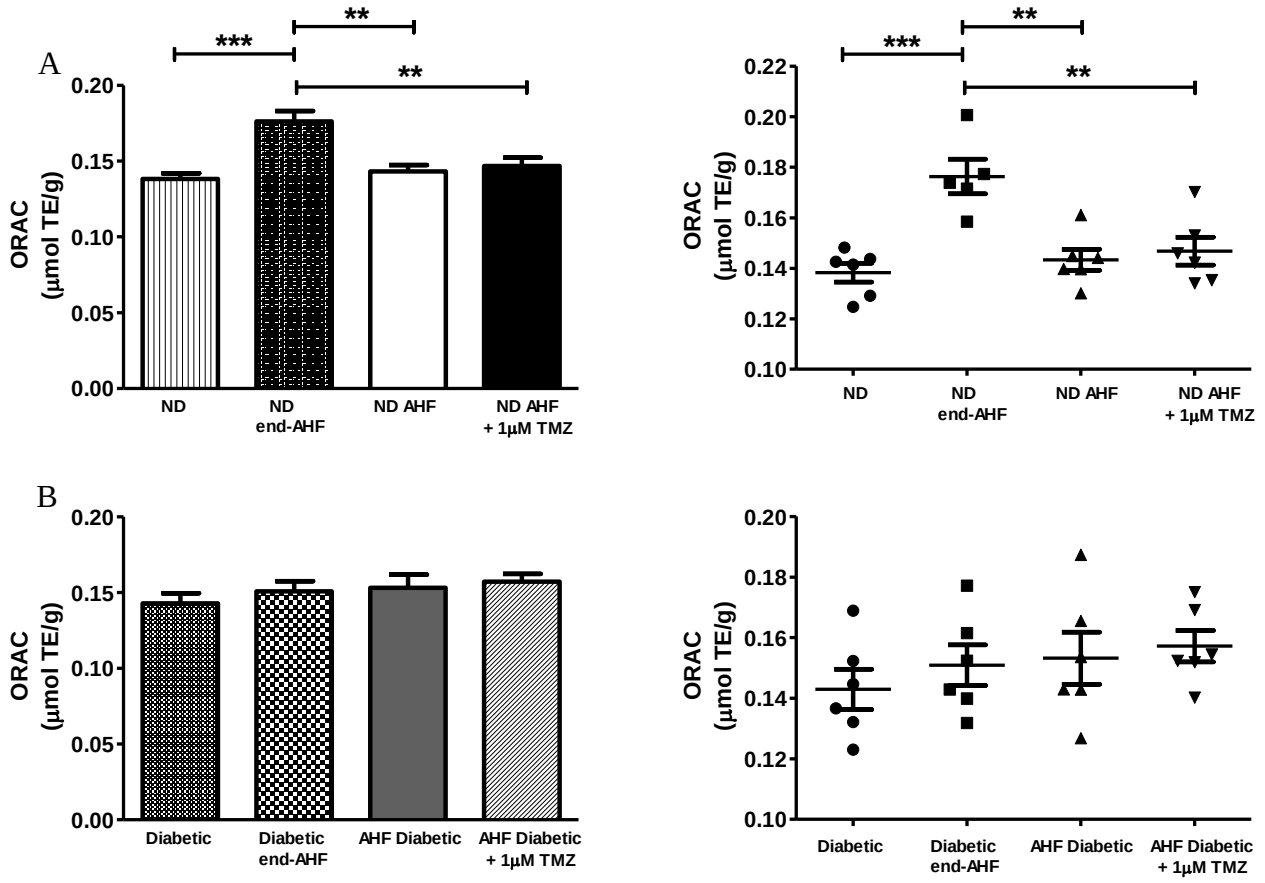

Figure 7.17. Hearts subjected to simulated AHF conditions and ORAC changes. Isolated non-diabetic and diabetic rat hearts were subjected to simulated AHF conditions i.e 30 min stabilization (11 mM or 30 mM glucose, non-diabetic and diabetic respectively, 35 min AHF (2.5 mM glucose, 1.5 mM palmitate) and 30 min of recovery (11 mM or 30 mM glucose, 1.5 mM palmitate). An additional group was added in which non-diabetic and diabetic hearts were only perfused until AHF (Non-diabetic end-AHF and diabetic end-AHF). Values are expressed as mean ± SEM (n=6).

7.5 Evaluation of NOGP activation in hearts subjected to AHF

We next determined the effects of NOGP activation on hearts subjected to AHF and how this may be altered with TMZ administration. Here we initially evaluated methylglyoxal as a marker of the AGE pathway. AHF diabetic hearts treated with TMZ, showed a significant decrease in methylglyoxal ($p<0.05$ *vs.* AHF diabetic) (Figure 7.18). However, we observed no changes in AGE protective systems GLO-I (Figure 7.19), RAGE (Figure 7.20) and FN3K (Figure 7.21) expression.

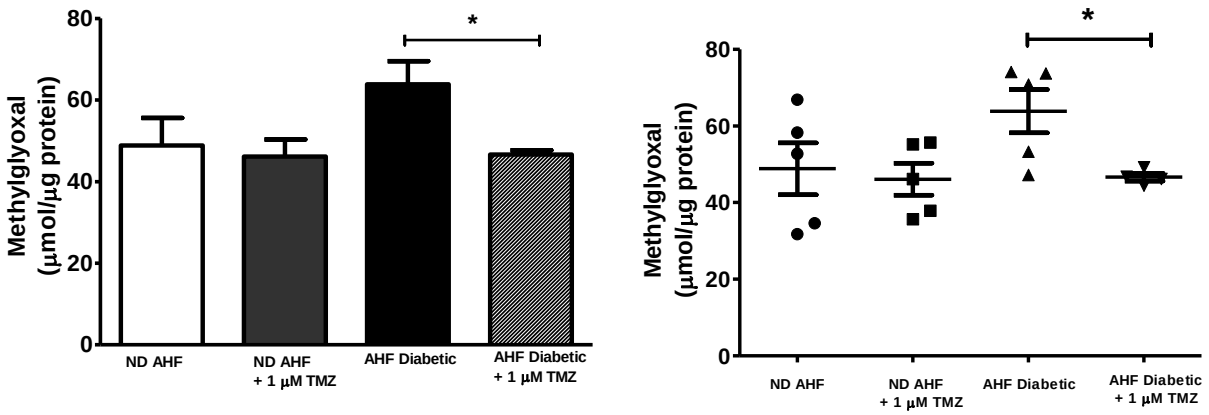

Figure 7.18. Methylglyoxal levels were downregulated in AHF diabetic hearts treated with TMZ. Values are expressed as mean ± SEM ($n\leq6$). *$p<0.05$ *vs.* AHF diabetic.

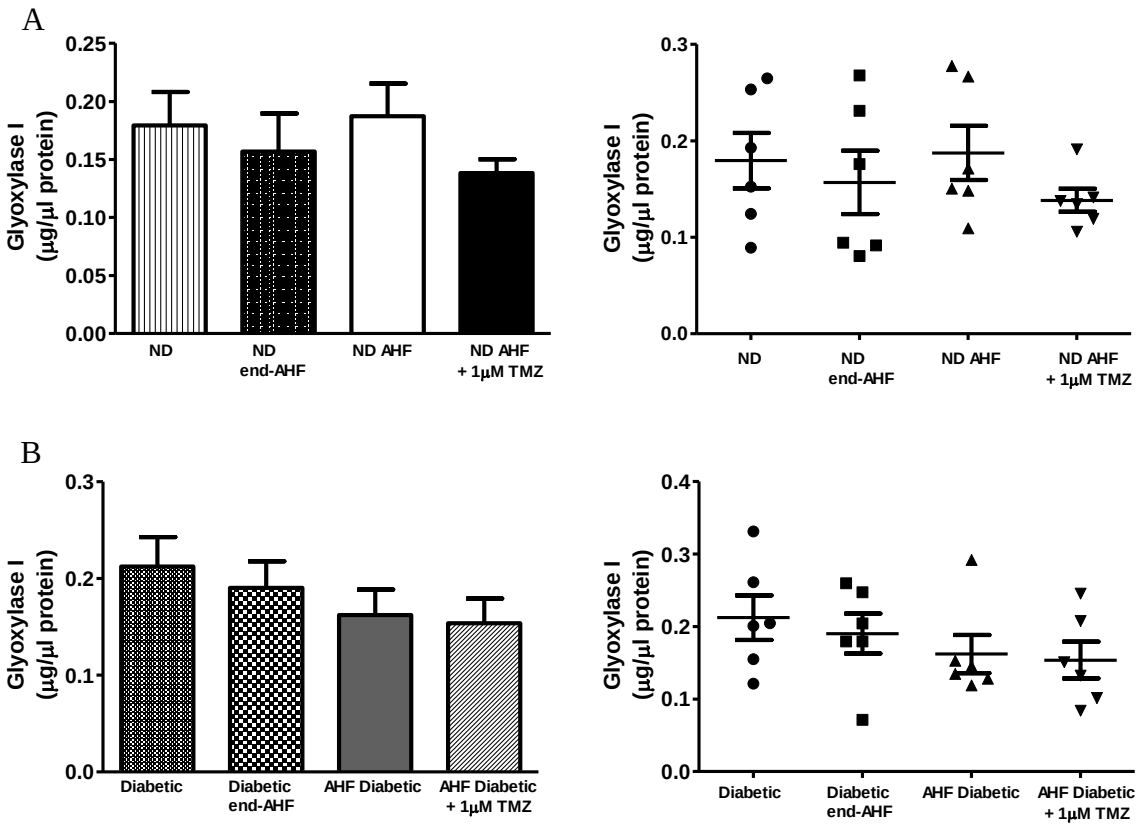

Figure 7.19. Trimetazidine administration has no effect on glyoxylase I. Values are expressed as mean ± SEM (n=6).

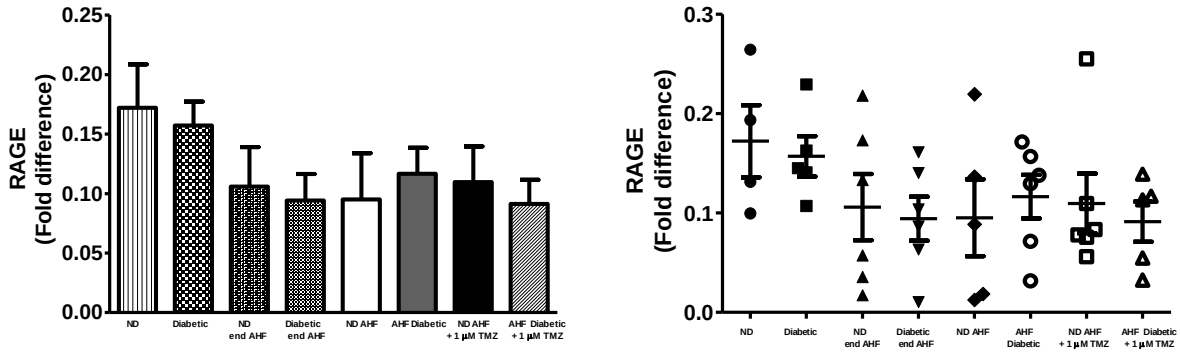

Figure 7.20. Trimetazidine administration has no significant effects on the expression of the receptor for advanced glycation end products. Total protein was extracted and subjected to Western blot analysis. Values are expressed as mean ± SEM (n=6).

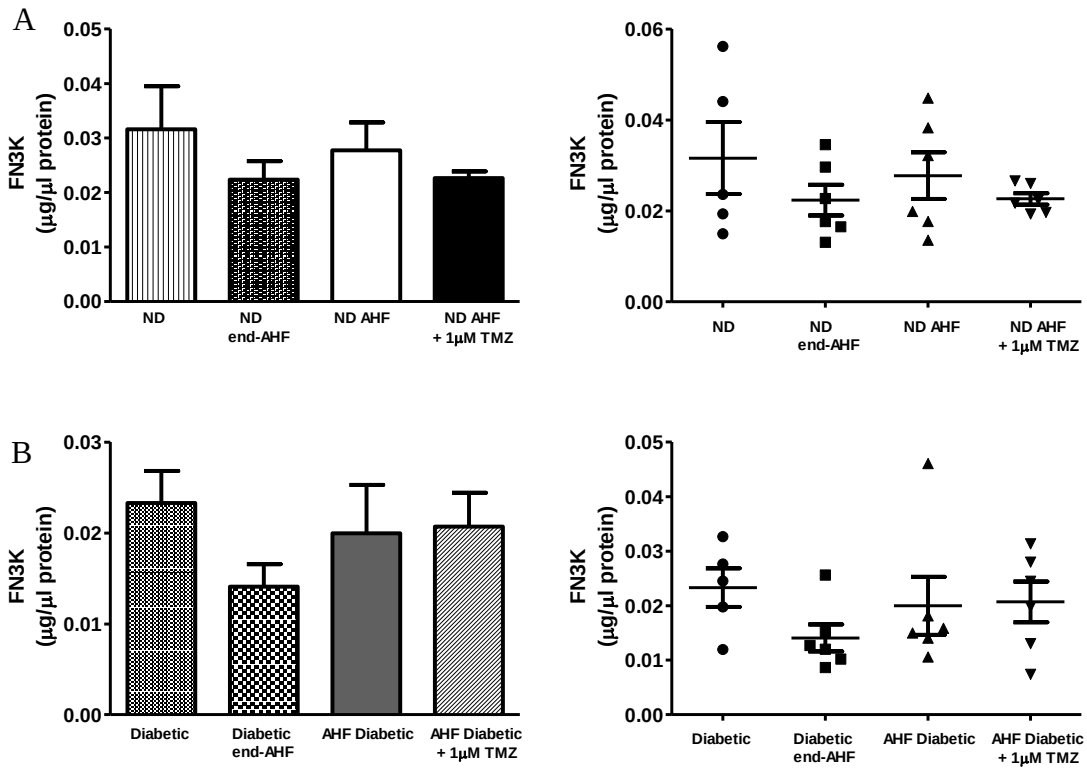

Figure 7.21. Fructosamine-3-kinase levels remain unchanged in non-diabetic and diabetic AHF hearts ± TMZ. Values are expressed as mean ± SEM (n≤6).

We also assessed activation of the polyol pathway that was upregulated in AHF diabetic hearts subjected to TMZ treatment (Figure 7.22).

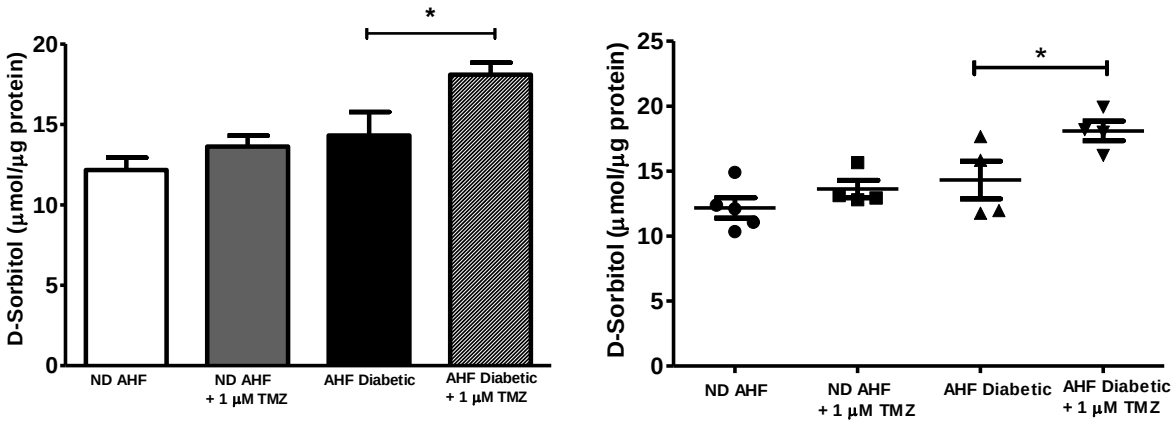

Figure 7.22. Polyol pathway assessment (D-sorbitol levels) with AHF ± TMZ treatment. Values are expressed as mean ± SEM (n≤6). *p<0.05 *vs.* AHF diabetic.

7.6 Evaluation of oxidative stress in an *in vitro* setting using H9c2 rat cardiomyoblasts

Since the in SOD2 expression data did not reveal useful information regarding the potential antioxidant effects of TMZ, we further evaluated this within an *in vitro* setting. Here we used H9c2 cells treated ± palmitate ± TMZ and assessed the levels of intracellular ROS (DCF staining) and mitochondrial (MitoSOX staining) ROS levels by flow cytometry. Our results indicate that treatment of H9c2 cells with palmitate leads to increased mitochondrial ROS (p<0.01 *vs.* control) and that TMZ attenuates this (Figure 7.23 B). Of note, our treatments elicited no significant effect on total intracellular ROS as determined by DCF staining (Figure 7.23 A).

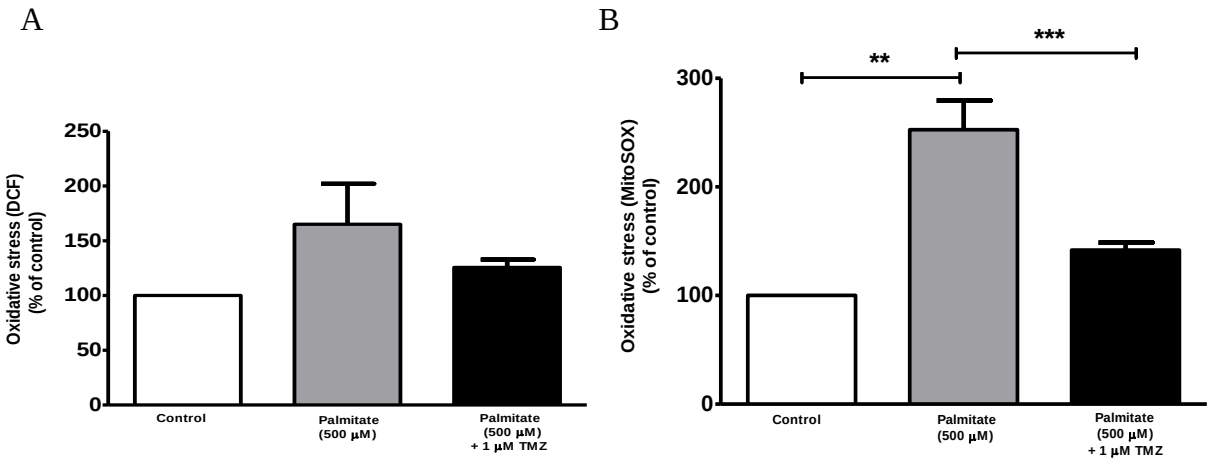

Figure 7.23. Mitochondrial ROS is lowered in response to TMZ treatment. H9c2 cells were subjected to 500 µM palmitate treatment for 21 hours and treated with TMZ for the next 3 hours. (A) Total intracellular ROS (DCF), (B) Mitochondrial ROS (MitoSOX). Values are expressed as mean ± SEM (n≥5). **p<0.01 *vs.* control; ***p<0.001 *vs.* control.

7.7 Increased caspase 3/7 activity in response to palmitate treatment in H9c2 cells

To further elucidate the protective effects of TMZ treatment we next evaluated caspase 3/7 activity, hydroxyacyl-CoA dehydrogenase (HADHA/HADHB) and acyl-CoA dehydrogenase very long chain (ACADVL) as markers of apoptosis and FA oxidation, respectively. Our results indicate that H9c2 cells treated with palmitate displayed an increase in caspase 3/7 activity (p<0.001 *vs.* control) (Figure 7.24 A). However, there were no significant differences with TMZ treatment as well as for HADHA/HADHB and ACADVL expression levels (Figure 7.24 B and C).

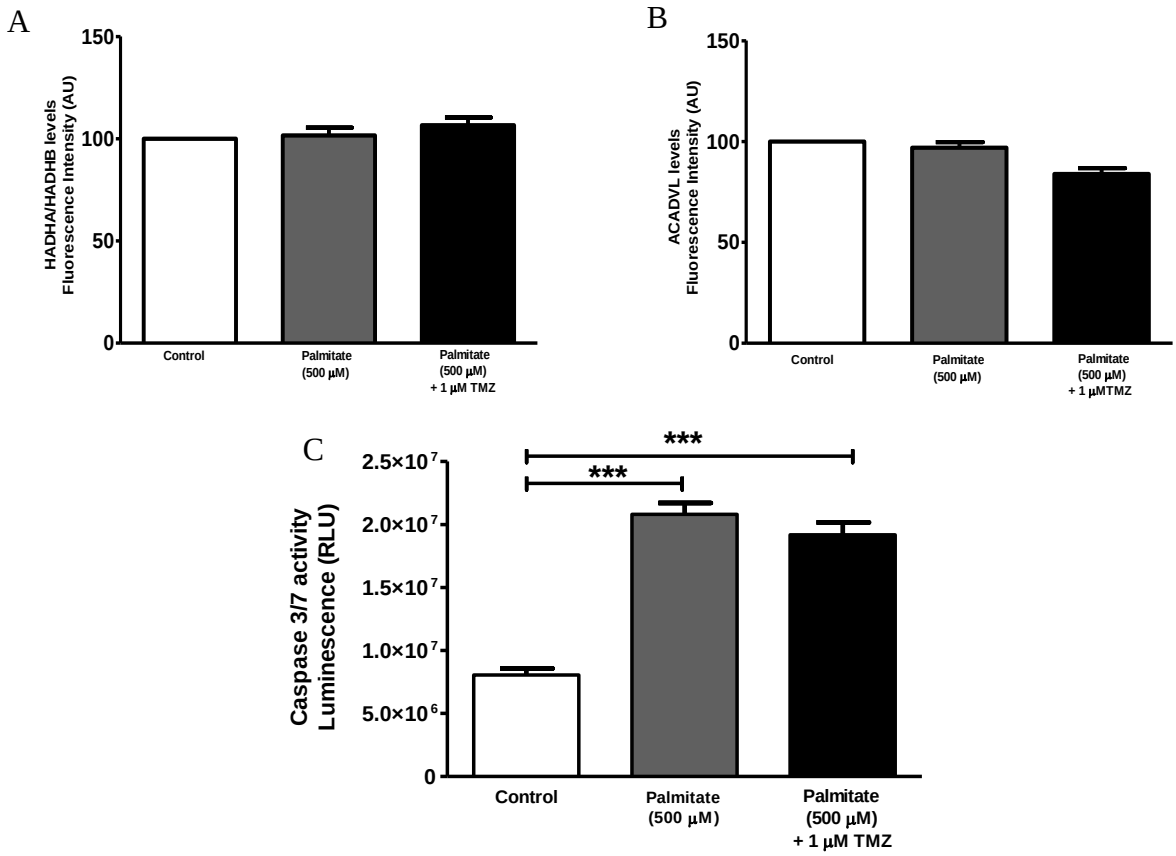

Figure 7.24. Palmitate treatment increased caspase 3/7 activity. H9c2 cells were subjected to 500 µM palmitate treatment for 21 hours and treated with TMZ for an additional 3 hours. (A) HADHA/HADHB levels, (B) ACADVL levels, (C) Caspase 3/7 activity.

8 CHAPTER 8

Discussion

AHF is a complex life-threatening complex condition that requires rapid therapeutic interventions in order to alleviate associated, damaging outcomes (McMurray *et al*., 2013). However, current AHF treatments primarily focus on providing hemodynamic stabilization and symptomatic relief (Nieminen, 2005). As such therapies can elicit detrimental side-effects (refer Chapter 4 of this thesis) there is an urgent need for the development of novel therapeutic interventions. For this study we therefore focused on metabolic modulation and investigated the anti-anginal drug TMZ as a therapeutic intervention for AHF. TMZ classically functions by inhibiting FA β-oxidation and favoring glucose oxidation (Kantor *et al*., 2000) that should limit the damaging effects of FAs that occur with HF (Essop and Opie, 2004). ***We thus hypothesized that acute TMZ treatment offers cardioprotection to diabetic rat hearts subjected to ex vivo AHF.*** The main outcomes of this study were: 1) the successful establishment of an *ex vivo* diabetic rat model of AHF; 2) TMZ blunts cardiac dysfunction in diabetic hearts subjected to AHF; and 3) TMZ treatment downregulates myocardial AGEs in diabetic hearts exposed to AHF. 4) Our cell data indicate that TMZ may mediate some of its cardioprotective effects by attenuating ROS.

8.1 The successful establishment of an *ex vivo* diabetic rat model of AHF

We initially set out to establish an *ex vivo* perfusion diabetic rat model of *de novo* AHF that consists of three components, i.e. 1) stabilization phase - characterized by a perfusion pressure of 100 cm H_2O where the sole fuel substrate was either 11 mM glucose (non-diabetic hearts) or 30 mM glucose (diabetic hearts); 2) AHF phase - characterized by lowering the perfusion pressure to 20 cm H_2O and the glucose concentration in the perfusate to 2.5 mM. In parallel, FFA availability was raised to supraphysiological concentrations (1.5 mM) to mimic elevated levels usually found in the failing heart; and 3) recovery phase - perfusion is returned to 100 cm H_2O without altering the palmitate (1.5 mM) concentration, while glucose availability is restored to 11 mM and 30 mM for non-diabetic and diabetic hearts, respectively (Figure 6).

To our knowledge this is one of a few, if not the first, to establish an *ex vivo* model of AHF for the diabetic rat heart. This developmental component of this study was very challenging and technically demanding. This consumed a substantial amount of time allocated for completion of the study. However, after repeated attempts and optimization steps we were able to successfully establish the model in our laboratory and this advance should now facilitate testing of additional therapeutic agents in the setting of *ex vivo* AHF. We also provide additional insights into the *ex vivo* AHF model as we now include assessments of changes at the end of the AHF phase. Here the collective data show a sharp decline in heart function together with lower coronary flow following AHF. Of note, changes in our coronary flow (Figure 7.8) data were expected as pressures are reduced in our model of AHF - to 20 cm H_2O. The reduction in coronary flow during the AHF phase isn't as a result of heart failure but rather the reduction in the perfusion

pressure. In addition, there is increased apoptosis (pBAD/BAD) (Figure 7.13). However, there was no evidence of increased infarct sizes (Figure 7.3) in both non-diabetic and diabetic perfused hearts. Of note, an *ex vivo* ischemia-reperfusion model is also accompanied by a low-flow phase as in our AHF model. What are the differences between our AHF model and a ischemia-reperfusion model? The *ex vivo* ischemia-reperfusion model has either global or regional ischemia with reduced oxygen and nutrient supply to the heart. In comparison to our AHF model; our low-flow phase has constant oxygenated nutrient supply to the heart. Secondly ischemia is often accompanied by necrosis which is absent in our model. This was a somewhat unexpected finding as we postulated increased necrosis following AHF. We are unclear why this may be the case and suggest that additional experiments be completed with larger sample sizes in order to confirm whether this is indeed the case. In addition, an assessment of both molecular and histological markers of necrosis may also provide further insights into this issue. We also found that there is evidence of increased oxidative stress after AHF (higher TBARS) – in both diabetic and no-diabetic hearts (Figure 7.15). In support, there is increased ORAC (Figure 7.17) in non-diabetic hearts indicating an attempt to counteract this stress. However, this was not found in the diabetic heart and suggests that this could potentially compromise its ability to recover optimally during the recovery phase. This may therefore be a potential reason why diabetic hearts show greater impairment during the recovery phase when compared to non-diabetic counterparts. However, the GSH/GSSG (Figure 7.16) data do not support this notion as non-diabetic hearts exhibited lower levels after AHF. We are unclear why this may be the case and further studies are required to validate this finding.

How does the current model differ from the well-established ischemia-reperfusion experimental system? The AHF model has a constant flow of CO_2/O_2 gassed nutrient Krebs buffer throughout all three phases of the protocol that distinguishes it from the classical ischemic heart protocol. For the latter, ischemia is simulated by decreasing or completely cutting off the flow of oxygenated nutrients to the heart (Sakai *et al*., 2016). In our opinion, this is one of the key factors that distinguishes the *ex vivo* AHF model from a classic ischemia-reperfusion model.

Our functional data revealed a robust decrease in contractile function during the AHF phase for both non-diabetic and diabetic hearts (Figure 7.1 and 7.2). These data (for non-diabetic hearts) are in agreement with the *ex vivo* rat model established by others (Opie *et al*., 2010). The findings also demonstrate that the combination of diabetes together with AHF results in a more damaging outcome compared to the non-diabetic AHF hearts and may occur due to a lack of anti-oxidant capacity. The established model is therefore ideal to further test therapeutic interventions for conditions where diabetes co-presents with AHF.

8.2 TMZ blunts cardiac dysfunction in diabetic hearts subjected to AHF

When TMZ was acutely administered we found that it blunted cardiac dysfunction only in the diabetic heart. Here such treatment improved contractile functional parameters during the recovery period (Figure 7.5). With regard to LVeSP and LVeDP we observed a trend where the systolic pressure was slightly elevated and the diastolic pressure decreased in AHF diabetic TMZ hearts, although not statistically significant (Figure 7.7). The latter indicates a potential improvement in the filling of the heart. As the model generated is novel, there are no published

animal studies that will allow for a comparative analysis of findings generated in this study. However, there are clinical studies that agree with our data. For example, some demonstrated improved contractility in the diabetic heart by TMZ treatment (Rosano *et al*., 2006), while others showed that it decreased FA oxidation and increased glucose oxidation in diabetic patients with chronic HF, together with improved cardiac function (Monti *et al*., 2006).

TMZ classically functions by selectively inhibiting long-chain 3-KAT, the final enzyme in the FA β-oxidation spiral (Kantor *et al*., 2000) and this in turn increases glucose oxidation by upregulating PDH. In light of this, we assessed the cardiac expression levels of long-chain 3-KAT and PDH. The 3-KAT protein levels were lower with AHF as expected, although this was not the case for AHF together with diabetes (Figure 7.9). Moreover, PDH protein levels were not significantly altered by TMZ treatment (Figure 7.10). Of note, MacInnes *et al*. (2003) found that TMZ did not inhibit long-chain 3-KAT enzyme activity as expected (MacInnes *et al*., 2003) and the authors suggested that TMZ may exert its beneficial effects by other mechanisms. We are uncertain why TMZ treatment resulted in differences in 3-KAT expression data (AHF versus AHF + diabetes) and found no additional literature to further help elucidate such discordant findings. In light of this, we propose that future studies should a) determine 3-KAT and PDH enzyme activities and b) evaluate additional TMZ targets.

8.3 TMZ may mediate some of its therapeutic effects by attenuating the AGE pathway

As the failing heart is also associated with diminished mitochondrial respiration, greater ROS production and increased apoptosis we evaluated protein expression levels of several markers of

such processes. Here the data revealed a significant increase in pBAD/BAD expression in both non-diabetic and diabetic hearts treated with TMZ. These findings therefore show that TMZ triggers anti-apoptotic effects in acutely failing hearts. Of note, the effect was observed in both non-diabetic and diabetic hearts, although TMZ did not result in improvement of cardiac function in the former group. Thus it is likely that TMZ is also acting on other damaging pathways that are specifically activated within the diabetic heart. TMZ did not exert any significant anti-apoptotic effects our *in vitro* model (H9c2 cardiomyoblasts) - in response to high FA availability. Although there was a modest decrease in caspase activity with TMZ treatment, this effect was not statistically significant. The differences between apoptosis data generated by the *ex vivo* and *in vitro* models may be due to the nature of experimental systems (*in vitro* versus *ex vivo*), different TMZ dosages employed and also the length of treatments. Further studies are required to reveal the precise reasons for such differences.

As a study by Ruiz-Meana (2005) demonstrated antioxidant properties of TMZ with ischemia-reperfusion (Ruiz-Meana, 2005), we investigated its potential antioxidant capacity by completing various assessments. To gain additional insights, we evaluated the direct effects of TMZ on oxidative stress in H9c2 cardiomyoblasts. Here TMZ treatment resulted in a significant decrease in mitochondrial ROS generation (Figure 7.24) and this finding is consistent with the premise that it acts on additional intracellular targets to elicit its therapeutic effects. However, our data generated from heart tissues collected at the end of the recovery phase are not consistent with the *in vitro* findings. Here we found that TMZ treatment did not result in significant changes for any of the oxidative stress markers evaluated in this study. Thus the question whether TMZ indeed acts as an anti-oxidant mediator in our experimental system remains unclear and further studies

are required to resolve the matter. We propose that a time-dependent study be conducted where heart tissues are collected at various time intervals following the AHF phase. It is possible that TMZ effects may occur relatively earlier-on during the recovery phase and may thus be missed by the time measurements are done at the end of the recovery phase. It is interesting to speculate, however, that TMZ is likely to act as an anti-oxidant but that this occurs shortly after the AHF phase in especially diabetic hearts, as the latter did not show the increased ORAC response after AHF (as for non-diabetic hearts). This makes for an interesting hypothesis to be further investigated.

It is also likely that by blunting FA oxidation in diabetic-AHF hearts TMZ should lower ROS production and downstream effects such as cardiac apoptosis (Essop and Opie, 2004). In parallel, TMZ may also act directly on the machinery that regulates cardiac oxidative stress. As oxidative stress depends on the balance between the generation of free radicals (largely by mitochondria) and its removal by anti-oxidant systems, additional *in vitro* studies are required to more directly test this proposal. Our data suggest that TMZ likely acts by limiting mitochondrial ROS generation (Figure 8.1) and not via the antioxidant surveillance systems as SOD2 expression levels, CDs, TBARS and ORAC did not change especially during the recovery phase.

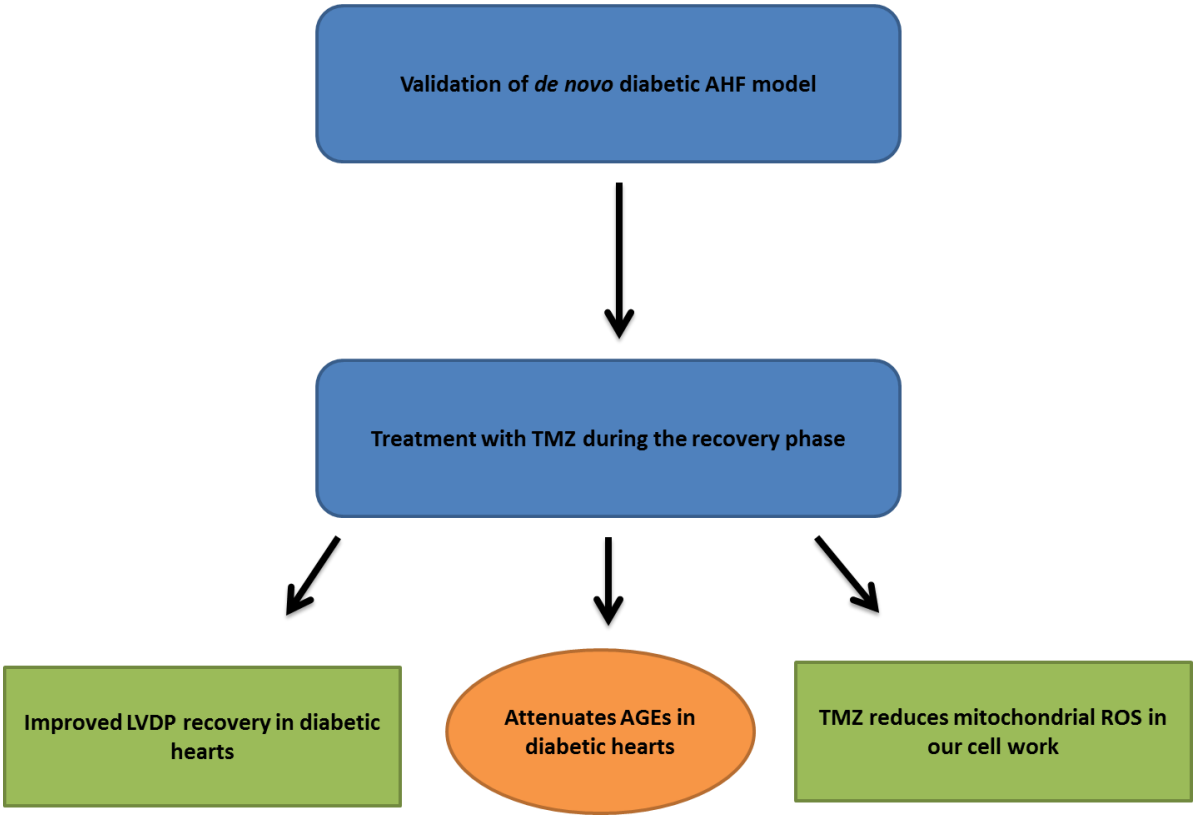

Figure 8.1. Treatment with TMZ improves recovery in diabetic hearts subjected to AHF

Since our laboratory previously implicated NOGPs as key mediators of diabetes-induced damage to the heart (Mapanga and Essop, 2015), we investigated the effects of TMZ on the AGE and polyol pathways. Here TMZ treatment resulted in a significant decrease in myocardial AGEs together with increased polyol pathway activation in diabetic-AHF hearts. The finding of higher polyol pathway activation (Figure 7.22) with TMZ treatment was surprising as this usually associated with damaging effects on the diabetic heart (Mapanga and Essop, 2015). We are uncertain regarding the mechanism of such activation and one possibility may be that as glucose metabolism increases there may be some ‘’spill over’’ into the polyol pathway. However, additional studies are required to assess the link between TMZ and activation of the polyol

pathway in the diabetic heart. Our laboratory recently proposed that AGEs are the most damaging of the NOGPs in the diabetic heart (Mapanga and Essop, 2015) and hence it is likely that additional cardio-protective effects of TMZ may be mediated by blunting of this pathway. In agreement, AGEs are implicated in the progression of HF and may result in both vascular and cardiac changes (Hartog *et al*., 2007). In support, Brownlee and colleagues established that the diabetic heart is associated with increased myocardial AGEs (Brownlee and Cerami, 1981). How does TMZ decrease the AGE pathway? This is unknown at present as this is the first study to uncover this link. We attempted to address this question by completing an evaluation of various markers of the AGE pathway but found no significance. Together our data suggest that TMZ likely does not exert its protective effects via the AGE pathway and hence it may acting via alternative pathways not here investigated. It is possible that the antioxidant effects of TMZ may lead to decreased AGE activation, as previously highlighted the link of ROS-mediated AGE activation with diabetes (Mapanga and Essop, 2015).

As previously mentioned our AHF model was adapted from an existing AHF model established by Deshpande *et al*., 2010. These authors focused on deciphering molecular markers and in addition they used pacing and altered concentrations of adrenaline, calcium, glucose and increased FA during AHF phase. In our study we focused on increased FA and reduced glucose in our perfusate to mimic metabolic alterations that occur in the failing heart. In addition the core of our model was that it was a diabetic AHF model of AHF. Seeing as though diabetes is accompanied with increased mortality in CVD inclusive of metabolic derangements such as reduced glucose uptake and elevated blood glucose and FAs (Aronson *et al*., 1997; Malmberg, 1997; Nesto and Zarich, 1998).The advantage of our model is to our knowledge it's the first to

test diabetic hearts in the context on AHF and this adds great value to our current knowledge. This opens an exciting opportunity for further studies in the field. However, the disadvantage is that we investigated AHF in the context of an *ex vivo* model although this is widely used in science it would be beneficial to attempt these studies in an *in vivo* setting. Secondly, our system is a representation of hypotensive AHF and it would be beneficial to test this model in the context of hypertensive AHF model.

8.4 Limitations of the study

For the Western blot analysis we did not include non-AHF control samples due to technical reasons (lack of adequate sample materials) - generation of such data would have added value to our understanding of the *ex vivo* AHF model here established. As hypertensive HF is the most common form of AHF in sub-Saharan Africa, future studies should be geared toward establishing a diabetic hypertensive AHF model which would add even greater insights into treatment strategies for AHF. For example, others found that *ex vivo* perfusions with pressures ≥ 180 mmHg lead to irreversible heart failure (Opie, 1965); this would therefore be a useful starting point to establish such an experimental model.

8.5 Conclusion

To our knowledge our study is the first of its kind to demonstrate that TMZ can improve contractile function in diabetic hearts subjected to *de novo* AHF. This opens up an exciting option for the treatment of AHF as TMZ acts by metabolic modulation and therefore elicits no hemodynamic effects. TMZ offered cardioprotection in diabetic hearts exposed to AHF. Our results indicate that TMZ reduces detrimental myocardial AGEs in diabetic hearts. However, we propose that TMZ may potentially trigger its protective effects by lowering mitochondrial ROS as indicated in our cell work. This requires further confirmatory studies and TMZ therefore emerges as a putative therapeutic target to be considered as sole and/or combined treatment (with more conventional drugs) for AHF patients. However, further studies are required to confirm this notion and to translate such basic research work into the clinical setting.

References

Aasum, E., Larsen, T.S., 1997. Pyruvate reverses fatty-acid-induced depression of ventricular function and calcium overload after hypothermia in guinea pig hearts. Cardiovasc. Res. 33, 370–377.

Adams, K.F., Fonarow, G.C., Emerman, C.L., LeJemtel, T.H., Costanzo, M.R., Abraham, W.T., Berkowitz, R.L., Galvao, M., Horton, D.P., 2005. Characteristics and outcomes of patients hospitalized for heart failure in the United States: rationale, design, and preliminary observations from the first 100,000 cases in the Acute Decompensated Heart Failure National Registry (ADHERE). Am. Heart J. 149, 209–16.

Adewole, A.D., Ikem, R.T., Adigun, A.Q., Akintomide, A.O., Balogun, M.O., Ajayi, A.A., 1996. A three year clinical review of the impact of angiotensin converting enzyme inhibitors on the intra hospital mortality of congestive heart failure in Nigerians. Cent. Afr. J. Med. 42, 253–255.

Alberti, K.G., Zimmet, P.Z., 1998. Definition, diagnosis and classification of diabetes mellitus and its complications. Part 1: diagnosis and classification of diabetes mellitus provisional report of a WHO consultation. Diabet. Med. 15, 539–553.

An, D., Rodrigues, B., 2006. Role of changes in cardiac metabolism in development of diabetic cardiomyopathy. Am J Physiol Hear. Circ Physiol 291, H1489–H1506.

Armbruster, D.A., 1987. Fructosamine: structure, analysis, and clinical usefulness. Clin. Chem. 33, 2153–2163.

Aronson, D., EJ, R., JH, C., 1997. Mechanisms determining course and outcome of diabetic patients who have had acute myocardial infarction. Ann. Intern. Med. 126, 296–306.

Asensi, M., Sastre, J., Pallardo, F. V., Lloret, A., Lehner, M., Garcia-De-La Asuncion, J., Viña, J., 1999. Ratio of reduced to oxidized glutathione as indicator of oxidative stress status and DNA damage. Methods Enzymol. 299, 267–276.

Avogaro, A., Nosadini, R., Doria, A., Fioretto, P., Velussi, M., Vigorito, C., Sacca, L., Toffolo, G., Cobelli, C., Trevisan, R., et, al., 1990. Myocardial metabolism in insulin-deficient diabetic humans without coronary artery disease. Am. J. Physiol. - Endocrinol. Metab. 258, E606–E618.

Bayeva, M., Sawicki, K.T., Ardehali, H., 2013. Taking diabetes to heart--deregulation of myocardial lipid metabolism in diabetic cardiomyopathy. J. Am. Heart Assoc. 2, e000433.

Beauloye, C., Marsin, A.-S., Bertrand, L., Vanoverschelde, J.-L., Rider, M.H., Hue, L., 2002. The stimulation of heart glycolysis by increased workload does not require AMP-activated protein kinase but a wortmannin-sensitive mechanism. FEBS Lett. 531, 324–328.

Belevich, I., Verkhovsky, M.I., Wikström, M., 2006. Proton-coupled electron transfer drives the proton pump of cytochrome c oxidase. Nature 440, 829–832.

Bergman, G., Atkinson, L., Metcalfe, J., Jackson, N., Jewitt, D.E., 1980. Beneficial effect of enhanced myocardial carbohydrate utilisation after oxfenicine (L-hydroxyphenylglycine) in angina pectoris. Eur. Heart J. 1, 247–253.

Bersin, R.M., Stacpoole, P.W., 1997. Dichloroacetate as metabolic therapy for myocardial ischemia and failure. Am. Heart J. 134, 841–855.

Bing, R.J., Siegel, A., Ungar, I., Gilbert, M., 1954. Metabolism of the human heart. Am. J. Med. 16, 504–515.

Bloomfield, G.S., Barasa, F., Doll, J., Velazquez, E.J., 2013. Heart failure in sub-Saharan Africa. Curr. Cardiol. Rev. 9, 157–73.

Blumenkranz, M.., 1993. The Effect of Intensive Treatment of Diabetes on the Development and Progression of Long-Term Complications in Insulin-Dependent Diabetes Mellitus. N. Engl. J. Med. 329, 977–986.

Bowker-Kinley, M.M., Davis, I.W., Wu, P., Harris, A.R., Popov, M.K., 1998. Evidence for existence of tissue-specific regulation of the mammalian pyruvate dehydrogenase complex. Biochem. J. 329, 191–196.

Bricknell, O.L., Opie, L.H., 1978. Effects of substrates on tissue metabolic changes in the isolated rat heart during underperfusion and on release of lactate dehydrogenase and arrhythmias during reperfusion. Circ. Res. 43, 102–115.

Brottier, L., Barat, J.L., Combe, C., Boussens, B., Bonnet, J., Bricaud, H., 1990. Therapeutic value of a cardioprotective agent in patients with severe ischaemic cardiomyopathy. Eur. Heart J. 11, 207–212.

Brownlee, M., 2005. The pathobiology of diabetic complications. Diabetes 54, 1615.

Brownlee, M., 2001. Biochemistry and molecular cell biology of diabetic complications. Nature 414, 813–820.

Brownlee, M., Cerami, A., 1981. The Biochemistry of the Complications of Diabetes Mellitus. Annu. Rev. Biochem. 50, 385–432.

Bui, A.L., Horwich, T.B., Fonarow, G.C., 2011. Epidemiology and risk profile of heart failure. Nat. Rev. Cardiol. 8, 30–41.

Burger, A.J., Elkayam, U., Neibaur, M.T., Haught, H., Ghali, J., Horton, D.P., Aronson, D., 2015a. Comparison of the occurrence of ventricular arrhythmias in patients with acutely decompensated congestive heart failure receiving dobutamine versus nesiritide therapy. Am. J. Cardiol. 88, 35–39.

Burger, A.J., Horton, D.P., LeJemtel, T., Ghali, J.K., Torre, G., Dennish, G., Koren, M., Dinerman, J., Silver, M., Cheng, M.L., Elkayam, U., 2015b. Effect of nesiritide (B-type natriuretic peptide) and dobutamine on ventricular arrhythmias in the treatment of patients with acutely decompensated congestive heart failure: The PRECEDENT study. Am. Heart J. 144, 1102–1108.

Cai, W., Ramdas, M., Zhu, L., Chen, X., Striker, G., Vlassara, H., 2012. Oral advanced glycation end products(AGEs) promote insulin resistance and diabetes by depleting the antioxidant defenses AGEreceptor-1 and sirtuin1. Proc.Natl. Acad. Sci. 109, 15888–15893.

Carroll, J., 2005. The Post-translational Modifications of the Nuclear Encoded Subunits of Complex I from Bovine Heart Mitochondria. Mol. Cell. Proteomics 4, 693–699.

Carroll, J., 2002. Definition of the Nuclear Encoded Protein Composition of Bovine Heart Mitochondrial Complex I. Identification Of Two New Subunits. J. Biol. Chem. 277, 50311–50317.

Casademont, J., Miro, O., 2002. Electron transport chain defects in heart failure. Hear. Fail Rev 7, 131–139.

Cecchini, G., 2003. Function and Structure of Complex II of the Respiratory Chain. Annu. Rev. Biochem. 72, 77–109.

Ceriello, A., Quagliaro, L., D'Amico, M., Di Filippo, C., Marfella, R., Nappo, F., Berrino, L., Rossi, F., Giugliano, D., 2002. Acute hyperglycemia induces nitrotyrosine formation and apoptosis in perfused heart from rat. Diabetes 51, 1076–82.

Chance, B., Sies, H., Boveris, A., 1979. Hydroperoxide metabolism in mammalian organs. Physiol. Rev. 59, 527–605.

Chandler, M.P., Stanley, W.C., Morita, H., Suzuki, G., Roth, B.A., Blackburn, B., Wolff, A., Sabbah, H.N., 2002. Short-Term Treatment With Ranolazine Improves Mechanical Efficiency in Dogs With Chronic Heart Failure. Circ. Res. 91, 278–280.

Cheng, H.-M., González, R.G., 1986. The effect of high glucose and oxidative stress on lens metabolism, aldose reductase, and senile cataractogenesis. Metabolism 35, 10–14.

Chiarelli, F., Marcovecchio, M., 2013. The molecular mechanisms underlying diabetic complications. Int. J. Pediatr. Endocrinol. 2013, O1.

Chierchia, S.L., Fragasso, G., 1993. Metabolic management of ischaemic heart disease. Eur. Heart J. 14, 2–5.

Clarke, B., 1996. Ranolazine Increases Active Pyruvate Dehydrogenase in Perfused Normoxic Rat Hearts: Evidence for an Indirect Mechanism. J. Mol. Cell. Cardiol. 28, 341–350.

Cleland, J.G.F., Swedberg, K., Follath, F., Komajda, M., Cohen-Solal, A., Aguilar, J.C., Dietz, R., Gavazzi, A., Hobbs, R., Korewicki, J., Madeira, H.C., Moiseyev, V.S., Preda, I., Van Gilst, W.H., Widimsky, J., Freemantle, N., Eastaugh, J., Mason, J., 2003. The EuroHeart Failure survey programme - A survey on the quality of care among patients with heart failure in Europe. Part 1: Patient characteristics and diagnosis. Eur. Heart J. 24, 442–463.

Cohen, M.P., Clements, R.S., Cohen, J.A., Shearman, C.W., 1996. Glycated Albumin Promotes a Generalized Vasculopathy in thedb/dbMouse. Biochem. Biophys. Res. Commun. 218, 72–75.

Cooper, H.A., Dries, D.L., Davis, C.E., Shen, Y.L., Domanski, M.J., 1999. Left Ventricular Dysfunction. Circulation 100, 1311–1315.

Cowie, M.R., Mosterdft, A., Wood, D.A., Deckers, J.W., Sutton, G.C., Grobbeef, D.E., 1997. Review Article The epidemiology of heart failure. Eur. Heart J. 18, 208–225.

Cross, H.R., Opie, L.H., Radda, G.K., Clarke, K., 1996. Is a High Glycogen Content Beneficial or Detrimental to the Ischemic Rat Heart?: A Controversy Resolved. Circ. Res. 78, 482–491.

Cuffe, M., Califf, R., Adams, K., Benza, A., Bourge, R., Colucci, N., Massie, B., O'Connor, C., Pina, I., Quigg, R., Silver, M., Gheorghiade, M., 2002. Short-term intravenous milrinone for acute exacerbation of chronic heart failure: A randomized controlled trial. JAMA 287, 1541–1547.

Dalal, S., Beunza, J.J., Volmink, J., Adebamowo, C., Bajunirwe, F., Njelekela, M., Mozaffarian, D., Fawzi, W., Willett, W., Adami, H.-O., Holmes, M.D., 2011. Non-communicable diseases in sub-Saharan Africa: what we know now. Int. J. Epidemiol. 40, 885–901.

Damasceno, A., Cotter, G., Mayosi, B.M., Medicina, F. De, Mondlane, U.E., Carolina, N., Unit, C., Cardiovascular, S., Hani, C., Hospital, B., Africa, S., Hospital, G.S., Town, C., 2007. Heart failure in Sub-Saharan Africa: Time for Action. JACC 50, 1688–93.

Damasceno, A., Mayosi, B., Sani, M., Al, E., 2012. The causes, treatment, and outcome of acute heart failure in 1006 africans from 9 countries: Results of the sub-saharan africa survey of heart failure. Arch. Intern. Med. 172, 1386–1394.

Day, J.F., Thornberg, R.W., Thrope, S.R., Baynes, J.W., 1979. Non-enzymatic glycosylation of rat albumin. Studies in vitro and in vivo. J.Biol.Chem. 254, 9394–9400.

Delpierre, G., Van Schaftingen, E., 2003. Fructosamine 3-kinase, an enzyme involved in protein deglycation. Biochem. Soc. Trans. 31, 1354–1357.

Depre, C., Rider, M.H., Hue, L., 1998. Mechanisms of control of heart glycolysis. Eur. J. Biochem. 258, 277–290. doi:10.1046/j.1432-1327.1998.2580277.x

Depre, C., Rider, M.H., Veitch, K., Hue, L., 1993. Role of fructose 2,6-bisphosphate in the control of heart glycolysis. J. Biol. Chem. 268, 13274–9.

Deshpande, G.P., McCarthy, J., Mardikar, H., Lecour, S., Opie, L., 2010. Effects of sphingosine-1-phosphate on acute contractile heart failure (ACHF). Cardiovasc. Drugs Ther. 24, 459–460.

Detry, J.M., Sellier, P., Pennaforte, S., Cokkinos, D., Dargie, H., Mathes, P., 1994. Trimetazidine: a new concept in the treatment of angina. Comparison with propranolol in patients with stable angina. Trimetazidine European Multicenter Study Group. Br. J. Clin. Pharmacol. 37, 279–288.

Dézsi, C.A., 2015. Trimetazidine in Practice : Review of the Clinical and Experimental Evidence. Am. J. Ther. 9, 1–9.

Di Napoli, P., Chierchia, S., Taccardi, A.A., Grilli, A., Felaco, M., Caterina, R. De, Barsotti, A., 2007. Trimetazidine improves post-ischemic recovery by preserving endothelial nitric oxide synthase expression in isolated working rat hearts. Nitric Oxide - Biol. Chem. 16, 228–236.

di Rago, J.P., Netter, P., Slonimski, P.P., 1990. Intragenic suppressors reveal long distance interactions between inactivating and reactivating amino acid replacements generating three-dimensional constraints in the structure of mitochondrial cytochrome b. J.Biol.Chem. 265, 15750–15757.

Dimmeler, S., 2011. Cardiovascular disease review series. EMBO Mol. Med. 3, 697.

Dobson, G.P., Himmelreich, U., 2002. Heart design : free ADP scales with absolute mitochondrial and myofibrillar volumes from mouse to human. Biochim. Biophys. Acta 1553, 261–267.

Doria-Medina, C.L., Lund, D.D., Pasley, A., Sandra, A., Sivitz, W.I., 1993. Immunolocalization of GLUT-1 glucose transporter in rat skeletal muscle and in normal and hypoxic cardiac tissue. Am. J. Physiol. - Endocrinol. Metab. 265, E454–E464.

Doust, J. a, Pietrzak, E., Dobson, A., Glasziou, P., 2005. How well does B-type natriuretic peptide predict death and cardiac events in patients with heart failure: systematic review. BMJ 330, 625.

Drexler, B., Heinisch, C., Balmelli, C., Lassus, J., Siirilä-Waris, K., Arenja, N., Socrates, T., Noveanu, M., Potocki, M., Meune, C., Haaf, P., Degen, C., Breidthardt, T., Reichlin, T., Nieminen, M.S., Veli-Pekka, H., Osswald, S., Mueller, C., 2012. Quantifying cardiac hemodynamic stress and cardiomyocyte damage in ischemic and nonischemic acute heart failure. Circ. Hear. Fail. 5, 17–24.

Dröse, S., Zwicker, K., Brandt, U., 2002. Full recovery of the NADH:ubiquinone activity of complex I (NADH:ubiquinone oxidoreductase) from Yarrowia lipolytica by the addition of phospholipids. Biochim. Biophys. Acta - Bioenerg. 1556, 65–72.

Dyck, J.R.B., 2004. Malonyl Coenzyme A Decarboxylase Inhibition Protects the Ischemic Heart by Inhibiting Fatty Acid Oxidation and Stimulating Glucose Oxidation. Circ. Res. 94, e78–e84.

Essop, M.F., 2007. Cardiac metabolic adaptations in response to chronic hypoxia. J. Physiol. 584, 715–726.

Essop, M.F., Opie, L.H., 2004. Metabolic therapy for heart failure. Eur. Heart J. 25, 1765–1768.

Fillmore, N., Lopaschuk, G.D., 2011. Impact of fatty acid oxidation on cardiac efficiency. Hear. Metab. 53, 33–37.

Fonarow, G.C., Abraham, W.T., Albert, N.M., Gattis Stough, W., Gheorghiade, M., Greenberg, B.H., O'Connor, C.M., Nunez, E., Yancy, C.W., Young, J.B., 2008. Day of Admission and Clinical Outcomes for Patients Hospitalized for Heart Failure: Findings From the Organized Program to Initiate Lifesaving Treatment in Hospitalized Patients With Heart Failure (OPTIMIZE-HF). Circ. Hear. Fail. 1, 50–57.

Fragasso, G., Palloshi, A., Puccetti, P., Silipigni, C., Rossodivita, A., Pala, M., Calori, G., Alfieri, O., Margonato, A., 2006a. A Randomized Clinical Trial of Trimetazidine, a Partial Free Fatty Acid Oxidation Inhibitor, in Patients With Heart Failure. J. Am. Coll. Cardiol. 48, 992–998.

Fragasso, G., Perseghin, G., De Cobelli, F., Esposito, A., Palloshi, A., Lattuada, G., Scifo, P., Calori, G., Del Maschio, A., Margonato, A., 2006b. Effects of metabolic modulation by trimetazidine on left ventricular function and phosphocreatine/adenosine triphosphate ratio in patients with heart failure. Eur. Heart J. 27, 942–948.

Fragasso, G., Piatti Md, P.M., Monti, L., Palloshi, A., Setola, E., Puccetti, P., Calori, G., Lopaschuk, G.D., Margonato, A., 2003. Short- and long-term beneficial effects of trimetazidine in patients with diabetes and ischemic cardiomyopathy. Am. Heart J. 146, E18.

Fragasso, G., Rosano, G., Baek, S.H., Sisakian, H., Di Napoli, P., Alberti, L., Calori, G., Kang, S.M., Sahakyan, L., Sanosyan, A., Vitale, C., Marazzi, G., Margonato, A., Belardinelli, R., 2013. Effect of partial fatty acid oxidation inhibition with trimetazidine on mortality and morbidity in heart failure: Results from an international multicentre retrospective cohort study. Int. J. Cardiol. 163, 320–325.

Fragasso, G., Salerno, A., Lattuada, G., Cuko, A., Calori, G., Scollo, A., Ragogna, F., Arioli, F., Bassanelli, G., Spoladore, R., Luzi, L., Margonato, A., Perseghin, G., 2011. Effect of partial inhibition of fatty acid oxidation by trimetazidine on whole body energy metabolism in patients with chronic heart failure. Heart 97, 1495–1500.

Fry, M., Green, D.E., 1981. Cardiolipin requirement for electron transfer in complex I and III of the mitochondrial respiratory chain. J. Biol. Chem. 256, 1874–1880.

Gambert, S., Vergely, C., Filomenko, R., Moreau, D., Bettaieb, A., Opie, L., Rochette, L., 2006. Adverse effects of free fatty acid associated with increased oxidative stress in postischemic isolated rat hearts. Mol. Cell. Biochem. 283, 147–152.

Garcia, C.K., Goldstein, J.L., Pathak, R.K., Anderson, R.G.W., Brown, M.S., 2015. Molecular characterization of a membrane transporter for lactate, pyruvate, and other monocarboxylates: Implications for the Cori cycle. Cell 76, 865–873.

Garland, P.B., Randle, P.J., Nwesholme, E.A., 1963. Citrate as an Intermediary in the Inhibition of Phosphofructokinase in Rat Heart Muscle by Fatty Acids, Ketone Bodies, Pyruvate, Diabetes and Starvation. Nature 200, 169–170.

Gheorghiade, M., Abraham, W.T., Albert, N.M., Greenberg, B.H., O'Connor, C.M., She, L., Stough, W.G., Yancy, C.W., Young, J.B., Fonarow, G.C., 2006. Systolic blood pressure at admission, clinical characteristics, and outcomes in patients hospitalized with acute heart failure. Jama 296, 2217–26.

Gheorghiade, M., Zannad, F., Sopko, G., Klein, L., Piña, I.L., Konstam, M. a., Massie, B.M., Roland, E., Targum, S., Collins, S.P., Filippatos, G., Tavazzi, L., 2005. Acute heart failure syndromes: Current state and framework for future research. Circulation 112, 3958–3968.

Giacco, F., Du, X., D'Agati, V.D., Milne, R., Sui, G., Geoffrion, M., Brownlee, M., 2014. Knockdown of glyoxalase 1 mimics diabetic nephropathy in nondiabetic mice. Diabetes 63, 291–299.

Gibala, M.J., Young, M.E., Taegtmeyer, H., 2000. Anaplerosis of the citric acid cycle: role in energy metabolism of heart and skeletal muscle. Acta Physiol. Scand. 168, 657–665.

Glatz, J.F.C., Luiken, J., Bonen, A., 2001. Involvement of membrane-associated proteins in the acute regulation of cellular fatty acid uptake. J. Mol. Neurosci. 16, 123–132.

Goldenthal, M.J., Marín-García, J., 2002. Fatty acid metabolism in cardiac failure: biochemical, genetic and cellular analysis. Cardiovasc. Res. 54, 516–527.

Goldfarb, A.H., Bruno, J.F., Buckenmeyer, P.J., 1986. Intensity and duration effects of exercise on heart cAMP, phosphorylase, and glycogen. J. Appl. Physiol. 60, 1268–1273.

Goldstein, D.E., Little, R.R., Wiedmeyer, H.M., England, J.D., McKenzie, E.M., 1986. Glycated hemoglobin: methodologies and clinical applications. Clin. Chem. 32, B64–70.

Golfman, L.S., Takeda, N., Dhalla, N.S., 1996. Cardiac membrane Ca2+-transport in alloxan-induced diabetes in rats. Diabetes Res. Clin. Pract. 31, 73–77.

Gu, K., Cowie, C.C., Harris, M.I., 1998. Mortality in Adults With and Without Diabetes in a National Cohort of the U.S. Population, 1971–1993. Diabetes Care 21, 1138–1145.

Gupte, S.S., Hackenbrock, C.R., 1988. Multidimensional diffusion modes and collision frequencies of cytochrome c with its redox partners. J. Biol. Chem. 263, 5241–7.

Hall, J.L., Stanley, W.C., Lopaschuk, G.D., Wisneski, J.A., Pizzurro, R.D., Hamilton, C.D., McCormack, J.G., 1996. Impaired pyruvate oxidation but normal glucose uptake in diabetic pig heart during dobutamine-induced work. Am. J. Physiol. - Hear. Circ. Physiol. 271, H2320–H2329.

Harpey, C., Clauser, P., Labrid, C., Freyria, J.-L., Poirier, J.-P., 1988. Trimetazidine, A Cellular Anti-ischemic Agent. Cardiovasc. Drug Rev. 6, 292–312.

Harris, R.A., Huang, B., Wu, P., 2001. Control of pyruvate dehydrogenase kinase gene expression. Adv. Enzyme Regul. 41, 269–288.

Hartog, J.W.L., Voors, A. a., Bakker, S.J.L., Smit, A.J., van Veldhuisen, D.J., 2007. Advanced glycation end-products (AGEs) and heart failure: Pathophysiology and clinical implications. Eur. J. Heart Fail. 9, 1146–1155.

Henry, C.G., Strauss, A.W., Keating, J.P., Hillman, R.E., 1981. Congestive cardiomyopathy associated with β-ketothiolase deficiency. J. Pediatr. 99, 754–757.

Herzig, S., Raemy, E., Montessuit, S., Veuthey, J., Zamboni, N., Westermann, B., Kunji, E.R.S., Martinou, J., 2012. Identification and Functional Expression of the Mitochondrial Pyruvate Carrier. Science (80-.). 337, 93–6.

Higgins, A.J., Morville, M., Burges, R.A., Blackburn, K.J., 1981. Mechanism of action of oxfenicine on muscle metabolism. Biochem. Biophys. Res. Commun. 100, 291–296.

Higgins, P.J., Bunn, H.F., 1981. Kinetic analysis of the nonenzymatic glycosylation of hemoglobin. J. Biol. Chem. 256, 5204–5208.

Hirst, J., 2005. Energy transduction by respiratory complex I - an evaluation of current knowledge. Biochem. Soc. Trans. 33, 525–529.

Hue, L., Rider, M.H., 1987. Role of fructose 2, 6-bisphosphate in the control of glycolysis in mammalian tissues. Biochem. J. 245, 313.

Hue, L., Taegtmeyer, H., 2009. The Randle cycle revisited: a new head for an old hat. Am. J. Physiol. Endocrinol. Metab. 297, E578–E591.

Humphries, K.M., Szweda, L.I., 1998. Selective Inactivation of α-Ketoglutarate Dehydrogenase and Pyruvate Dehydrogenase: Reaction of Lipoic Acid with 4-Hydroxy-2-nonenal. Biochemistry 37, 15835–15841.

Ikizler, M., Erkasap, N., Dernek, S., Batmaz, B., Kural, T., Kaygisiz, Z., 2006. Trimetazidine-Induced Enhancement of Myocardial Recovery during Reperfusion: A Comparative Study in Diabetic and Non-diabetic Rat Hearts. Arch. Med. Res. 37, 700–708.

Ishiki, M., Klip, A., 2005. Minireview: Recent Developments in the Regulation of Glucose Transporter-4 Traffic: New Signals, Locations, and Partners. Endocrinology 146, 5071–5078.

James, D.E., Strube, M., Muecdler, M., 1989. Molecular cloning and characterization of an insulin-regulatable glucose transporter. Nature 338, 83–87.

Jaswal, J.S., Keung, W., Wang, W., Ussher, J.R., Lopaschuk, G.D., 2011. Targeting fatty acid and carbohydrate oxidation - A novel therapeutic intervention in the ischemic and failing heart. Biochim. Biophys. Acta - Mol. Cell Res. 1813, 1333–1350.

Jennings, R.B., 1970. Myocardial ischemia—Observations, definitions and speculations. J. Mol. Cell. Cardiol. 1, 345–349.

Johannsson, E., Nagelhus, E.A., McCullagh, K.J.A., Sejersted, O.M., Blackstad, T.W., Bonen, A., Ottersen, O.P., 1997. Cellular and Subcellular Expression of the Monocarboxylate Transporter MCT1 in Rat Heart: A High-Resolution Immunogold Analysis. Circ. Res. 80, 400–407.

Johnson, R.N., Metcalf, P.A., Baker, J.R., 1983. Fructosamine: a new approach to the estimation of serum glycosylprotein. An index of diabetic control. Clin. Chim. Acta. 127, 87–95.

Jowett, B.Y.M., Quastel, J.H., 1933. The Glyoxalase Activity of the Red Blood Cell: The Function of Glutathione. Biochem. J. 27, 486 – 498.

Kannel, W.B., McGee, D.L., 1979. Diabetes and cardiovascular disease: The framingham study. JAMA 241, 2035–2038.

Kantor, P.F., Lopaschuk, G.D., Opie, L.H., 2001. Heart Physiology and Pathophysiology, Heart Physiology and Pathophysiology. Elsevier.

Kantor, P.F., Lucien, A., Kozak, R., Lopaschuk, G.D., 2000. The antianginal drug trimetazidine shifts cardiac energy metabolism from fatty acid oxidation to glucose oxidation by inhibiting mitochondrial long-chain 3-ketoacyl coenzyme A thiolase. Circ. Res. 86, 580–588.

Karbowska, J., Kochan, Z., Smolenski, R.T., 2003. Peroxisome proliferator-activated receptor alpha is downregulated in the failing human heart. Cell. Mol. Biol. Lett. 8, 49–53.

Katz, A., 2000. Heart Failure:Pathophysiology, Molecular Biology and Clinical Management. Lippincott Williams & Wilkins, Philadelphia, PA.

Katz, A.M., Katz, P.B., 1962. Diseases of the heart in the works of Hippocrates. Br. Heart J. 24, 257–264.

Kelly, D.P., Strauss, A.W., 1994. Inherited Cardiomyopathies. N. Engl. J. Med. 330, 913–919.

Kengne, A.P., Turnbull, F., MacMahon, S., 2010. The Framingham Study, Diabetes Mellitus and Cardiovascular Disease: Turning Back the Clock. Prog. Cardiovasc. Dis. 53, 45–51.

Kerbey, A.L., Randle, P.J., Cooper, R.H., Whitehouse, S., Pask, H.T., Denton, R.M., 1976. Regulation of pyruvate dehydrogenase in rat heart. Mechanism of regulation of proportions of dephosphorylated and phosphorylated enzyme by oxidation of fatty acids and ketone bodies and of effects of diabetes: role of coenzyme A, acetyl-coenzyme A and red. Biochem. J. 154, 327–348.

Kerner, J., Hoppel, C., 2000. Fatty acid import into mitochondria. Biochim. Biophys. Acta - Mol. Cell Biol. Lipids 1486, 1–17.

Khan, M., Meduru, S., Mostafa, M., Khan, S., Hideg, K., Kuppusamy, P., 2010. Trimetazidine, Administered at the Onset of Reperfusion, Ameliorates Myocardial Dysfunction and Injury by Activation of p38 Mitogen-Activated Protein Kinase and Akt Signaling, Journal of Pharmacology and Experimental Therapeutics.

Kingue, S., Dzudie, A., Menanga, A., Akono, M., Ouankou, M., Muna, W., 2005. [A new look at adult chronic heart failure in Africa in the age of the Doppler echocardiography: experience of the medicine department at Yaounde General Hospital]. Ann. Cardiol. Angeiol. (Paris). 54, 276–83.

Kloner, R. a., Nesto, R.W., 2008. Glucose-insulin-potassium for acute myocardial infarction: Continuing controversy over cardioprotection. Circulation 117, 2523–2533.

Kolwicz, S.C., Olson, D.P., Marney, L.C., Garcia-Menendez, L., Synovec, R.E., Tian, R., 2012. Cardiac-specific deletion of acetyl CoA carboxylase 2 prevents metabolic remodeling during pressure-overload hypertrophy. Circ. Res. 111, 728–38.

Koonen, D.P.Y., Glatz, J.F.C., Bonen, A., Luiken, J.J.F.P., 2005. Long-chain fatty acid uptake and FAT/CD36 translocation in heart and skeletal muscle. Biochim. Biophys. Acta - Mol. Cell Biol. Lipids 1736, 163–180.

Kruszynska, Y.T., McCormack, J.G., McIntyre, N., 1991. Effects of glycogen stores and non-esterified fatty acid availability on insulin-stimulated glucose metabolism and tissue pyruvate dehydrogenase activity in the rat. Diabetologia 34, 205–211.

Kunau, W.-H., Dommes, V., Schulz, H., 1995. β-Oxidation of fatty acids in mitochondria, peroxisomes, and bacteria: A century of continued progress. Prog. Lipid Res. 34, 267–342.

Kusunoki, H., Miyata, S., Ohara, T., Liu, B.-F., Uriuhara, A., Kojima, H., Suzuki, K., Miyazaki, H., Yamashita, Y., Inaba, K., Kasuga, M., 2003. Relation Between Serum 3-Deoxyglucosone and Development of diabetic microangiopathy. Diabetes Care 26, 1889–1894.

Laybutt, D.R., Chisholm, D.J., Kraegen, E.W., 1997. Specific adaptations in muscle and adipose tissue in response to chronic systemic glucose oversupply in rats. Am. J. Physiol. - Endocrinol. Metab. 273, E1–E9.

Lee, A.Y., Chung, S.S., 1999. Contributions of polyol pathway to oxidative stress in diabetic cataract. FASEB J. 13, 23–30.

Lindenfeld, J., Albert, N.M., Boehmer, J.P., Collins, S.P., Ezekowitz, J.A., Givertz, M.M., Katz, S.D., Klapholz, M., Moser, D.K., Rogers, J.G., Starling, R.C., Stevenson, W.G., Tang, W.H.W., Teerlink, J.R., Walsh, M.N., 2010. HFSA 2010 Comprehensive Heart Failure Practice Guideline. J. Card. Fail. 16, e1–194.

Liu, J., Li, J., Li, W.J., Wang, C.M., 2013. The role of uncoupling proteins in diabetes mellitus. J. Diabetes Res. 2013, 1–8.

Lopaschuk, G., Ussher, J., 2010. Myocardial fatty acid metabolism in health and disease. Physiol. Rev. 90, 207–258.

Lopaschuk, G.D., Barr, R., Thomas, P.D., Dyck, J.R.B., Lopaschuk, G.D., Barr, R., Thomas, P.D., Dyck, J.R.B., 2003. Response to Research Commentary Beneficial Effects of Trimetazidine in Ex Vivo Working Ischemic Hearts Are Due to a Stimulation of Glucose Oxidation Secondary to Inhibition of Long-Chain 3-Ketoacyl Coenzyme A Thiolase. Circ. Res. 93, e33–7.

Lopaschuk, G.D., Barr, R.L., 1997. Measurements of fatty acid and carbohydrate metabolism in the isolated working rat heart. Mol. Cell. Biochem. 172, 137–147.

Lopaschuk, G.D., Belke, D.D., Gamble, J., Itoi, T., Schönekess, B.O., 1994. Regulation of fatty acid oxidation in the mammalian heart in health and disease. Biochim. Biophys. Acta 1213, 263–276.

Lopaschuk, G.D., Folmes, C.D.L., Stanley, W.C., 2007. Cardiac energy metabolism in obesity. Circ. Res. 101, 335–347.

Lu, C., Dabrowski, P., Fragasso, G., Chierchia, S.L., 2015. Effects of trimetazidine on ischemic left ventricular dysfunction in patients with coronary artery disease. Am. J. Cardiol. 82, 898–901.

Ludwig, B., Bender, E., Arnold, S., Hüttemann, M., Lee, I., Kadenbach, B., 2001. Cytochrome c Oxidase and the Regulation of Oxidative Phosphorylation. ChemBioChem 2, 392–403.

Luiken, J.F.P., Coort, S.M., Koonen, D.Y., van der Horst, D., Bonen, A., Zorzano, A., Glatz, J.C., 2004. Regulation of cardiac long-chain fatty acid and glucose uptake by translocation of substrate transporters. Pflügers Arch. 448, 1–15.

MacDonald, M.R., Petrie, M.C., Varyani, F., Ostergren, J., Michelson, E.L., Young, J.B., Solomon, S.D., Granger, C.B., Swedberg, K., Yusuf, S., Pfeffer, M. a, McMurray, J.J. V, 2008. Impact of diabetes on outcomes in patients with low and preserved ejection fraction heart failure: an analysis of the Candesartan in Heart failure: Assessment of Reduction in Mortality and morbidity (CHARM) programme. Eur. Heart J. 29, 1377–1385.

MacInnes, A., Fairman, D., Binding, P., Rhodes, J., Wyatt, M., Phelan, A., Haddock, P., Karran, E., 2003. The Antianginal Agent Trimetazidine Does Not Exert Its Functional Benefit via Inhibition of Mitochondrial Long-Chain 3-Ketoacyl Coenzyme A Thiolase. Circ. Res. 93, 26e–32.

Malmberg, K., 1997. Prospective randomised study of intensive insulin treatment on long term survival after acute myocardial infarction in patients with diabetes mellitus. BMJ 314, 1512.

Mapanga, R.F., Essop, M.F., 2016. The damaging effects of hyperglycemia on cardiovascular function: spotlight on glucose metabolic pathways. Am. J. Physiol. - Hear. Circ. Physiol. 310, H153 – H173.

Mapanga, R.F., Joseph, D., Symington, B., Garson, K.-L., Kimar, C., Kelly-Laubscher, R., Essop, M.F., 2014. Detrimental effects of acute hyperglycaemia on the rat heart. Acta Physiol. (Oxf). 210, 546–64.

Marsin, a. S., Bertrand, L., Rider, M.H., Deprez, J., Beauloye, C., Vincent, M.F., Van den Berghe, G., Carling, D., Hue, L., 2000. Phosphorylation and activation of heart PFK-2 by AMPK has a role in the stimulation of glycolysis during ischaemia. Curr. Biol. 10, 1247–1255.

Marwick, T.H., 2008. Diabetic heart disease. Postgrad. Med. J. 84, 188–192.

Marzilli, M., 2003. Cardioprotective effects of trimetazidine: a review. Curr. Med. Res. Opin. 19, 661–672.

Marzilli, M., Klein, W.W., 2003. Efficacy and tolerability of trimetazidine in stable angina: a meta-analysis of randomized, double-blind, controlled trials. Coron. Artery Dis. 14, 171–9.

Massó, J.-F.M., Martí, I., Carrera, N., Poza, J.-J., López de Munain, A., 2005. Trimetazidine Induces Parkinsonism, Gait Disorders and Tremor. Therapie 60, 419–422.

Mayosi, B.M., Flisher, A.J., Lalloo, U.G., Sitas, F., Tollman, S.M., Bradshaw, D., 2009. The burden of non-communicable diseases in South Africa. Lancet 374, 934–947.

McGarry, J.D., Leatherman, G.F., Foster, D.W., 1978. Carnitine palmitoyltransferase I. The site of inhibition of hepatic fatty acid oxidation by malonyl-CoA. J. Biol. Chem. 253 , 4128–4136.

McGarry, J.D., Mannaerts, G.P., Foster, D.W., 1977. A possible role for malonyl-CoA in the regulation of hepatic fatty acid oxidation and ketogenesis. J. Clin. Invest. 60, 265–270.

McMurray, J.J. V., Adamopoulos, S., Anker, S.D., Auricchio, A., Bohm, M., Dickstein, K., Falk, V., Filippatos, G., Fonseca, C., Gomez-Sanchez, M. a., Jaarsma, T., Kober, L., Lip, G.Y.H., Maggioni, a. P., Parkhomenko, A., Pieske, B.M., Popescu, B. a., Ronnevik, P.K., Rutten, F.H., Schwitter, J., Seferovic, P., Stepinska, J., Trindade, P.T., Voors, a. a., Zannad, F., Zeiher, A., Bax, J.J., Baumgartner, H., Ceconi, C., Dean, V., Deaton, C., Fagard, R., Funck-Brentano, C., Hasdai, D., Hoes, A., Kirchhof, P., Knuuti, J., Kolh, P., McDonagh, T., Moulin, C., Popescu, B. a., Reiner, Z., Sechtem, U., Sirnes, P. a., Tendera, M., Torbicki, A., Vahanian, A., Windecker, S., McDonagh, T., Sechtem, U., Bonet, L. a., Avraamides, P., Ben Lamin, H. a., Brignole, M., Coca, A., Cowburn, P., Dargie, H., Elliott, P., Flachskampf, F. a., Guida, G.F., Hardman, S., Iung, B., Merkely, B., Mueller, C., Nanas, J.N., Nielsen, O.W., Orn, S., Parissis, J.T., Ponikowski, P., 2012. ESC Guidelines for the diagnosis and treatment of acute and chronic heart failure 2012: The Task Force for the Diagnosis and Treatment of Acute and Chronic Heart Failure 2012 of the European Society of Cardiology.

Developed in collaboration with the Heart. Eur. Heart J. 33, 1787–1847.

McMurray, J.J. V, Adamopoulos, S., Anker, S.D., Auricchio, A., Böhm, M., Dickstein, K., Falk, V., Filippatos, G., Fonseca, C., Gomez-Sanchez, M.A., Jaarsma, T., Køber, L., Lip, G.Y.H., Maggioni, A.P., Parkhomenko, A., Pieske, B.M., Popescu, B.A., Rønnevik, P.K., Rutten, F.H., Schwitter, J., Seferovic, P., Stepinska, J., Trindade, P.T., Voors, A.A., Zannad, F., Zeiher, A., 2013. Corrigendum to: ESC Guidelines for the diagnosis and treatment of acute and chronic heart failure 2012'[Eur Heart J 2012;33:1787–1847, doi:10.1093/eurheartj/ehs104. Eur. Heart J. 34, 158 LP – 158.

Meerwaldt, R., Lutgers, H.L., Links, T.P., Graaff, R., Baynes, J.W., Gans, R.O.B., Smit, A.J., 2007. Skin Autofluorescence Is a Strong Predictor of Cardiac Mortality in Diabetes. Diabetes Care 30, 107–112.

Mehta, R., Pascual, M., Soroko, S., Chertow, G., 2002. DIuretics, mortality, and nonrecovery of renal function in acute renal failure. JAMA 288, 2547–2553.

Mensah, G.A., 2008. Ischaemic heart disease in Africa. Heart 94, 836–43. doi:10.1136/hrt.2007.136523

Merkel, M., 2002. Lipoprotein lipase: genetics, lipid uptake, and regulation. J. Lipid Res. 43, 1997–2006.

Metra, M., Felker, G.M., Zacà, V., Bugatti, S., Lombardi, C., Bettari, L., Voors, A., Gheorghiade, M., Dei Cas, L., 2010. Acute heart failure: Multiple clinical profiles and mechanisms require tailored therapy. Int. J. Cardiol. 144, 175–179.

Miyata, T., Sugiyama, S., Saito, A., Kurokawa, K., 2001a. Reactive carbonyl compounds related

uremic toxicity (“carbonyl stress”). Kidney Int. Suppl.

Miyata, T., van Ypersele de Strihou, C., Imasawa, T., Yoshino, A., Ueda, Y., Ogura, H., Kominami, K., Onogi, H., Inagi, R., Nangaku, M., Kurokawa, K., 2001b. Glyoxalase I deficiency is associated with an unusual level of advanced glycation end products in a hemodialysis patient. Kidney Int. 60, 2351–2359.

Mohas, M., Kisfali, P., Baricza, E., Merei, A., Maasz, A., Cseh, J., Mikolas, E., Szijarto, I.A., Melegh, B., Wittmann, I., 2010. A polymorphism within the fructosamine-3-kinase gene is associated with HbA1c Levels and the onset of type 2 diabetes mellitus. Exp. Clin. Endocrinol. Diabetes 118, 209–212.

Monnier, V.M., Bautista, O., Kenny, D., Sell, D.R., Fogarty, J., Dahms, W., Cleary, P.A., Lachin, J., Genuth, S., 1999. Skin collagen glycation, glycoxidation, and crosslinking are lower in subjects with long-term intensive versus conventional therapy of type 1 diabetes: relevance of glycated collagen products versus HbA1c as markers of diabetic complications. DCCT Skin Co. Diabetes 48, 870–880.

Monti, L.D., Setola, E., Fragasso, G., Camisasca, R.P., Lucotti, P., Galluccio, E., Origgi, A., Margonato, A., Piatti, P., 2006. Metabolic and endothelial effects of trimetazidine on forearm skeletal muscle in patients with type 2 diabetes and ischemic cardiomyopathy. Am. J. Physiol. Endocrinol. Metab. 290, E54–E59.

Morrison, A.D., Clements, R.S., Travis, S.B., Oski, F., Winegrad, A.I., 1970. Glucose utilization by the polyol pathway in human erythrocytes. Biochem. Biophys. Res. Commun. 40, 199–205.

Murray, A.J., Anderson, R.E., Watson, G.C., Radda, G.K., Clarke, K., 2004. Uncoupling proteins in human heart. Lancet 364, 1786–1788.

Murray, C.J.L., Ezzati, M., Flaxman, A.D., Lim, S., Lozano, R., Michaud, C., Naghavi, M., Salomon, J.A., Shibuya, K., Vos, T., Wikler, D., Lopez, A.D., 2012. GBD 2010: design, definitions, and metrics. Lancet 380, 2063–2066.

Neely, J.R., Rovetto, M.J., Oram, J.F., 1972. Myocardial utilization of carbohydrate and lipids. Prog. Cardiovasc. Dis. 15, 289–329.

Nesto, R.W., Zarich, S., 1998. Acute Myocardial Infarction in Diabetes Mellitus Lessons Learned From ACE Inhibition. Circulation 97, 12–15.

Nichols, M., Townsend, N., Scarborough, P., Rayner, M., 2014. Cardiovascular disease in Europe 2014: epidemiological update. Eur. Heart J. 35, 2950–2959.

Nieminen, M.S., 2005. Pharmacological options for acute heart failure syndromes: Current treatments and unmet needs. Eur. Hear. Journal, Suppl. 7, 1–8.

Nieminen, M.S., Brutsaert, D., Dickstein, K., Drexler, H., Follath, F., Harjola, V.-P., Hochadel, M., Komajda, M., Lassus, J., Lopez-Sendon, J.L., Ponikowski, P., Tavazzi, L., 2006. EuroHeart Failure Survey II (EHFS II): a survey on hospitalized acute heart failure patients: description of population. Eur. Heart J. 27, 2725–2736.

Nishikawa, T., Edelstein, D., Brownlee, M., 2000a. The missing link: A single unifying mechanism for diabetic complications. Kidney Int 58, S26–S30.

Nishikawa, T., Edelstein, D., Du, X.L., Yamagishi, S., Matsumura, T., Kaneda, Y., Yorek, M.A., Beebe, D., Oates, P.J., Hammes, H.-P., Giardino, I., Brownlee, M., 2000b. Normalizing mitochondrial superoxide production blocks three pathways of hyperglycaemic damage. Nature 404, 787–790.

Norman, R., Gaziano, T., Laubscher, R., Steyn, K., Bradshaw, D., Comparative, A., 2007. Estimating the burden of disease attributable to high blood pressure in South Africa in 2000. South African Med. J. 97, 692–8.

Olson, A.L., Pessin, J.E., 1996. Structure, Function, and Regulation of the Mammalian Facilitative Glucose Transporter Gene Family. Annu. Rev. Nutr. 16, 235–256.

Onay-Besikci, A., Ozkan, S.A., 2008. Trimetazidine revisited: a comprehensive review of the pharmacological effects and analytical techniques for the determination of trimetazidine. Cardiovasc. Ther. 26, 147–165.

Opie, L., 1991. The Heart: Physiology and Metabolism. Rven, New York.

Opie, L., Deshpande, G., 2016. Acute heart failure: Can modern therapy delay or prevent death? South African Med. J. 106, 20.

Opie, L.H., 2004. The metabolic vicious cycle in heart failure. Lancet 364, 1733–4.

Opie, L.H., 1970. Effect of Fatty Acids on Contractility and Rhythm of the Heart. Nature 227, 1055–1056.

Opie, L.H., 1965. Coronary flow rate and perfusion pressure as determinants of mechanical function and oxidative metabolism of isolated perfused heart. J Physiol 180, 529–541.

Opie, L.H., Knuuti, J., 2009. The adrenergic-fatty acid load in heart failure. J. Am. Coll. Cardiol. 54, 1637–46.

Opie, L.H., Lecour, S., Mardikar, H., Deshpande, G.P., 2010. Cardiac survival strategies: an evolutionary hypothesis with rationale for metabolic therapy of acute heart failure. Trans. R. Soc. South Africa 65, 185–189.

Owen, O.E., Kalhan, S.C., Hanson, R.W., 2002. The Key Role of Anaplerosis and Cataplerosis for Citric Acid Cycle Function. J. Biol. Chem. 277, 30409–30412.

Oyoo, G.O., Ogola, E.N., 1999. Clinical and socio demographic aspects of congestive heart failure patients at Kenyatta National Hospital, Nairobi. East Afr. Med. J. 76, 23–27.

Ozbay, L., Unal, D.O., Erol, D., 2012. Food Effect on Bioavailability of Modified-Release Trimetazidine Tablets. J. Clin. Pharmacol. 52, 1535–1539.

Palmer, W., 1977. Biochemical Interfibrillar Muscle. Biol. Chem. 236, 8731–8739.

Panchal, A.R., Comte, B., Huang, H., Dudar, B., Roth, B., Chandler, M., Des Rosiers, C., Brunengraber, H., Stanley, W.C., 2001. Acute hibernation decreases myocardial pyruvate carboxylation and citrate release. Am. J. Physiol. Heart Circ. Physiol. 281, H1613–20.

Panchal, A.R., Comte, B., Huang, H., Kerwin, T., Darvish, A., Des Rosiers, C., Brunengraber, H., Stanley, W.C., 2000. Partitioning of pyruvate between oxidation and anaplerosis in swine hearts. Am. J. Physiol. Heart Circ. Physiol. 279, H2390–8.

Paradies, G., Petrosillo, G., Pistolese, M., Ruggiero, F.M., 2001. Reactive oxygen species generated by the mitochondrial respiratory chain affect the complex III activity via cardiolipin peroxidation in beef-heart submitochondrial particles. Mitochondrion 1, 151–159.

Park, J.H., Balmain, S., Berry, C., Morton, J.J., McMurray, J.J. V, 2010. Potentially detrimental cardiovascular effects of oxygen in patients with chronic left ventricular systolic dysfunction. Heart 96, 533–538.

Patel, M.S., Korotchkina, L.G., 2006. Regulation of the pyruvate dehydrogenase complex. Biochem. Soc. Trans. 34, 217–222.

Paulson, D.J., Ward, K.M., Shug, A.L., 1984. Malonyl CoA inhibition of carnitine palmityltransferase in rat heart mitochondria. FEBS Lett. 176, 381–384.

Pepine, C.J., Abrams, J., Marks, R.G., Morris, J.J., Scheidt, S.S., Handberg, E., 1994. Characteristics of a contemporary population with angina pectoris. Am. J. Cardiol. 74, 226–231.

Philbin, E.F., Cotto, M., Rocco, T.A., Jenkins, P.L., 1997. Association between diuretic use, clinical response, and death in acute heart failure. Am. J. Cardiol. 80, 519–22.

Piatti, P.M., Monti, L.D., Galli, L., Fragasso, G., Valsecchi, G., Conti, M., Gernone, F., Pontiroli, A.E., 2015. Relationship between endothelin-1 concentration and metabolic alterations typical of the insulin resistance syndrome. Metab. - Clin. Exp. 49, 748–752.

Popova, E.A., Mironova, R.S., Odjakova, M.K., 2010. Non-enzymatic glycosylation and deglycating enzymes. Biotechnol. Biotechnol. Equip. 24, 1928–1935.

Postic, C., Leturque, A., Printz, R.L., Maulard, P., Loizeau, M., Granner, D.K., Girard, J., 1994. Development and regulation of glucose transporter and hexokinase expression in rat. Am. J. Physiol. - Endocrinol. Metab. 266, E548–E559.

Quinlan, C.L., Costa, A.D.T., Costa, C.L., Pierre, S. V, Dos Santos, P., Garlid, K.D., 2008. Conditioning the heart induces formation of signalosomes that interact with mitochondria to open mitoKATP channels. Am. J. Physiol. Heart Circ. Physiol. 295, H953–H961.

Ragan, C.I., 1978. The role of phospholipids in the reduction of ubiquinone analogues by the mitochondrial reduced nicotinamide-adenine dinucleotide-ubiquinone oxidoreductase complex. Biochem. J. 172, 539–47.

Randle, P.J., 1986. Fuel selection in animals. Biochem. Soc. Trans. 14, 799–806.

Randle, P.J., Garland, P.B., Hales, C.N., Newsholme, E. a., 1963. The glucose fatty-acid cycle its role in insulin sensitivity and the metabolic disturbances of diabetes mellitus. Lancet 281, 785–789.

Randle, P.J., Newsholme, E.A., Garland, P.B., 1964. Regulation of glucose uptake by muscle. 8. Effects of fatty acids, ketone bodies and pyruvate, and of alloxan-diabetes and starvation, on the uptake and metabolic fate of glucose in rat heart and diaphragm muscles. Biochem. J. 93, 652–665.

Randle, P.J., Priestman, D.A., 1996. Shorter term and longer term regulation of pyruvate dehydrogenase kinases, in: Patel, M., Roche, T., Harris, R. (Eds.), Alpha-Keto Acid Dehydrogenase Complexes SE - 11, MCBU Molecular and Cell Biology Updates. Birkhäuser Basel, pp. 151–161.

Rider, M.H., Bertrand, L., Vertommen, D., Michels, P. a, Rousseau, G.G., Hue, L., 2004. 6-Phosphofructo-2-Kinase/Fructose-2,6-Bisphosphatase: Head-To-Head With a Bifunctional Enzyme That Controls Glycolysis. Biochem. J. 381, 561–579.

Roden, M., Price, T.B., Perseghin, G., Petersen, K.F., Rothman, D.L., Cline, G.W., Shulman, G.I., 1996. Mechanism of free fatty acid-induced insulin resistance in humans. J. Clin. Invest. 97, 2859–2865.

Roglic, G., Unwin, N., Bennett, P.H., Mathers, C., Tuomilehto, J., Nag, S., Connolly, V., King, H., 2005. The burden of mortality attributable to diabetes: Realistic estimates for the year 2000. Diabetes Care 28, 2130–2135.

Rosano, G.M.C., Vitale, C., Fragasso, G., 2006. Metabolic therapy for patients with diabetes mellitus and coronary artery disease. Am. J. Cardiol. 98, 14J–18J.

Rosano, G.M.C., Vitale, C., Spoletini, I., 2015. Metabolic approach to heart failure: The role of metabolic modulators. Egypt. Hear. J.

Ruiz-Meana, M., 2005. Trimetazidine, Oxidative Stress, and Cell Injury During Myocardial Reperfusion. Rev. Española Cardiol. 58, 895–897.

Russell, R.R., Bergeron, R., Shulman, G.I., Young, L.H., 1999. Translocation of myocardial GLUT-4 and increased glucose uptake through activation of AMPK by AICAR. Am. J. Physiol. - Hear. Circ. Physiol. 277, H643–H649.

Russell, R.R.. 3rd, Taegtmeyer, H., 1991. Pyruvate carboxylation prevents the decline in contractile function of rat hearts oxidizing acetoacetate. Am J Physiol Hear. Circ Physiol 261, H1756–1762.

Sack, M.N., Kelly, D.P., 1998. The energy substrate switch during development of heart failure: gene regulatory mechanisms (Review). Int. J. Mol. Med. 1, 17–41.

Sakai, K., Gebhard, M.M., Spieckermann, P.G., Bretschneider, H.J., 2016. Enzyme release resulting from total ischemia and reperfusion in the isolated, perfused guinea pig heart. J. Mol. Cell. Cardiol. 7, 827–840.

Santalucia, T., 1999. Factors Involved in GLUT-1 Glucose Transporter Gene Transcription in Cardiac Muscle. J. Biol. Chem. 274, 17626–17634.

Santalucía, T., Camps, M., Castelló, A., Muñoz, P., Nuel, A., Testar, X., Palacin, M., Zorzano, A., 1992. Developmental regulation of GLUT-1 (erythroid/Hep G2) and GLUT-4 (muscle/fat) glucose transporter expression in rat heart, skeletal muscle, and brown adipose tissue. Endocrinology 130, 837–846.

Schaffer, J.E., 2002. Fatty acid transport: the roads taken. Am. J. Physiol. Endocrinol. Metab. 282, E239–46.

Schulz, H., 2008. Oxidation of fatty acids in eukaryotes, in: Biochemistry of Lipids, Lipoproteins and Membranes. pp. 131–154.

Schulz, H., 1994. Regulation of Fatty Acid Oxidation in Heart. J. Nutr. 165–171.

Sellier, P., Broustet, J.-P., 2003. Assessment of anti-ischemic and antianginal effect at trough plasma concentration and safety of trimetazidine MR 35 mg in patients with stable angina pectoris: a multicenter, double-blind, placebo-controlled study. Am. J. Cardiovasc. Drugs 3, 361–369.

Sharma, S., Adrogue, J. V, Golfman, L., Uray, I., Lemm, J., Youker, K., Noon, G.P., Frazier, O.H., Taegtmeyer, H., 2004. Intramyocardial lipid accumulation in the failing human heart resembles the lipotoxic rat heart. FASEB J. 18, 1692–1700.

Silver, M.A., Horton, D.P., Ghali, J.K., Elkayam, U., 2002. Effect of nesiritide versus dobutamine on short-term outcomes in the treatment of patients with acutely decompensated heart failure. J. Am. Coll. Cardiol. 39, 798–803.

Siostrzonek, P., Koreny, M., Delle-Karth, G., Haumer, M., Koller-Strametz, J., Heinz, G., 2000. Milrinone therapy in catecholamine-dependent critically ill patients with heart failure. Acta Anaesthesiol. Scand. 44, 403–409.

Sliwa, K., Mayosi, B.M., 2013. Recent advances in the epidemiology, pathogenesis and prognosis of acute heart failure and cardiomyopathy in Africa. Heart 99, 1317–22.

Sliwa, K., Mocumbi, A.O., 2010. Forgotten cardiovascular diseases in Africa. Clin. Res. Cardiol. 99, 65–74.

Stanley, W.C., 2001. Changes in cardiac metabolism: a critical step from stable angina to ischaemic cardiomyopathy. Eur. Hear. J. Suppl. 3, O2–O7.

Stanley, W.C., Lopaschuk, G.D., Hall, J.L., McCormack, J.G., 1997a. Regulation of myocardial carbohydrate metabolism under normal and ischaemic conditions. Potential for pharmacological interventions. Cardiovasc. Res. 33, 243–257.

Stanley, W.C., Lopaschuk, G.D., McCormack, J.G., 1997b. Regulation of energy substrate metabolism in the diabetic heart. Cardiovasc. Res. 34, 25–33.

Stanley, W.C., Recchia, F.A., Lopaschuk, G.D., 2005. Myocardial Substrate Metabolism in the Normal and Failing Heart. Physiol. Rev. 85, 1093–1129.

Steyn, K., Sliwa, K., Hawken, S., Commerford, P., Onen, C., Damasceno, A., Ounpuu, S., Yusuf, S., Africa, for the I.I. in, 2005a. Risk Factors Associated With Myocardial Infarction in Africa. Circulation 112, 3554–3561.

Steyn, K., Sliwa, K., Hawken, S., Commerford, P., Onen, C., Damasceno, A., Ounpuu, S., Yusuf, S., Africa, for the I.I. in, 2005b. Risk Factors Associated With Myocardial Infarction in Africa: The INTERHEART Africa Study. Circulation 112, 3554–3561.

Szwed, H., Hradec, J., Préda, I., 2001. Anti-ischaemic efficacy and tolerability of trimetazidine administered to patients with angina pectoris: results of three studies. Coron. Artery Dis. 12 Suppl 1, S25–8.

Taegtmeyer, H., Hems, R., Krebs, H. a, 1980. Utilization of energy-providing substrates in the isolated working rat heart. Biochem. J. 186, 701–711.

Thornalley, P.J., 1990. The glyoxalase system: new developments towards functional characterization of a metabolic pathway fundamental to biological life. Biochem. J. 269, 1–11.

Tsutsui, H., Kinugawa, S., Matsushima, S., 2011. Oxidative stress and heart failure. AJP-Heart Circ Physiol 301, 2181–2190.

Ungar, I., Gilbert, M., Siegel, A., Blain, J.M., Bing, R.J., 2015. Studies on myocardial metabolism. Am. J. Med. 18, 385–396.

Ussher, J.R., Wang, W., Gandhi, M., Keung, W., Samokhvalov, V., Oka, T., Wagg, C.S., Jaswal, J.S., Harris, R.A., Clanachan, A.S., Dyck, J.R.B., Lopaschuk, G.D., 2012. Stimulation of glucose oxidation protects against acute myocardial infarction and reperfusion injury. Cardiovasc. Res. 94, 359–369.

Van Bilsen, M., Van Nieuwenhoven, F. a., Van Der Vusse, G.J., 2009. Metabolic remodelling of the failing heart: Beneficial or detrimental? Cardiovasc. Res. 81, 420–428.

van der Vusse, G.J., van Bilsen, M., Glatz, J.F., 2000. Cardiac fatty acid uptake and transport in health and disease. Cardiovasc. Res. 45, 279–293.

Vitale, C., Spoletini, I., Malorni, W., Perrone-Filardi, P., Volterrani, M., Rosano, G.M.C., 2015. Efficacy of trimetazidine on functional capacity in symptomatic patients with stable exertional angina — The VASCO-angina study. Int. J. Cardiol. 168, 1078–1081.

Vitale, C., Wajngaten, M., Sposato, B., Gebara, O., Rossini, P., Fini, M., Volterrani, M., Rosano, G.M.C., 2004. Trimetazidine improves left ventricular function and quality of life in elderly patients with coronary artery disease. Eur. Heart J. 25, 1814–1821.

Wang, X., Hole, D.G., Da Costa, T.H., Evans, R.D., 1998. Alterations in myocardial lipid metabolism during lactation in the rat. Am. J. Physiol. 275, E265–E271.

Weiss, R.G., Maslov, M., 2004. Normal myocardial metabolism: Fueling cardiac contraction. Adv. Stud. Med. 4, 457–463.

Whitehouse, S., Cooper, R.H., Randle, P.J., 1974. Mechanism of activation of pyruvate dehydrogenase by dichloroacetate and other halogenated carboxylic acids. Biochem. J. 141, 761–774.

Wisneski, J.A., Gertz, E.W., Neese, R.A., Gruenke, L.D., Craig, J.C., 1985. Dual carbon-labeled isotope experiments using D-[6-14C] glucose and L-[1,2,3-13C3] lactate: A new approach for investigating human myocardial metabolism during ischemia. J. Am. Coll. Cardiol. 5, 1138–1146.

Wittstein, I.S., 2012. Stress cardiomyopathy: A syndrome of catecholamine-mediated myocardial stunning? Cell. Mol. Neurobiol. 32, 847–857.

Wittstein, I.S., Thiemann, D.R., Lima, J.A.C., Baughman, K.L., Schuman, S.P., Gerstenblith, G., Wu, K.C., Rade, J.J., Bivalacqua, T.J., Champion, H.C., 2005. Neurohumoral Features of Myocardial Stunning Due to Sudden Emotional Stress. N. Engl. J. Med. 352, 1045–1057.

Xu, X., Hua, Y., Nair, S., Zhang, Y., Ren, J., 2013. Akt2 knockout preserves cardiac function in high-fat diet-induced obesity by rescuing cardiac autophagosome maturation. J. Mol. Cell Biol.

Yabe-Nishimura, C., 1998. Aldose Reductase in Glucose Toxicity : A Potential Target for the Prevention of Diabetic Complications. Am. Soc. Pharmacol. Exp. Ther. 50, 21–33.

Yankovskaya, V., Horsefield, R., Törnroth, S., Luna-Chavez, C., Miyoshi, H., Léger, C., Byrne, B., Cecchini, G., Iwata, S., 2003. Architecture of Succinate Dehydrogenase and Reactive Oxygen Species Generation. Science (80-.). 299, 700–704.

Yoshikawa, S., 2003. A cytochrome c oxidase proton pumping mechanism that excludes the O2 reduction site. FEBS Lett. 555, 8–12.

Yoshikawa, S., Muramoto, K., Shinzawa-Itoh, K., Aoyama, H., Tsukihara, T., Ogura, T., Shimokata, K., Katayama, Y., Shimada, H., 2006. Reaction mechanism of bovine heart cytochrome c oxidase. Biochim. Biophys. Acta 1757, 395–400.

Young, L.H., Coven, D.L., Russell, R.R., 2000. Cellular and molecular regulation of cardiac glucose transport. J Nucl Cardiol 7, 267–276.

Young, L.H., Renfu, Y., Russell, R., Hu, X., Caplan, M., Ren, J., Shulman, G.I., Sinusas, A.J., 1997. Low-Flow Ischemia Leads to Translocation of Canine Heart GLUT-4 and GLUT-1 Glucose Transporters to the Sarcolemma In Vivo. Circulation 95, 415–422.

Appendix A

UNIVERSITEIT·STELLENBOSCH·UNIVERSITY
jou kennisvennoot • your knowledge partner

Protocol Approval

Date: 30-May-2013

PI Name: Kimar, Charlene CP

Protocol #: SU-ACUM13-00020

Title: Perturbed metabolic pathways and the onset of cardio-metabolic diseases in a Rat model.

Dear Charlene Kimar, the Initial Application, was reviewed on 30-May-2013 by the Research Ethics Committee: Animal Care and Use via committee review procedures and was approved. Please note that this clearance is only valid for a period of twelve months. Ethics clearance of protocols spanning more than one year must be renewed annually through submission of a progress report, up to a maximum of three years.

Applicants are reminded that they are expected to comply with accepted standards for the use of animals in research and teaching as reflected in the South African National Standards 10386: 2008. The SANS 10386: 2008 document is available on the Division for Research Developments website www.sun.ac.za/research.

Please remember to use your protocol number, SU-ACUM13-00020 on any documents or correspondence with the REC: ACU concerning your research protocol.

Please note that the REC: ACU has the prerogative and authority to ask further questions, seek additional information, require further modifications or monitor the conduct of your research.

We wish you the best as you conduct your research.

If you have any questions or need further help, please contact the REC: ACU secretariat at WABEUKES@SUN.AC.ZA or .

Sincerely,

Winston Beukes

REC: ACU Secretariat

Research Ethics Committee: Animal Care and Use

Appendix B

UNIVERSITEIT·STELLENBOSCH·UNIVERSITY
jou kennisvennoot • your knowledge partner

Approved with Stipulations

Date: 20-Apr-2016

PI Name: Kimar, Charlene CP

Protocol #: SU-ACUM13-00003

Title: Perturbed metabolic pathways and the onset of cardio-metabolic diseases

Dear Charlene Kimar, the Amendment submission was reviewed on by Research Ethics Committee: Animal Care and Use via committee review procedures and was approved on condition that the following stipulations are adhered to:

a) 60 animals (6 groups, n=10) for analysis of oxidative stress and metabolic pathways.

b) 40 animals (4 groups, n=10) to test for the presence of necrosis.

Total = 100 animals

Applicants are reminded that they are expected to comply with accepted standards for the use of animals in research and teaching as reflected in the South African National Standards 10386: 2008. The SANS 10386: 2008 document is available on the Division for Research Developments website www.sun.ac.za/research.

As provided for in the Veterinary and Para-Veterinary Professions Act, 1982. It is the principal investigator's responsibility to ensure that all study participants are registered with or have been authorised by the South African Veterinary Council (SAVC) to perform the procedures on animals, or will be performing the procedures under the direct and continuous supervision of a SAVC-registered veterinary professional or SAVC-registered para-veterinary professional, who are acting within the scope of practice for their profession.

Please remember to use your protocol number, SU-ACUM13-00003 on any documents or correspondence with the REC: ACU concerning your research protocol.

Any event not consistent with routine expected outcomes that results in any unexpected animal welfare issue (death, disease, or prolonged distress) or human health risks (zoonotic disease or exposure, injuries) must be reported to the committee, by creating an Adverse Event submission within the system.

If you have any questions or need further help, please contact the REC: ACU secretariat at WABEUKES@SUN.AC.ZA or 0218089003.

Sincerely,

Winston Beukes

Appendix C

Preparation of citrate buffer for dissolving streptozotocin

An amount of 0.192 g citric acid (0.1 M) was dissolved in 10 ml dist H_20 (Solution A) and separately 0.294 g sodium citrate (0.1 M) was dissolved in 10 ml (Solution B). An amount of 1.8 ml of Solution A was added to 8.2 ml Solution B and brought to a final volume of 100 ml with dH_20. The pH was adjusted to 6.2 with sodium hydroxide or hydrochloric acid.

Appendix D

Preparation of Krebs-Henseleit buffer

Krebs-Henseleit stock solutions

1. NaCl (277 g/2 L) (118.5 mM)
2. $NaHCO_3$ (84 g/2 L) (25 mM)
3. KCL (11.8 g/1 L) (4.75 mM)
4. $MgSO_4$.7H20 (9.8 g/L) (1.19 mM)
5. KH_2PO_4 (8g/L) (1.18 mM)
6. $CaCl_2$ dehydrate (20 g/L) (1.36 mM)

To prepare a 5 L Krebs-Henseleit buffer, mix 250 ml of solution 1 and 2, add 150 ml of solution 3 and 4. Thereafter add 5 and 6 and stir the solution. Add the appropriate amount of glucose, either 10 g (11 mM) for baseline glucose or 27 g (30 mM) for high glucose concentrations.

Appendix E

Mitochondrial protein isolation

The Isolation buffer provided in the mitochondrial isolation kit (Abcam, MitoSciences,Eugene OR) was supplemented with the following protease inhibitors:

- 1 mM phenylmethylsulfonyl (PMSF) added before use
- 1 µg/ml leupeptin
- 1 µg/ml aprotonin
- 1 mM sodium orthovanadate (Na_3VO_4)
- 1 mM sodium fluoride (NaF)

Appendix F

Modified RIPA buffer

For 100 ml of modified RIPA buffer

- 50 mM (790 mg) Tris base to 75 ml dH20. Add 900 mg NaCl. Adjust the pH to 7.4 using HCL.
- 10 ml 10% Nonidet-P40 (NP-40) (final concentration of 1%)
- 2.5 ml of 10% sodium-deoxycholate (final concentration 0.25%)
- 1 mM EDTA, pH 7.4 (final volume of 100 ml)
- 1 mM phenylmethylsulfonyl (PMSF) added before use
- 1 µg/ml leupeptin (10 µl)
- 1 µg/ml aprotonin (10 µl)
- 1 mM sodium orthovanadate (Na_3VO_4) (final volume of 100 ml)
- 1 mM sodium fluoride (NaF) (final volume of 100 ml)
- 1% Triton X

This buffer is made to 100 ml with dH_2O, aliquoted and stored at – 20°C

Appendix G

Bradford protein quantification

Bradford stock solution (5x)

Dilute 500 mg Coomassie Brilliant blue G250 in 250 ml 95% ethanol

Add 500 ml phosphoric acid, mix thoroughly

Adjust volume to 1 L with dH_20

Filter solution and store at 4°C

Bradford working solution

Dilute stock solution in a 1:5 ratio with dH_20

Filter with 2 filter papers

* The filtered working solution should be light brown in color: light sensitive

Bradford method

1. Thaw 1 mg/ml BSA stock (stored in freezer)
2. Thaw protein samples on ice - keep in ice at all times
3. Prepare BSA working solution by diluting 100 µl BSA stock in 400 µl dH_2O, vortex
4. Label 7 tubes for the standard curve and 1 tube for each sample. Samples were prepared in duplicate
5. Add BSA and dH_2O according to the table below

Standard (µg protein)	BSA (µl)	dH_2O (µl)
Blank	0	100
2	10	90
4	20	80
8	40	60
12	60	40
16	80	20
20	100	0

6. Add 95 µl dH2O and 5 µl protein sample (tissue or cell proteins)
7. Vortex all tubes briefly
8. Add 900 µl Bradford working solution to each tube and vortex again

9. Incubate tubes at room temperature for 5 min
10. Switch on the spectrophotometer, allow it to calibrate, then set the wavelength to 595 nm
11. Read absorbance of standards and samples twice for each tube
12. If the absorbance of samples fall outside the range of the highest standard, dilute with RIPA
13. Use Bradford graph program to plot a standard curve and unknown protein (µg) values.
14. Prepare samples with loading buffer of equal protein amounts (µg)

Appendix H

Western blot protocol

Preparation of sample buffer

Laemmli sample buffer
dH_2O – 3.8 ml
0.5 M Tris-HCL, pH 6.8 - 1 ml
Glycerol – 0.8 ml
10% (w/v) SDS -1.6 ml
0.05% (w/v) bromophenol blue – 0.4 ml

Sample preparation

1. Set the heating block to 95°C
2. Prepare a working solution of sample buffer by addition of 850 µl Laemmli buffer to 150 µl β-mercaptoethanol (prepare in fume cabinet), vortex thoroughly
3. Calculate the appropriate concentration of each sample (e.g. 20 µg per sample), and calculate the number of samples needed
4. Label microcentrifuge tubes for each sample and sample set
5. Add a volume of working sample buffer equivalent to 1/3 of total sample volume (2/3 protein +1/3 sample buffer)
6. Add appropriate volume of protein to each tube and punch holes in lid of each tube
7. Heat samples in a 95°C heating block for 5 min
8. Centrifuge each tube briefly for approximately 10 seconds and place on ice
9. Samples can now be loaded on SDS-PAGE gels or stored at – 20°C

Western blot buffers

Blocking buffer	Constituents
1% w/v BSA	1 g BSA in 100 ml 1x TBS-T
5% non-fat milk	5 g non-fat milk powder in 100 ml
	1x TBS-T

* Blocking buffer dependent on the specifications of the specific antibody

SDS-PAGE

1. Clean spacer plates and short plates, casting frames, stands and rubber gaskets

2. Place gasket in groves at the base of the stand and assemble glass plates in green frames with the short plate facing the front. Make sure to tighten the clips to secure the plates.

3. Place the assembled plates onto the rubber gasket in the base of the casting frame and securing it with a clip.

4. Add dH2O between plates to check for leakage.

5. Get two small beakers for the resolving and stacking gels

6. Gels were make up using TGX™ and TGX stain-free FastCast acrylamide kit (Bio-Rad, Hercules CA) according to the following table:

	Stacker	Resolver
Resolver A	-	3 ml x n
Resolver B	-	3 ml x n
Stacker A	1 ml x n	-
Stacker B	1 ml x n	-
TEMED	2 µl x n	3 µl x n
10% APS	10 µl x n	30 µl x n

7. The resolving acrylamide gel solution was prepared by combining equal volumes of resolver A and B solutions.
8. Add the required volume of TEMED and freshly made 10% APS to the combined resolver A and B solution and mix well.
9. Carefully pipette the resolving gel solution into the glass plates using a Pasteur pipette – be sure to avoid introducing bubbles.
10. Prepare the stacking acrylamide gel solution by combining equal volumes of stacker A and B solutions.
11. Add the required volume of TEMED and freshly made 10% APS to the combined solution and mix well.
12. Pipette the stacking gel solution into the glass plates using a Pasteur pipette.
13. Insert the gel combs – be sure to avoid introducing bubbles.

14. Allow the gel to set for 30 – 45 min.
15. Load molecular weight protein marker and protein samples.
16. Gels were electrophoresed at 100 V (constant) and 400 mA until the protein marker reached the bottom of the gel.

Electrotransfer

Proteins were transferred onto the membrane using trans-blot® turbo midi PVDF transfer packs (Bio-Rad, Hercules CA) in the following manner:

1. Place the membrane and the bottom stack on the cassette base. Make sure to use a blot roller to remove any air bubbles- The anode stack and membrane are located at the bottom.
2. Place 2 mini gels onto the membrane and gently use a blot roller to remove any air bubbles.
3. Place the second wetted transfer stack on top of the gel. This will serve as a top ion stack. Be sure to remove any air bubbles.
4. Close and lock the cassette lid and insert the cassette into the Trans-Blot Turbo System® (Bio-Rad, Hercules CA).

Appendix I

Respresentative Western blot images used as a loading control

3-KAT

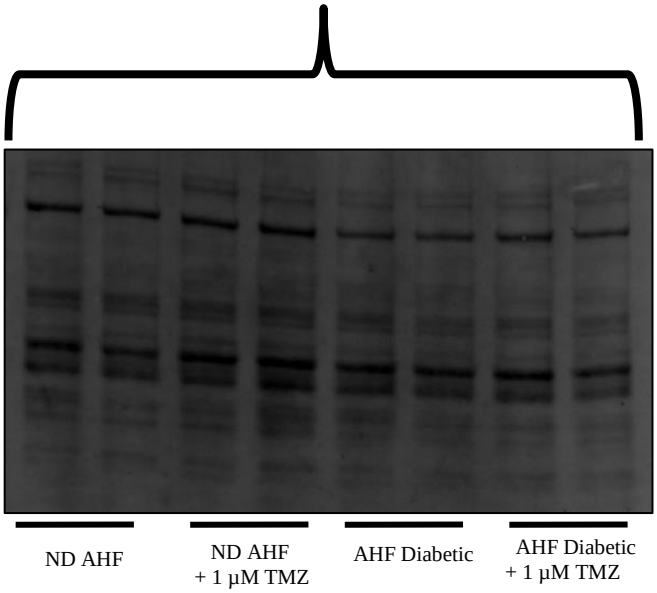

PDH

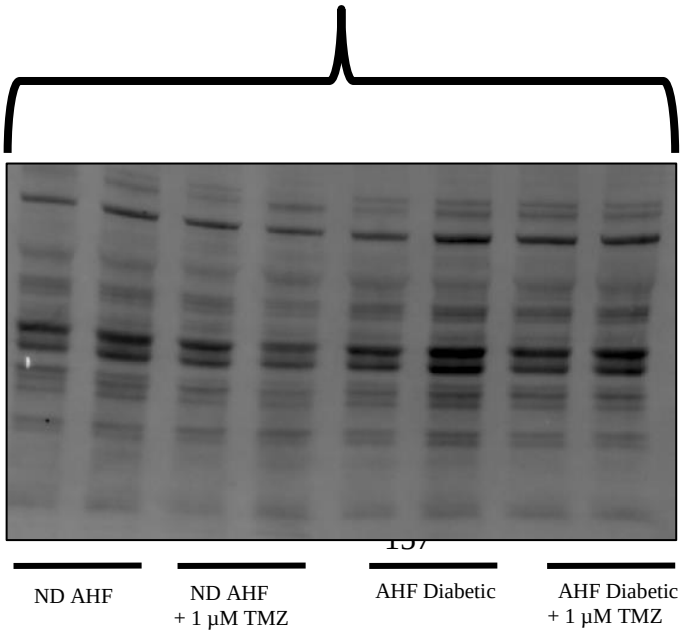

SOD2

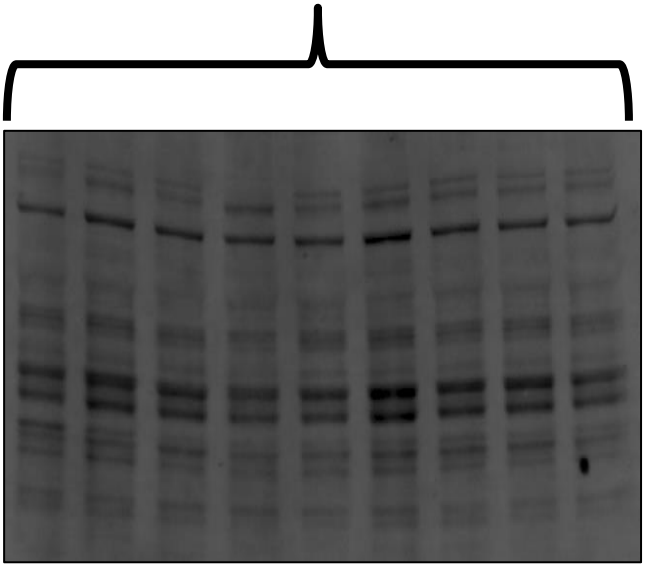

UCP2

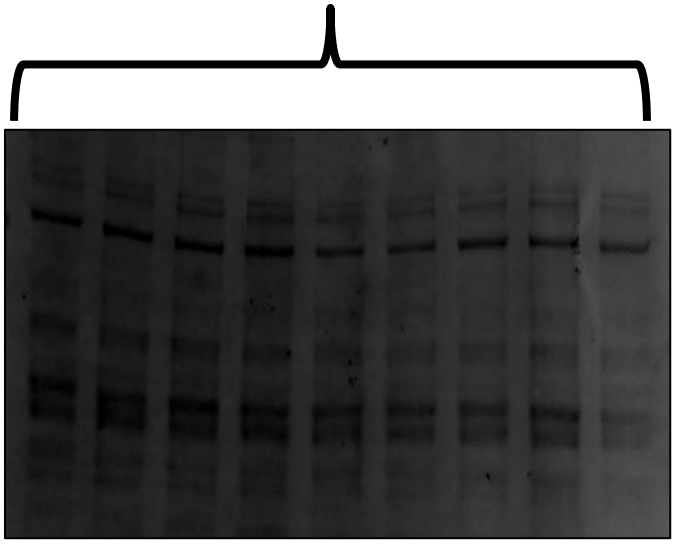

Appendix J

Oxygen Radical Absorbance Capacity Solutions

Tube	Standard concentration (µM)	Trolox stock solution (µl)	Phosphate Buffer (µl)
A	0	0	750
B	83	125	625
C	167	250	500
D	250	375	375
E	333	500	250
F	417	625	125

Phosphate buffer (75 mM, pH 7.4)

Solution 1: Weigh 1.035 g sodium di-hydrogen orthophosphate-1-hydrate in 100 ml beaker with the addition of 100 ml dH_2O until dissolved. Solution 2: Weigh 1.335 g di-sodium hydrogen orthophosphate dehydrate in 100 ml beaker with the addition of 100 ml dH_2O. Mix 18 ml of solution 1 with 82 ml of solution 2. Solution stored at 4 °C until needed.

Trolox (control) (250 µM stock):

Weigh 0.00312 g 6-Hydroxy-2 5,7,8-tetra-methylchroman-2carboxylic acid in 50 centrifuge tube and add 50 ml phosphate buffer until dissolved. This solution should yield an absorbance of 0.670 ± 0.015 at 289 nm.

Trolox standard (500 µM stock):

Weigh 0.00625 g 6-Hydroxy-2 5,7,8-tetra-methylchroman-2carboxylic acid and add 50 ml phosphate buffer until dissolved. This solution should yield an absorbance of 0.670 ± 0.015 at 289 nm.

Fluorescein sodium salt:

Dissolve 0.0225 g fluorescein sodium salt in 50 ml phosphate buffer. Store in dark container at 4 °C

Peroxyl radical:

Weigh 0.150 g 2,2'-Azobis (2-mthylpropionamidine) dihydrochloride (25 mg/L) into a 15 ml centrifuge tube. This solution should be prepared fresh.